The mathematics of thin structures

Jean-François Babadjian, Giovanni Di Fratta, Irene Fonseca, Gilles A Francfort, Marta Lewicka, Cyrill B Muratov

QUARTERLY OF APPLIED MATHEMATICS
VOLUME , NUMBER 0
XXXX XXXX, PAGES 000–000

THE MATHEMATICS OF THIN STRUCTURES

By

JEAN-FRANÇOIS BABADJIAN (*Université Paris-Saclay, CNRS, Laboratoire de mathématiques d'Orsay, 91405, Orsay, France*),

GIOVANNI DI FRATTA (*Dipartimento di Matematica e Applicazioni "R. Caccioppoli", Università degli Studi di Napoli "Federico II", Napoli, Italy*),

IRENE FONSECA (*Department of Mathematical Sciences, Carnegie Mellon University, 5000 Forbes Avenue, Pittsburgh, PA 15213, USA*),

GILLES A. FRANCFORT (*Université Paris-Nord, LAGA, Avenue J.-B. Clément, 93430 - Villetaneuse, France & Courant Institute, New York University, 251 Mercer St., NYC, NY 10012, USA*),

MARTA LEWICKA (*Marta Lewicka: University of Pittsburgh, Department of Mathematics, 139 University Place, Pittsburgh, PA 15260*),

AND

CYRILL B. MURATOV (*Department of Mathematical Sciences, New Jersey Institute of Technology, Newark, NJ 07102, USA*)

Abstract. This article offers various mathematical contributions to the behavior of thin films. The common thread is to view thin film behavior as the variational limit of a three-dimensional domain with a related behavior when the thickness of that domain vanishes. After a short review in Section 1 of the various regimes that can arise when such an asymptotic process is performed in the classical elastic case, giving rise to various well-known models in plate theory (membrane, bending, Von Karmann, etc...), the other sections address various extensions of those initial results. Section 2 adds brittleness and delamination and investigates the brittle membrane regime. Sections 4 and 5 focus on micromagnetics, rather than elasticity, this once again in the membrane regime and discuss magnetic skyrmions and domain walls, respectively. Finally, Section 3 revisits the classical setting in a non-Euclidean setting induced by the presence of a pre-strain in the model.

E-mail address: jean-francois.babadjian@universite-paris-saclay.fr
E-mail address: giovanni.difratta@unina.it
E-mail address: fonseca@andrew.cmu.edu
E-mail address: gilles.francfort@univ-paris13.fr, gilles.francfort@cims.nyu.edu
E-mail address: lewicka@pitt.edu
E-mail address: muratov@njit.edu

Contents

1. The Mathematics of Thin Structures – An introduction (by G. Francfort and I. Fonseca).

1.1. *Introduction.* This collection of articles attempts to provide a wide ranging, while not encompassing all views of the current mathematical investigations into thin structures. Rather than enumerate and detail the various topics that have been either included or excluded from this volume, we prefer to describe briefly the main historical steps that have led to the kind of pursuit which is described in the following presentations.

The original concern was a simple one: What happens to a thin three-dimensional elastic body when its thickness vanishes asymptotically? In other words, consider a domain of the form $\Omega^\varepsilon := \omega \times (-\varepsilon/2, \varepsilon/2)$ with $\omega \subset \mathbb{R}^2$ open, bounded, Lipschitz domain, and $\varepsilon > 0$.

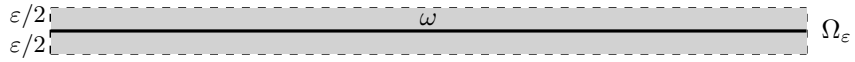

FIG. 1. The thin domain

That domain is occupied by an elastic material with $W : \mathbb{R}^{3\times 3} \to \bar{\mathbb{R}}$ as elastic energy density, so that the internal energy of the body is

$$E_\varepsilon(U^\varepsilon) := \int_{\Omega^\varepsilon} W(\nabla U^\varepsilon)\, dx,$$

where U^ε is the elastic minimizer of the associated potential energy.[1] What is the stored energy in the limit two dimensional body ω as $\varepsilon \searrow 0$?

It was realized early on that the limit stored energy critically depends on the order of E_ε in ε, giving rise to a great variety of asymptotic behaviors. Given a thin domain and a set of boundary conditions and loads, there is no natural way to guess what the

[1] In this presentation, as well as in those of the various contributors, a variational attitude is adopted. It consists in assuming that elastic equilibrium is achieved through minimization of the potential energy for the relevant boundary conditions and loads. Of course, while this is strictly equivalent to assuming equilibrium in a linearized context, it is not so in a nonlinear framework and much remains to be done on that front.

relevant order is, so the classification is not so useful from a practical standpoint, except maybe for the potential corrections that the obtained asymptotic models suggest vis à vis the classical models used by engineers. Nevertheless, this is where the mathematical effort has concentrated, and our goal in this short introduction is to review the classical tenet of the theory precisely in terms of the ε-order of the internal energy.

In the sequel and unless otherwise stated, we assume the following on the elastic energy W, as was first posited in [16],

$$\begin{cases} W : \mathbb{R}^{3\times 3} \to \bar{\mathbb{R}}^+ \text{ is continuous} \\ W(F) = \infty \text{ if } \det F \leq 0 \text{ (preservation of orientation } + \text{non interpenetration)} \\ W(RF) = W(F) \text{ for all } R \in SO(3) \text{ (frame indifference)} \\ W(Id) = 0 \text{ (no pre-stress)} \\ W \text{ is } C^2 \text{ near } Id \\ W(F) \geq c \operatorname{dist}^2(F, SO(3)) = c|\sqrt{F^T F} - Id|^2 \text{ for some } c > 0 \\ \qquad\qquad\qquad\qquad\qquad\qquad \text{(linear behavior near the identity)}, \end{cases} \tag{1.1}$$

which are the classical features of a so-called hyperelastic energy. In (1.1), Id is the identity matrix.

Remark 1.1. Note that the last property in (1.1) implies that $\partial W/\partial F(Id) = 0$, and that the quadratic form

$$Q_3(M) := \frac{\partial^2 W}{\partial F^2}(Id)M \cdot M, \ M \text{ symmetric } 3 \times 3 \text{ matrix}, \tag{1.2}$$

satisfies $Q_3(M) \geq c \operatorname{tr} M^T M$. Further,

$$W(Id + hA) \geq Q_3(hA) - o(|hA|^2).$$

The first step in the analysis is always the same. One should rescale the problem so as to deal with a fixed domain $\Omega = \omega \times (-1/2, 1/2)$. The associated rescaling is $x_3 \mapsto x_3/\varepsilon$, resulting in

$$E_\varepsilon(U^\varepsilon) = \varepsilon \int_\Omega W(\nabla^\varepsilon u^\varepsilon)\, dx, \tag{1.3}$$

where $u^\varepsilon(x_\alpha, x_3) := U^\varepsilon(x_\alpha, \varepsilon x_3)$ and $\nabla^\varepsilon := \left(\nabla', 1/\varepsilon \dfrac{\partial}{\partial x_3}\right)$, ∇' denoting the in-plane partial derivatives $\partial/\partial x_1, \partial/\partial x_2$.

We define

$$\mathcal{E}^\varepsilon(v) := \int_\Omega W(\nabla^\varepsilon v)\, dx$$

so that $E^\varepsilon(U^\varepsilon) = \varepsilon \mathcal{E}(u^\varepsilon)$.

The goal is then to investigate the asymptotic behavior of $E_\varepsilon/\varepsilon^\beta$. In mathematical terms, this amounts to a study of

- The compactness of (approximate) minimizers u^ε of $\mathcal{E}^\varepsilon/\varepsilon^{\beta-1}$ under the assumption that

$$\sup_\varepsilon \mathcal{E}^\varepsilon(u^\varepsilon)/\varepsilon^{\beta-1} < \infty; \tag{1.4}$$

- The Γ-convergence, in the topology for which compactness is attained as per the previous item, of $\mathcal{E}^\varepsilon/\varepsilon^{\beta-1}$.

It is clear from (1.3) that the first order for which a non trivial limit may be obtained is $\beta = 1$. This will give rise to the so-called membrane regime detailed in Subsection 1.2.1. Then, the regimes $\beta > 1$ will produce a variety of different models that conform more or less to classical engineering models, as described in Subsections 1.2.3, 1.2.4 and 1.2.5. All results pertaining to regimes for which $\beta > 1$ heavily hinge on an approximate rigidity theorem established in [91]. Subsection 1.2.2 will detail that result and the way it is used in establishing the relevant Γ-limits in Subsections 1.2.3, 1.2.4 and 1.2.5.

Each of the following subsections in Section 1.2 is short (and even very short), and essentially reduces to a mere statement of the most important results pertaining to the relevant scaling, together with a rapid sketch of some of the underlying mathematical arguments. The focus is almost exclusively on the derivation of a lower bound for the $\Gamma - \liminf$ which, hopefully, will be optimal. In all that follows, we assume familiarity with the notion of $\Gamma(X)$-convergence, X being a metrizable topological space (see [54]).

Finally, in Section 1.3, we address a few of the problems or concerns that can be raised as to the significance of the models described in Section 1.2 in the hope that some of those will provide motivation for future research.

Notationwise, if M is a 3×3 matrix, we denote by $|M|$ its Frobenius norm, that is $(\text{tr } M^T M)^{1/2}$ (associated to the Frobenius inner product $M \cdot N := \text{tr } M^T N$), and we use x' to denote the planar coordinates x_1, x_2. The rest of the notation is standard.

1.2. *The various regimes.* In this section, we quickly describe the main regimes that can be obtained when β varies.

REMARK 1.2. In Section 3, Marta Lewicka will offer a similar analysis with the additional non trivial feature that hers is a non-Euclidean setting induced by the presence of a pre-strain in the model. In that framework, $E^\varepsilon(U^\varepsilon)$ is modified and becomes $\int_{\Omega^\varepsilon} W(\nabla U^\varepsilon g^{-1/2})\, dx$ where g is the smooth Riemannian metric associated with the pre-strain of the thin domain.

1.2.1. *Membranes ($\beta = 1$; Le Dret-Raoult).* The scaling $\beta = 1$ is historically the first one to be addressed in [137]. Unfortunately, the analysis in that paper does not allow for an energy satisfying (1.1). Instead, one should have, for some $C > 0$,

$$W : \mathbb{R}^{3\times 3}\mathbb{R} \text{ is continuous, and } \frac{1}{C}|F|^p - C \leq W(F) \leq C(|F|^p + 1),\ 1 < p < \infty, \quad (1.5)$$

which of course goes against the requirement that $W(F) \nearrow \infty$ as $\det F \to 0^+$.

In such a setting, coercivity immediately implies that a sequence $\{u^\varepsilon\}$ satisfying (1.4) will have a weak-$L^p(\Omega;\mathbb{R}^{3\times 3})$-converging subsequence of gradients with, as limit the gradient of an x_3-independent function $u = u(x')$. With this in mind, a first result is as follows:

THEOREM 1.3. Under assumption (1.5)

- For a subsequence (still indexed by ε), if u^ε satisfies (1.4), then
  weakly in $W^{1,p}(\Omega;\mathbb{R}^3)$, with u a function of x' solely;

- $\mathcal{E}^\varepsilon$ $\Gamma(L^p(\Omega;\mathbb{R}^3))$-converges to

$$\mathcal{E}_m(u) = \begin{cases} \int_\omega Q\overline{W}(\nabla' u)dx', \ u \in W^{1,p}(\Omega,\mathbb{R}^3), u \text{ independent of } x_3 \\ \infty, \ else, \end{cases}$$

where, for $F \in \mathbb{R}^{3\times 2}$, $\overline{W}(F) := \inf_{z\in\mathbb{R}^3} W(F,z)$, and $Q\overline{W}$ is the 3×2-quasiconvex envelope of $\overline{W}$, that is

$$Q\overline{W}(F) := \inf_\varphi \left\{ \fint_A \overline{W}(F+\nabla'\varphi) : \varphi \in C_c^\infty(A;\mathbb{R}^3) \right\}$$

for some (any) bounded open set $A \in \mathbb{R}^2$ with $\mathcal{L}^2(\partial A) = 0$.

REMARK 1.4. Note that, if W satisfies frame indifference (see (1.1)), then so does $Q\overline{W}$. Also, if $F \in \mathbb{R}^{3\times 2}$ is such that $|F|^2 \leq 1$, then $Q\overline{W}(F) = 0$. Indeed, in such a case, the singular values v_1, v_2 of F are both in $[0,1]$. The affine deformation $u = (v_1x_1, v_2x_2, 0)^T$ is such that $\nabla' u^T \nabla' u = F^T F$ and thus, because of frame indifference, $Q\overline{W}(F) = Q\overline{W}(\nabla' u)$. But the sequence $\{u_\varepsilon\}$ given by $u^\varepsilon := (v_1x_1 + \varepsilon\theta_1(x_1/\varepsilon), v_2x_2 + \varepsilon\theta_2(x_2/\varepsilon), 0)^T$ with

$$\theta_i(t) := \begin{cases} (1-v_i)t & \text{if } 0 \leq t \leq (1+v_i)/2, \\ -(1+v_i)(t-1) & \text{if } (1+v_i)/2 \leq t \leq 1, \end{cases}$$

converges strongly to u in $L^2(\Omega;\mathbb{R}^3)$, while its reduced gradient $\nabla' u^\varepsilon$ only takes the values

$$J_{\pm,\pm} := \begin{pmatrix} \pm 1 & 0 \\ 0 & \pm 1 \\ 0 & 0 \end{pmatrix}.$$

Since $Q\overline{W}(J_{\pm,\pm}) \leq W(J_{\pm,\pm})$, and by (1.1) $W(J_{\pm,\pm}) = W(Id) = 0$, we deduce that $Q\overline{W}(\nabla' u^\varepsilon) = 0$ and, in turn, by lower semicontinuity we conclude that $Q\overline{W}(\nabla' u) \equiv 0$.

This shows that the membrane regime does not react to compression, and forces us to go beyond that scaling in the next subsections.

The previous theorem result, in spite of its intrinsic defect with regard to orientation preservation and non interpenetration, spurred a plethora of investigations in a variety of fields ranging from micro-magnetics, optimal design, fracture, to homogenization among others. We will not dwell upon those here, pointing instead to Section 2 by Jean-François Babadjian on brittle membranes and of both Section 4 by Giovanni Di Fratta and Section 5 by Cyrill Muratov on micromagnetics in this volume. In Section 2 an additional energy is added to the elastic energy to account for delamination of the membrane from its substrate and/or fracture within the membrane, and the author analyzes the competition between those two processes. In Section 4 elasticity is replaced by magnetism while the membrane is not a flat one, but a curved one (ω is replaced by a smooth surface embedded in $\mathbb{R}^3$) and the author investigates the appearance of magnetic skyrmions. In Section 5, the emphasis is on the study of magnetic domains in thin films (those regions with aligned magnetic spins) and on the transition layers between the domains (the magnetic walls).

To this day, the handling of conditions (1.1) seems to be out of reach. The studies that come nearest to achieving that goal are those of [50, 207] which investigate the incompressible case, that is what happens when the energy is infinite if $\det F \neq 1$ and

satisfies (1.5). In that case, the limit model is exactly that obtained in the previous theorem and incompressibility is lost in the limit.

Finally, let us emphasize that one could refine the results of Theorem 1.3 in a variety of ways. As an example, one could also impose that, in the search for a Γ-limit, one also require that, for a converging sequence $\{w^\varepsilon\}$, the weak $L^p(\Omega;\mathbb{R}^3)$-limit of the term $1/\varepsilon\partial w^\varepsilon/\partial x_3$ be given (and not only that of the strong $L^p(\Omega;\mathbb{R}^3)$-limit of w^ε). In that case, the results are much more intricate and the limit behavior is most likely nonlocal. We refer the reader to [27] for details.

1.2.2. *Rigidity (*Friesecke-James-Müller*).* Say that $u \in W^{1,2}(\Omega;\mathbb{R}^n)$ is such that $\nabla u(x) = R(x) \in SO(n)$, for a.e. $x \in \Omega$. Then, since $\operatorname{div}\operatorname{cof}\nabla u = 0$, we get $0 = \operatorname{div}\operatorname{cof} R = \operatorname{div} R = \triangle u$, and u is harmonic. Hence, we may consider derivatives of u of any order, and because $|R|^2 = 1$, we have

$$0 = \triangle|R|^2 = \triangle(|\nabla u|^2) = |\nabla^2 u|^2,$$

($\nabla^2 u$ is the Hessian matrix of each component of u), and thus ∇u is a constant rotation. This is a classical exact rigidity result à la Liouville. The approximate rigidity result uncovered in [91] states a similar result, provided that ∇u is L^2-close to a rotation, namely,

THEOREM 1.5. Let $\Omega \subset \mathbb{R}^n, n \geq 2$, be a bounded Lipschitz domain. Then there exists $C(\Omega)$, invariant by translation and dilation, such that, for all $u \in W^{1,2}(\Omega,\mathbb{R}^n)$, there exists $R \in SO(n)$ with

$$\|\nabla u - R\|_{L^2(\Omega;\mathbb{R}^{n\times n})} \leq C(\Omega)\|\operatorname{dist}(\nabla u, SO(n)\|_{L^2(\Omega)}.$$

This result has proved a milestone in many fields. For our part, we apply it to the setting at hand, recalling the bound from below on $W(F)$ in (1.1). We obtain that, for ε small, there exists $R^\varepsilon \in SO(3)$ such that

$$\int_{S_{a,\varepsilon}} |\nabla^\varepsilon u^\varepsilon - R^\varepsilon|^2 \, dx \leq C \int_{S_{a,\varepsilon}} \operatorname{dist}(\nabla^\varepsilon u, SO(3))^2 \, dx,$$

where $S_{a,\varepsilon} := (a + (-\varepsilon/2, \varepsilon/2))^2) \times (-1/2, 1/2)$, $a \in \varepsilon\mathbb{Z}^2$ and C is independent of a, ε. Provided that (1.4) holds, the previous estimate gives rise to a piecewise constant rotation field $R^\varepsilon(x')$ such that

$$\int_{\omega\times(-1/2,1/2)} |\nabla^\varepsilon u^\varepsilon - R^\varepsilon|^2 \, dx \leq C\varepsilon^{\beta-1} \tag{1.6}$$

and, with a little bit of work, it is not hard to show that, for some $C' > 0$,

$$\int_\omega |R^\varepsilon(x'+z) - R^\varepsilon(x')|^2 \, dx' \leq C'\varepsilon^{\beta-1}\left(\left|\frac{z}{\varepsilon}\right|^2 + 1\right). \tag{1.7}$$

If $\beta \geq 3$, from (1.7), we immediately infer that

$$\limsup_{z\to 0}\sup_\varepsilon \|R^\varepsilon(\cdot + z) - R^\varepsilon(\cdot)\|_{L^2(\Omega,\mathbb{R}^3)} = 0$$

so that, by the Fréchet-Kolmogorov theorem,

$$R^\varepsilon \overset{L^2(\Omega;\mathbb{R}^{3\times 3})}{\longrightarrow} \bar{R} \in W^{1,2}(\omega; SO(3))$$

and thus, with (1.6),

$$\nabla^\varepsilon u^\varepsilon \text{ and } R^\varepsilon \overset{L^2(\Omega;\mathbb{R}^{3\times 3})}{\longrightarrow} \bar{R} \in W^{1,2}(\omega, SO(3)). \tag{1.8}$$

In particular, we get that

$$\nabla^\varepsilon u^\varepsilon \overset{L^2(\Omega;\mathbb{R}^{3\times 3})}{\longrightarrow} (\nabla' u, b) \text{ with } b(x') = \frac{\partial u}{\partial x_1}(x') \wedge \frac{\partial u}{\partial x_2}(x'). \tag{1.9}$$

If $\beta < 3$, the only information we derive from (1.6) is that

$$\nabla^\varepsilon u^\varepsilon \text{ and } R^\varepsilon \overset{\text{weakly in } L^2(\Omega;\mathbb{R}^{3\times 3})}{\rightharpoonup} (\nabla' u, b) \text{ with } |\nabla' u|^2 \leq 1. \tag{1.10}$$

In such a case, u is called a short map.

1.2.3. *In between ($1 < \beta < 3$; Conti-Maggi).* Strangely enough, not much is known about the regime $1 < \beta < 3$ in addition to (1.10). In [52], it is proved that, when $\beta < 8/3$ the $\Gamma(L^2)$-limit of $\mathcal{E}/\varepsilon^{\beta-1}$ is 0 for short maps and ∞ else while, for $8/3 \leq \beta \leq 3$, the $\Gamma(L^2)$-limit has not been characterized as of yet.

The difficulty in this case lies in the construction of a recovery sequence. This relies upon the possibility of approaching uniformly a $W^{1,\infty}(\Omega;\mathbb{R}^3)$-short map u by C^1-isometries u_k, that is such that, for some b_k, $(\nabla u_k, b_k) \in SO(3)$; this is the famous Nash-Kuiper theorem.

In [52], the authors relate their results to Origami constructions and, further, to paper crumpling, an association which may, or may not be relevant because of the irreversibility of the folding process.

1.2.4. *Bending ($\beta = 3$; Friesecke-James-Müller).* If $\beta = 3$, then from (1.6) we immediately conclude that, up to a subsequence,

$$G^\varepsilon := 1/\varepsilon((R^\varepsilon)^T \nabla^\varepsilon u^\varepsilon - Id) \overset{\text{weakly in } L^2(\Omega;\mathbb{R}^{3\times 3})}{\rightharpoonup} G \tag{1.11}$$

and thus that, since, by frame indifference, $W(\nabla^\varepsilon u^\varepsilon) = W(Id + \varepsilon G^\varepsilon)$, we get, thanks to Remark 1.1,

$$\mathcal{E}^\varepsilon(u^\varepsilon)/\varepsilon^2 \geq 1/2 \int_\Omega Q_3(G^\varepsilon)\ dx - o(1)$$

where Q_3 was defined in (1.2). Hence

$$\liminf_\varepsilon \mathcal{E}^\varepsilon(u^\varepsilon)/\varepsilon^2 \geq 1/2 \int_\Omega Q_2(G'')\ dx \tag{1.12}$$

where, for any $M \in \mathbb{R}^{2\times 2}$,

$$Q_2(M) := \inf_{z,z' \in \mathbb{R}^2, z" \in \mathbb{R}} Q_3 \left(\begin{pmatrix} M & z \\ z' & z" \end{pmatrix} \right) \tag{1.13}$$

where we use the notation F'' to denote the 2×2 matrix with entries F_{ij}, $1 \leq i, j \leq 2$, while F' stands for the 3×2 matrix with entries $F_{i,j}$, $1 \leq i \leq 3$, $1 \leq j \leq 2$.

It remains to identify G'' in (1.12). To that effect, recalling that $b = b(x')$ is the strong $L^2(\Omega;\mathbb{R}^3)$-limit of $\{1/\varepsilon\ \partial u^\varepsilon/\partial x_3\}$, we have

$$\frac{1}{\varepsilon z} \int_{x_3}^{x_3+z} \frac{\partial u^\varepsilon}{\partial x_3}\ dz = \frac{1}{\varepsilon z}(u^\varepsilon(x', x_3 + z) - u^\varepsilon(x', x_3)) \overset{L^2(\Omega;\mathbb{R}^3)}{\longrightarrow} b,$$

hence

$$\frac{1}{z}((R^\varepsilon G^\varepsilon)'(x', x_3+z) - (R^\varepsilon G^\varepsilon)'(x', x_3)) = \frac{1}{z}\left[\frac{(\nabla' u^\varepsilon(x', x_3+z) - \nabla' u^\varepsilon(x', x_3))}{\varepsilon}\right] \overset{H^{-1}(\Omega;\mathbb{R}^{3\times 3})}{\longrightarrow} \nabla' b(x').$$

Consequently, from (1.8), (1.11),

$$\left[\bar{R}\left(\frac{G(x', x_3+z) - G(x', x_3)}{z}\right)\right]' = \nabla' b,$$

and, letting $z \searrow 0$, $\left[\bar{R}\partial G/\partial x_3\right]' = \nabla' b$, from which simple algebra leads to

$$\left[\frac{\partial G}{\partial x_3}\right]'' = (\nabla' u(x'))^T \nabla' b(x'), \tag{1.14}$$

which is thus an x_3-independent quantity. Finally we conclude that

$$G''(x', x_3) = G''(x', 0) + x_3 \left[\frac{\partial G}{\partial x_3}\right]''(x')$$

and so, recalling (1.12), (1.14),

$$\begin{aligned}\liminf_\varepsilon \mathcal{E}^\varepsilon(u^\varepsilon)/\varepsilon^2 &\geq 1/2 \int_\omega Q_2(G''(x', 0))\, dx + 1/24 \int_\omega Q_2\left((\nabla' u(x'))^T \nabla' b(x')\right)\, dx' \\ &\geq 1/24 \int_\omega Q_2\left((\nabla' u(x'))^T \nabla' b(x')\right)\, dx'. \end{aligned} \tag{1.15}$$

Inequality (1.15) actually provides the correct Γ-limit, as could be checked by constructing a recovery sequence roughly of the form $U^\varepsilon := \hat{u}(x') + \varepsilon x_3 \hat{b}(x') + \varepsilon x_3^2 \hat{d}(x')$, where $\hat{u}$ is an isometry, $\hat{b} := \partial\hat{u}/\partial x_1 \wedge \partial\hat{u}/\partial x_2$, and $\hat{d}$ is such that $Q_3(\hat{R}^T(\nabla' b, d)) = Q_2((\nabla'\hat{u})^T \nabla'\hat{b})$, with $\hat{R} := (\nabla'\hat{u}, \hat{b})$.

So we obtain the following:

THEOREM 1.6. Under assumption (1.1)

- For a subsequence (still indexed by ε), if u^ε satisfies (1.4), then $\nabla^\varepsilon u^\varepsilon \longrightarrow (\nabla' u, b)$ strongly in $L^2(\Omega; \mathbb{R}^{3\times 3})$, where $(\nabla' u, b) \in W^{1,2}(\Omega; SO(3))$ and is a function of x' solely;
- $\mathcal{E}^\varepsilon/\varepsilon^2$ $\Gamma(L^2(\Omega;\mathbb{R}^3))$-converges to

$$\mathcal{E}_b(v) := \begin{cases} 1/24 \int_\omega Q_2((\nabla' v)^T \nabla' c) dx', & \text{if } (\nabla' v, c) \text{ satisfies } (\nabla' v, c) \in W^{1,2}(\Omega; SO(3)) \\ & \text{and is a function of } x' \text{ solely} \\ \infty, \ else, \end{cases}$$

  where Q_2 was defined in (1.13).

The above regime is usually referred to as that of nonlinear bending.

REMARK 1.7. Note that $(\nabla' v, c) \in SO(3)$, therefore $c \cdot \dfrac{\partial v}{\partial x_1} = c \cdot \dfrac{\partial v}{\partial x_2} = 0$. Differentiating these equations with respect to x_1 and to x_2, shows that the term $(\nabla' v)^T \nabla' c$ can be equivalently written as $(\nabla')^2 v \cdot c$ (the reduced Hessian of u).

1.2.5. *von Kármán like ($\beta > 3$; Friesecke-James-Müller).* First we remark that, when $\beta > 3$, then (1.7) implies that $\bar{R}$ is a constant. Then, because of frame indifference, we may as well assume that $\bar{R} = Id$. The argument for deriving a Γ-liminf roughly follow those expounded in the previous subsection, but with β-dependent scalings; for example the quantity G^ε in (1.11) is now

$$G^\varepsilon := \varepsilon^{\frac{1-\beta}{2}}((R^\varepsilon)^T \nabla^\varepsilon u^\varepsilon - Id).$$

We refer the interested reader to [92, Theorems 2,3] and only detail somewhat the result in the true von Kármán case, that is that when $\beta = 5$.

In the setting of Subsection 1.2.2, we define

$$y^\varepsilon := (\bar{R}^\varepsilon)^T u^\varepsilon - c^\varepsilon,$$

where $\bar{R}^\varepsilon$ is a constant ε-dependent rotation obtained from R^ε defined in (1.6) and c^ε is a suitable constant so that $\int_\Omega (y^\varepsilon - (x', \varepsilon x_3))\ dx = 0$ (see [92, Lemma 1] for details). We further define the averaged in-plane and out-of-plane displacements

$$\begin{cases} h^\varepsilon_{1,2} := 1/\varepsilon^2 \displaystyle\int_{-1/2}^{1/2} (y^\varepsilon_{1,2} - x_{1,2})\ dx_3, \\ v^\varepsilon := 1/\varepsilon \displaystyle\int_{-1/2}^{1/2} y^\varepsilon_3\ dx_3. \end{cases} \tag{1.16}$$

Then it is easily obtained that

$$\begin{cases} h^\varepsilon \overset{W^{1,2}(\omega;\mathbb{R}^2)}{\longrightarrow} h, \\ v^\varepsilon \overset{W^{1,2}(\omega)}{\longrightarrow} v. \end{cases} \tag{1.17}$$

The Γ-convergence theorem is as follows:

THEOREM 1.8. Under assumption (1.1)

- For a subsequence (still indexed by ε), if u^ε satisfies (1.4), then $\{h^\varepsilon\}, \{v^\varepsilon\}$ constructed through (1.16) from u^ε satisfy convergences (1.17);
- $\mathcal{E}^\varepsilon/\varepsilon^4$ Γ-converges (for the topology associated with the convergences (1.17)) to

$$\mathcal{E}_{vk}(h, v) := 1/2 \int_\omega Q_2(1/2[\nabla' h + (\nabla' h)^T] + \nabla' v \otimes \nabla' v)\ dx' + 1/24 \int_\omega Q_2((\nabla')^2 v)\ dx,$$

  where Q_2 was defined in (1.13).

The von Kármán model has always been contentious. While widely used by engineers, it has been criticized by many famous scientists, not least among them Clifford Truesdell.[2] At worst the above theorem demonstrates that such a model is compatible with the variational view of nonlinear elasticity under appropriate rescaling.

REMARK 1.9. For $3 < \beta < 5$, the obtained regime sits between the nonlinear bending and the von Kármán regimes, while for $\beta > 5$ we recover in the limit the setting of linear Kirchhoff-Love plate theory which can also be obtained through 3d to 2d dimensional reduction starting from linear elasticity as first established in [46].

[2] "An analyst may regard that theory as handed down by some higher power (a Hungarian wizard, say) and study it as a matter of pure analysis. To do so for the von Kármán theory is particularly tempting because nobody can make sense out of the "derivations". " [208, Page 601].

1.3. *Boundary conditions, forces and other considerations.* From a mathematical standpoint, the regime $\beta = 1$ distinguishes itself from all others on two grounds. On the one hand, as already explained, it does not allow for energies satisfying (1.1). But, on the other hand, it gives rise to a model which is local in the sense that the Γ-limit can be localized to any open subdomain A of ω and remains the same (just replace Ω by $A \times (-1/2, 1/2)$ in the definition of $\mathcal{E}^\varepsilon$). This is so because, as a function of A, the integration domain in the plane, that Γ-limit is a measure, as can be established through what is sometimes called the fundamental estimate (see e.g. [31, Chapter 11]). In particular, that estimate implies that the obtained membrane model (or, equivalently the Γ-limit) is impervious to the kind of boundary conditions that are imposed on the converging sequences. As such, it is a *bona fide* constitutive model for thin plates.

Not so for the other regimes where the Γ-convergence process cannot be localized, and where the only kind of boundary conditions that can be imposed are enslaved by the limit kinematics. For example, in the nonlinear bending regime ($\beta = 3$), those must be of the form

$$u^\varepsilon_{\lfloor \partial\omega \times (-1/2,1/2)} = \hat{u}(x') + x_3 \varepsilon \hat{b}(x')$$

where $\hat{u} \in W^{2,2}(\omega; \mathbb{R}^3)$ is such that $(\nabla' \hat{u}, \hat{b}) \in SO(3)$ a.e. in Ω.

If, however, the domain is laterally clamped ($u^\varepsilon_{\lfloor \partial\omega \times (-1/2,1/2)} = 0$), the resulting model (called Föppl-von Kármán) is completely different for all scalings $1 < \beta < 5$ as demonstrated in [53].

For this reason, one could possibly wonder whether the obtained Γ-limits are truly constitutive models, and not only classes of asymptotic solutions to specific boundary value problems.

In this respect, a related issue is that of forces. Indeed, in most works on dimensional reduction, the relevant scaling, which cannot, as we just saw, be connected to the boundary conditions except in the membrane regime, is dictated by the scaling of the forces; this is, for example, the adopted classification in [92]. Now, the volume forces that allow such a hierarchy generate an additional contribution to the energy in the unscaled domain of the form

$$-\int_{\Omega^\varepsilon} f^\varepsilon \cdot V \, dx, \tag{1.18}$$

the relevant scaling becoming dependent on how f^ε varies with ε. Those kinds of forces are referred to as dead forces. However, a contribution to the potential energy of the form (1.18) is rather useless when contemplating an equilibrium problem in finite elasticity. As a matter of fact, from an engineering standpoint, the only dead force is gravity, hardly an ε-dependent load! All other applied forces, be they the representation of volume or surface loads, are active forces and generate a contribution to the potential energy that includes non linear terms involving the gradient of the deformation. For example, an hydrostatic pressure p applied to the boundary of the domain generates an additional contribution of the form

$$p \int_{\Omega^\varepsilon} \det \nabla V \, dx,$$

a term which is of the same order of nonlinearity as the elastic energy itself.

Furthermore, as already alluded to in the introduction, if confronted with a boundary value problem for a thin domain of thickness ε and a set of boundary conditions and loads, how is one to decide what the appropriate ε-scaling is for such loads (and boundary conditions). This conundrum would be resolved if one could somehow establish quantitative error estimates for, e.g., $u^\varepsilon - u$, u^ε being a minimizer for the ε-rescaled problem. Unfortunately, no such results are available.

2. Fracture versus delamination of thin films (by J.F. Babadjian).

2.1. *Introduction.*

2.1.1. *Motivation.* Thin films can essentially experience two different fracture modes: either transverse cracks which split the body into several pieces, or planar cracks leading to debonding effects and delaminated surfaces. These phenomena can be observed in real life as, e.g. the stickers identifying research labs at the Ecole Polytechnique in Palaiseau, France, which was the starting place of this project. A thin vinyl sticker is bonded to a metal panel and exposed to atmospheric conditions. Among others, the variation of temperature generates inelastic mismatch strains leading to transverse cracking and possibly debonding. A few panels relative to numbers in the range "401"–"408", all of the same material and subject to similar loading conditions, show recurring crack patterns.

FIG. 2. Cracked lettering at Ecole Polytechnique, Palaiseau, France

Many works have attempted to explain these types of phenomena from mechanical, mathematical or numerical points of view. A comprehensive review of common fracture patterns may be found in [162, 215].

From a mathematical standpoint, static fractures in (nonlinearly elastic) thin films have been investigated by means of a Γ-convergence analysis that allows the identification of an effective reduced 2D model (see [30, 26, 13]). In [12] a quasi-static evolution model of cracks in thin films is studied, proving the convergence of the full three-dimensional evolution to the reduced two-dimensional one (see also [89] in the case of linear elasticity with topological restrictions on the admissible cracks). The dimension reduction of a bilayer thin film allowing for debonding at the interface has been investigated in [22], debonding being penalized by a phenomenological interfacial energy paying for the jump

of the deformation at the interface. The limit models are discussed according to the weight of interfacial energy. Rigorous derivations of decohesion-type energies have been given in [9, 10] by means of a homogenization procedure. In these works the interfacial energy appears as the limit of a Neumann sieve, debonding being regarded as the effect of the interaction of two thin films through a suitably periodically distributed contact zone.

More recently, [56, 161, 87] have also derived similar cohesive fracture models by means of a phase field Ambrosio-Tortorelli approximation involving an internal damage variable. Finally, several works have focused on the quasi-static evolution of debonding problems with a prescribed debonding zone. In particular, [194] modeled the debonding phenomenon through an internal variable representing the volume fraction of adhesive contact between the layers. However, none of these works is able to rigorously justify the models used by the engineering fracture mechanics community to model the cracks of thin film/substrate systems [162].

In [163], a two-dimensional model of a thin film bonded on a thin substrate has been introduced and studied. In this model, transverse cracks Γ and debonded regions Δ are respectively 1-dimensional and 2-dimensional subsets of a given reference configuration $\omega \subset \mathbb{R}^2$. The kinematic unknown is the planar displacement $u : \omega \to \mathbb{R}^2$ and its associated elastic strain is given by the symmetric part of its gradient $e(u) = (\nabla u + \nabla u^T)/2$. For external loadings given by an inelastic deformation in the film $e_0 : \omega \to \mathbb{M}^{2\times 2}_{\rm sym}$ (the set of 2×2 symmetric matrices) and a prescribed displacement $u_0 : \omega \to \mathbb{R}^2$ in the substrate, the total energy associated to the triple (Γ, Δ, u) is given by

$$\mathcal{E}(\Gamma, \Delta, u) := \mathcal{P}(\Gamma, \Delta, u) + \mathcal{S}(\Gamma, \Delta),$$

where

$$\mathcal{P}(\Gamma, \Delta, u) := \frac{1}{2} \int_{\omega \setminus \Gamma} \mathbf{A}(e(u) - e_0) : (e(u) - e_0)\, dx + \frac{1}{2} \int_{\omega \setminus \Delta} K(u - u_0) \cdot (u - u_0)\, dx$$

is the potential energy, and

$$\mathcal{S}(\Gamma, \Delta) = \mathcal{H}^1(\Gamma) + \mathcal{L}^2(\Delta)$$

is the fracture energy of transverse cracks Γ and delaminated surfaces Δ. In the previous expressions, the elastic term is interpreted as the energy of a brittle membrane subject to inelastic strains e_0 lying on a brittle elastic foundation of stiffness K, whereas in the surface term, transverse cracks Γ and debonded regions Δ are penalized by a Griffith-type surface energy proportional to their length (through the 1-dimensional Hausdorff measure $\mathcal{H}^1$) and area (through the 2-dimensional Lebesgue measure $\mathcal{L}^2$), respectively. The contribution of the elastic foundation is extended only to the bonded portion of the film $\omega \setminus \Delta$.

The object of this note is to show that it is possible to rigorously derive the previous phenomenological model introduced in [163], starting from three-dimensional brittle fracture in the context of linear elasticity, by letting the thickness of the film tend to zero. It corresponds to joint works in collaboration with Blaise Bourdin, Duvan Henao, Andres Leon Baldelli and Corrado Maurini (see [164, 15]).

2.1.2. *Description of the problem.* Let us consider a system

$$\Omega^\varepsilon = \Omega_f^\varepsilon \cup \Omega_b^\varepsilon \cup \Omega_s^\varepsilon$$

made of a thin film $\Omega_f^\varepsilon = \omega \times (0, \varepsilon)$ ($\omega \subset \mathbb{R}^2$ is a smooth bounded open set) deposited on an infinite substrate $\Omega_s^\varepsilon = \omega \times (-\infty, -\varepsilon)$ through a bonding layer $\Omega_b^\varepsilon = \omega \times [-\varepsilon, 0]$. We assume that Ω^ε stands for the reference configuration of an isotropic linearly elastic body allowing for cracks. This body is subjected to two types of planar loadings:

- a prescribed (smooth) planar displacement $u_0 : \omega \to \mathbb{R}^2$ in the substrate (identified with a function $u_0 : \Omega_s^\varepsilon \to \mathbb{R}^3$ with zero last component);
- a (smooth) inelastic strain $e_0 = \omega \to \mathbb{M}^{2\times 2}_{\rm sym}$ (identified with a function $e_0 : \Omega_f^\varepsilon \cup \Omega_b^\varepsilon \to \mathbb{M}^{3\times 3}_{\rm sym}$ with zero entries on the third row and the third column).

According to the variational approach to fracture (see [102, 88, 28]), for a given crack $\Gamma \subset \overline{\Omega}^\varepsilon$ of finite area and a given displacement $v : \Omega^\varepsilon \setminus \Gamma \to \mathbb{R}^3$ satisfying $v = u_0$ in Ω_s^ε, we define the Griffith energy as the sum of the elastic energy (computed outside the crack) and the surface energy (penalizing the presence of cracks) by

$$(v, \Gamma) \mapsto \frac{1}{2} \int_{\Omega^\varepsilon \setminus \Gamma} \mathbf{A}^\varepsilon (e(v) - e_0) : (e(v) - e_0)\, dx + \int_\Gamma \kappa^\varepsilon \, d\mathcal{H}^2.$$

In the previous expression, $\mathbf{A}^\varepsilon$ stands for Hooke's law and κ^ε is the toughness, which are ε-dependent material parameters possibly depending on the spatial variable. The notation $\mathcal{H}^k$ stands for the k-dimensional Hausdorff measure which coincides with the usual notion of surface (for $k = 2$) or length (for $k = 1$) for smooth enough geometrical objects.

Of course, the dependence of $\mathbf{A}^\varepsilon$ and κ^ε on ε can lead to many different limit theories. In this work, we focus on the following scaling

$$\mathbf{A}^\varepsilon = \mathbf{A}_f \mathbf{1}_{\Omega_f^\varepsilon} + \varepsilon^2 \mathbf{A}_b \mathbf{1}_{\Omega_b^\varepsilon}, \quad \kappa^\varepsilon = \kappa_f \mathbf{1}_{\Omega_f^\varepsilon} + \varepsilon \kappa_b \mathbf{1}_{\Omega_b^\varepsilon},$$

where $\mathbf{A}_f$ and $\mathbf{A}_b$ are the (isotropic) Hooke's law of the film and the bonding layer, respectively, and $\kappa_f > 0$, $\kappa_b > 0$ are the toughnesses of the film and the bonding layer, respectively.

The first difficulty is to define a convenient mathematical framework. Since the displacement v might jump across the crack Γ and following the seminal idea of the Italian school of De Giorgi for free discontinuity problems, we can identify Γ to the jump set of v. The previous energy turns out to be well defined in the space $SBD^2(\Omega^\varepsilon)$ of special functions of bounded deformation, i.e. integrable vector fields v such that the distributional symmetric gradient $Ev = (Dv + Dv^T)/2$ is a bounded $\mathbb{M}^{3\times 3}_{\rm sym}$-valued measure of the form

$$Ev = e(v)\mathcal{L}^3 + (v^+ - v^-) \odot \nu_v \mathcal{H}^2 \llcorner J_v$$

(see [206, 203, 8, 14]). In the previous expression, $e(v) \in L^2(\Omega^\varepsilon; \mathbb{M}^{3\times 3}_{\rm sym})$ is the absolutely continuous part of Ev with respect to the Lebesgue measure $\mathcal{L}^3$. The jump set J_v is a countably $\mathcal{H}^2$-rectifiable set with $\mathcal{H}^2(J_v) < \infty$, on which it is possible to define a generalized unit normal ν_v and one-sided traces $v^\pm$ according to this orientation.

In this context, we define the energy $J(\varepsilon) : SBD^2(\Omega^\varepsilon) \to \mathbb{R}^+$ by

$$\begin{aligned} J(\varepsilon)(v) &= \frac{1}{2}\int_{\Omega^\varepsilon\setminus J_v} \mathbf{A}^\varepsilon(e(v)-e_0) : (e(v)-e_0)\,dx + \int_{J_v}\kappa^\varepsilon\,d\mathcal{H}^2 \\ &= \frac{1}{2}\int_{\Omega_f^\varepsilon\setminus J_v} \mathbf{A}_f(e(v)-e_0) : (e(v)-e_0)\,dx + \kappa_f\mathcal{H}^2(J_v\cap\Omega_f^\varepsilon) \\ &\quad + \frac{\varepsilon^2}{2}\int_{\Omega_b^\varepsilon\setminus J_v} \mathbf{A}_b(e(v)-e_0) : (e(v)-e_0)\,dx + \varepsilon\kappa_b\mathcal{H}^2(J_v\cap\Omega_b^\varepsilon). \end{aligned}$$

Note that there is no energetic contribution of the substrate since the displacement is prescribed and smooth in there. However, cracks are allowed to touch the interface $\{x_3 = -\varepsilon\}$ between the bonding layer and the substrate.

Our objective is to understand the asymptotic behavior of the previous energy functional as $\varepsilon \to 0$ in the sense of Γ-convergence which will give information on the asymptotic behavior of minimizers and the minimal value of $J(\varepsilon)$.

REMARK 2.1. In order to simplify the presentation, we will henceforth assume that $e_0 = 0$ and $u_0 = 0$.

2.1.3. *Rescaling.* As usual in dimension reduction problems, we reformulate the problem on a fixed domain independent of ε. Contrary to nonlinear elasticity where one only rescales the variable, we rescale here both the variables and the components of the displacement, as commonly done in linear elasticity (see [45]).

To this aim, we set $\Omega = \Omega^1$, $\Omega_f = \Omega_f^1$, $\Omega_b = \Omega_b^1$ and $\Omega_s = \Omega_s^1$. For $x = (x_1, x_2, x_3) = (x', x_3) \in \Omega$, with $x' = (x_1, x_2)$, we define for $\alpha = 1, 2$,

$$u_\alpha(x', x_3) = v_\alpha(x', \varepsilon x_3), \quad u_3(x', x_3) = \varepsilon v_3(x', \varepsilon x_3).$$

Then, for all $u \in SBD^2(\Omega)$ with $u = 0$ in Ω_s (recall Remark 2.1), we define

$$J_\varepsilon(u) = \varepsilon^{-1}J(\varepsilon)(v) = J_\varepsilon^f(u) + J_\varepsilon^b(u),$$

where

$$\begin{aligned} J_\varepsilon^f(u) &:= \frac{1}{2}\int_{\Omega_f\setminus J_u} \mathbf{A}_f e^\varepsilon(u) : e^\varepsilon(u)\,dx + \kappa_f\int_{J_u\cap\Omega_f} \left|\left((\nu_u)', \varepsilon^{-1}(\nu_u)_3\right)\right| d\mathcal{H}^2, \\ J_\varepsilon^b(u) &:= \frac{\varepsilon^2}{2}\int_{\Omega_b\setminus J_u} \mathbf{A}_b e^\varepsilon(u) : e^\varepsilon(u)\,dx + \kappa_b\varepsilon\int_{J_u\cap\Omega_b} \left|\left((\nu_u)', \varepsilon^{-1}(\nu_u)_3\right)\right| d\mathcal{H}^2, \end{aligned}$$

and

$$e^\varepsilon(u) := \begin{pmatrix} e_{11}(u) & e_{12}(u) & \varepsilon^{-1}e_{13}(u) \\ e_{12}(u) & e_{22}(u) & \varepsilon^{-1}e_{23}(u) \\ \varepsilon^{-1}e_{13}(u) & \varepsilon^{-1}e_{23}(u) & \varepsilon^{-2}e_{33}(u) \end{pmatrix}$$

is the rescaled elastic strain.

2.2. *Dimension reduction in linear elasticity.* In this first part, we focus on the energy in the thin film in the absence of cracks. The problem can be straightforwardly formulated in the framework of Sobolev space owing to Korn's inequality: for $u \in H^1(\Omega_f; \mathbb{R}^3)$, we only consider the elastic energy

$$J_\varepsilon^f(u) = \frac{1}{2}\int_{\Omega_f} \mathbf{A}_f e^\varepsilon(u) : e^\varepsilon(u)\,dx.$$

Denoting by λ_f and μ_f the Lamé coefficients of the film (which satisfy the usual ellipticity conditions $\mu_f > 0$ and $3\lambda_f + 2\mu_f > 0$) and recalling the isotropy hypothesis, the previous energy can be expressed as

$$\begin{aligned} J^f_\varepsilon(u) \quad := \quad & \int_{\Omega_f} \Big[\frac{\lambda_f}{2} e_{\alpha\alpha}(u) e_{\beta\beta}(u) + \mu_f e_{\alpha\beta}(u) e_{\alpha\beta}(u) \Big] \, dx \\ & + \varepsilon^{-2} \int_{\Omega_f} \Big[\lambda_f e_{\alpha\alpha}(u) e_{33}(u) + 2\mu_f e_{\alpha 3}(u) e_{\alpha 3}(u) \Big] \, dx \\ & + \varepsilon^{-4} \int_{\Omega_f} \frac{\lambda_f + 2\mu_f}{2} e_{33}(u) e_{33}(u) \, dx, \end{aligned}$$

where, from now on, we use Einstein's summation convention over repeating indexes. The diverging coefficients in front of both last integrals imply that if $u_\varepsilon \in H^1(\Omega_f; \mathbb{R}^3)$ is such that $u_\varepsilon \to u$ in $L^2(\Omega_f; \mathbb{R}^3)$ and $J^f_\varepsilon(u_\varepsilon) \leq C$, the limit admissible displacement u must satisfy $e_{i3}(u) = 0$ for $i = 1, 2, 3$, which means that

$$u_3(x', x_3) = \bar{u}_3(x'), \quad u_\alpha(x', x_3) = \bar{u}_\alpha(x') + \left(\frac{1}{2} - x_3 \right) \partial_\alpha \bar{u}_3(x') \quad \text{for } \alpha = 1, 2.$$

Such displacements are called Kirchhoff-Love displacements and the space of all Kirchhoff-Love displacements is denoted by $KL(\Omega_f)$.

The following Γ-convergence result can be found e.g. in [29] (see also [45]).

THEOREM 2.2. The functional J^f_ε Γ-convergence in $H^1(\Omega_f; \mathbb{R}^3)$, with respect to the strong $L^2(\Omega_f; \mathbb{R}^3)$ topology, to the functional $J^f_0 : H^1(\Omega_f; \mathbb{R}^3) \to [0, \infty]$ given by

$$J^f_0(u) = \begin{cases} \displaystyle\int_{\Omega_f} \Big[\frac{\lambda_f \mu_f}{\lambda_f + 2\mu_f} e_{\alpha\alpha}(u) e_{\beta\beta}(u) + \mu_f e_{\alpha\beta}(u) e_{\alpha\beta}(u) \Big] \, dx & \text{if } u \in KL(\Omega_f), \\ \infty & \text{otherwise.} \end{cases}$$

Using the Kirchhoff-Love structure of the displacement u, the previous functional decouples into

$$\begin{aligned} J^f_0(u) \quad = \quad & \int_\omega \Big[\frac{\lambda_f \mu_f}{\lambda_f + 2\mu_f} e_{\alpha\alpha}(\bar{u}) e_{\beta\beta}(\bar{u}) + \mu_f e_{\alpha\beta}(\bar{u}) e_{\alpha\beta}(\bar{u}) \Big] \, dx' \\ & + \frac{1}{12} \int_\omega \Big[\frac{\lambda_f \mu_f}{\lambda_f + 2\mu_f} e_{\alpha\alpha}(\nabla \bar{u}_3) e_{\beta\beta}(\nabla \bar{u}_3) + \mu_f e_{\alpha\beta}(\nabla \bar{u}_3) e_{\alpha\beta}(\nabla \bar{u}_3) \Big] \, dx'. \end{aligned}$$

The first term is a membrane energy term which accounts for stretching effect, while the second one stands for a bending energy term involving higher order derivatives. From the point of view the Euler-Lagrange equation, this last term leads to the biharmonic equation of plates.

2.3. *Winkler elastic foundation.* We now enrich the previous analysis by adding the information on the bonding layer and the substrate, but still assuming the absence of cracks. In this framework, the space of all kinematically admissible displacements is given by

$$\mathcal{A} := \{ v \in H^1(\Omega; \mathbb{R}^3) : \ v = 0 \text{ in } \Omega_s \},$$

where we recall that $\Omega = \Omega_f \cup \Omega_b \cup \Omega_s$. For $u \in H^1(\Omega;\mathbb{R}^3)$, the total energy is given by

$$\widetilde{J}_\varepsilon(u) = \begin{cases} \dfrac{1}{2}\displaystyle\int_{\Omega_f} \mathbf{A}_f e^\varepsilon(u) : e^\varepsilon(u)\,dx + \dfrac{\varepsilon^2}{2}\int_{\Omega_b} \mathbf{A}_b e^\varepsilon(u) : e^\varepsilon(u)\,dx & \text{if } u \in \mathcal{A}, \\ \infty & \text{otherwise,} \end{cases}$$

or still, using the isotropy hypothesis and denoting by λ_b and μ_b the Lamé coefficients of the bonding layer (which again satisfy the ellipticity conditions $\mu_b > 0$ and $3\lambda_b + 2\mu_b > 0$), for $u \in \mathcal{A}$,

$$\begin{aligned} \widetilde{J}_\varepsilon(u) \quad := \quad & \int_{\Omega_f} \Big[\frac{\lambda_f}{2} e_{\alpha\alpha}(u) e_{\beta\beta}(u) + \mu_f e_{\alpha\beta}(u) e_{\alpha\beta}(u)\Big]\,dx \\ & + \varepsilon^{-2}\int_{\Omega_f} \Big[\lambda_f e_{\alpha\alpha}(u) e_{33}(u) + 2\mu_f e_{\alpha 3}(u) e_{\alpha 3}(u)\Big]\,dx \\ & + \varepsilon^{-4}\int_{\Omega_f} \frac{\lambda_f + 2\mu_f}{2} e_{33}(u) e_{33}(u)\,dx \\ & + \varepsilon^{2}\int_{\Omega_b} \Big[\frac{\lambda_b}{2} e_{\alpha\alpha}(u) e_{\beta\beta}(u) + \mu_b e_{\alpha\beta}(u) e_{\alpha\beta}(u)\Big]\,dx \\ & + \int_{\Omega_b} \Big[\lambda_b e_{\alpha\alpha}(u) e_{33}(u) + 2\mu_b e_{\alpha 3}(u) e_{\alpha 3}(u)\Big]\,dx \\ & + \varepsilon^{-2}\int_{\Omega_b} \frac{\lambda_b + 2\mu_b}{2} e_{33}(u) e_{33}(u)\,dx. \end{aligned}$$

According to the analysis of the previous section, if $u_\varepsilon \in \mathcal{A}$ satisfies $u_\varepsilon \to u$ in $L^2(\Omega_f;\mathbb{R}^3)$ and $\widetilde{J}_\varepsilon(u_\varepsilon) \le C$, the limit admissible displacement u must at least be of Kirchhoff-Love type. Using further the condition $u_\varepsilon = 0$ in Ω_s in the substrate as well as, from the third and last terms of the energy,

$$\int_{\Omega_f \cup \Omega_b} |\partial_3 (u_\varepsilon)_3|^2\,dx = \int_{\Omega_f \cup \Omega_b} |e_{33}(u_\varepsilon)|^2\,dx \sim \varepsilon^2,$$

we infer that u must also satisfy $u_3 = 0$. Inserting this information in the Kirchhoff-Love structure yields $u(x', x_3) = (\bar{u}(x'), 0)$ which means that u is a planar displacement. As a consequence all flexural terms appearing in J_0^f (in Theorem 2.2) cancel and there only remain the membrane terms

$$\int_\omega \Big[\frac{\lambda_f \mu_f}{\lambda_f + 2\mu_f} e_{\alpha\alpha}(\bar{u}) e_{\beta\beta}(\bar{u}) + \mu_f e_{\alpha\beta}(\bar{u}) e_{\alpha\beta}(\bar{u})\Big]\,dx'.$$

The bonding layer does not only contribute to specifying limit admissible displacements, but also to an additional energetic term which arises from the only first order term in the bonding layer,

$$2\mu_b \int_{\Omega_b} e_{\alpha 3}(u_\varepsilon) e_{\alpha 3}(u_\varepsilon)\,dx.$$

In the $\varepsilon \to 0$ limit, this term leads to a cohesive type energy of the form

$$\frac{\mu_b}{2}\int_\omega |\bar{u}|^2\,dx'$$

penalizing the mismatch between the prescribed displacement in the substrate (recall that from Remark 2.1 we assume $u_0 = 0$) and the displacement in the film.

In summary, the following Γ-convergence result holds (see [15]) corresponding to the derivation of a Winkler foundation (see [213]).

THEOREM 2.3. The functional $\widetilde{J}_\varepsilon$ Γ-convergence in $H^1(\Omega;\mathbb{R}^3)$, with respect to the strong $L^2(\Omega_f;\mathbb{R}^3)$ topology, to the functional $\widetilde{J}_0 : H^1(\Omega;\mathbb{R}^3) \to [0,\infty]$ given by

$$\widetilde{J}_0(u) = \begin{cases} \displaystyle\int_\omega \Big[\frac{\lambda_f\mu_f}{\lambda_f+2\mu_f} e_{\alpha\alpha}(\bar u)e_{\beta\beta}(\bar u) + \mu_f e_{\alpha\beta}(\bar u)e_{\alpha\beta}(\bar u)\Big]\,dx' + \frac{\mu_b}{2}\displaystyle\int_\omega |\bar u|^2\,dx' & \text{if } \begin{cases} u=(\bar u,0),\\ \bar u\in H^1(\omega;\mathbb{R}^2), \end{cases}\\ \infty & \text{otherwise.} \end{cases}$$

2.4. *Transerve cracks.* We next introduce cracks into the model. We first focus on the energy in the film Ω_f which allows for cracks, without taking care of the bonding layer and the substrate. For all $u \in SBD^2(\Omega_f)$, the (Griffith) energy is defined by

$$\begin{aligned} \widetilde{J}^f_\varepsilon(u) &= \frac{1}{2}\int_{\Omega_f\setminus J_u} \mathbf{A}_f e^\varepsilon(u) : e^\varepsilon(u)\,dx + \kappa_f \int_{J_u\cap\Omega_f} \big|\big((\nu_u)', \varepsilon^{-1}(\nu_u)_3\big)\big|\,d\mathcal{H}^2\\ &= \int_{\Omega_f\setminus J_u} \Big[\frac{\lambda_f}{2} e_{\alpha\alpha}(u)e_{\beta\beta}(u) + \mu_f e_{\alpha\beta}(u)e_{\alpha\beta}(u)\Big]\,dx\\ &\quad +\varepsilon^{-2}\int_{\Omega_f\setminus J_u} \Big[\lambda_f e_{\alpha\alpha}(u)e_{33}(u) + 2\mu_f e_{\alpha3}(u)e_{\alpha3}(u)\Big]\,dx\\ &\quad +\varepsilon^{-4}\int_{\Omega_f\setminus J_u} \frac{\lambda_f+2\mu_f}{2} e_{33}(u)e_{33}(u)\,dx + \kappa_f\int_{J_u\cap\Omega_f} \big|\big((\nu_u)', \varepsilon^{-1}(\nu_u)_3\big)\big|\,d\mathcal{H}^2. \end{aligned}$$

In order to guess what kind of limit admissible displacement one should expect, let us consider a sequence of displacements $\{u_\varepsilon\}$ in $SBD^2(\Omega_f)$ such that $\widetilde{J}^f_\varepsilon(u_\varepsilon) \le C$. Assuming further the uniform bound $\|u_\varepsilon\|_\infty \le C$, we can apply a compactness and lower semicontinuity result in SBD (see [19]) which ensures that, up to a subsquence, there exists $u \in SBD^2(\Omega_f)$ such that $u_\varepsilon \to u$ in $L^2(\Omega_f;\mathbb{R}^3)$, $e(u_\varepsilon) \rightharpoonup e(u)$ weakly in $L^2(\Omega_f;\mathbb{M}^{3\times3}_{\rm sym})$ and $\mathcal{H}^2(J_u) \le \liminf_\varepsilon \mathcal{H}^2(J_{u_\varepsilon})$. Using the energy bound, we infer that $e_{i3}(u) = 0$ in Ω_f and $(\nu_u)_3 = 0$ on J_u. These last conditions ensure that $D_3u_3 = E_{33}u = \partial_3u_3\mathcal{L}^3 + (u_3^+ - u_3^-)(\nu_u)_3\mathcal{H}^2\llcorner J_u = 0$. Unfortunately, the full displacement u might fail to be of Kirchhoff-Love type as in the case of pure elasticity (see Theorem 2.2) because

$$E_{\alpha3}u = \frac{(u_3^+ - u_3^-)(\nu_u)_\alpha}{2}\mathcal{H}^2\llcorner J_u \neq 0, \quad \alpha = 1,2.$$

However, it has been established in [15], that such displacements enjoy a Kirchhoff-Love type structure "outside the jump set" in the sense that $u_3 \in SBV^2(\omega)$, the approximate gradient of u_3, denoted by $\nabla u_3 = (\partial_1u_3, \partial_2u_3) \in SBD(\omega)$, $\bar u = \int_0^1 (u_1(\cdot,s), u_2(\cdot,s))\,ds \in SBD(\omega)$ and

$$u_\alpha(x) = \bar u_\alpha(x') + \left(\frac{1}{2} - x_3\right)\partial_\alpha u_3(x'), \quad J_u = (J_{\bar u}\cup J_{u_3}\cup J_{\nabla u_3})\times(0,1).$$

Thus, the jump set (which is assimilated to the crack) associated with an admissible limit displacement is transverse in the sense that it is invariant with respect to the vertical direction.

The following Γ-convergence result has been proved in [15].

THEOREM 2.4. Under a uniform bound assumption, the functional $\widetilde{J}^f_\varepsilon$ Γ-converges in $SBD^2(\Omega)$, with respect to the strong $L^2(\Omega_f;\mathbb{R}^3)$ topology, to the functional $\widetilde{J}_0 : SBD^2(\Omega_f) \to [0,\infty]$ defined by

$$\begin{aligned}\widetilde{J}_0(u) &= \int_{\Omega_f\setminus J_u}\Big[\frac{\lambda_f\mu_f}{\lambda_f+2\mu_f}e_{\alpha\alpha}(u)e_{\beta\beta}(u)+\mu_f e_{\alpha\beta}(u)e_{\alpha\beta}(u)\Big]\,dx+\kappa_f\mathcal{H}^2(J_u)\\ &= \int_{\omega\setminus J_{\bar u}}\Big[\frac{\lambda_f\mu_f}{\lambda_f+2\mu_f}e_{\alpha\alpha}(\bar u)e_{\beta\beta}(\bar u)+\mu_f e_{\alpha\beta}(\bar u)e_{\alpha\beta}(\bar u)\Big]\,dx'\\ &\quad+\frac{1}{12}\int_{\omega\setminus J_{\nabla u_3}}\Big[\frac{\lambda_f\mu_f}{\lambda_f+2\mu_f}e_{\alpha\alpha}(\nabla u_3)e_{\beta\beta}(\nabla u_3)+\mu_f e_{\alpha\beta}(\nabla u_3)e_{\alpha\beta}(\nabla u_3)\Big]\,dx'\\ &\quad+\kappa_f\mathcal{H}^1(J_{\bar u}\cup J_{u_3}\cup J_{\nabla u_3}),\end{aligned}$$

if

$$\begin{cases} u_3\in SBV(\omega),\quad \nabla u_3\in SBD(\omega),\\ \bar u:=\int_0^1(u_1(\cdot,x_3),u_2(\cdot,x_3))\,dx_3\in SBD(\omega),\\ u_\alpha(x)=\bar u_\alpha(x')+\Big(\frac12-x_3\Big)\partial_\alpha u_3(x')\ \text{for}\ \alpha=1,2,\\ J_u=(J_{\bar u}\cup J_{u_3}\cup J_{\nabla u_3})\times(0,1)\end{cases}$$

and $\widetilde{J}_0(u)=\infty$ otherwise.

REMARK 2.5. The uniform bound assumption means that we work inside a fixed "box", i.e. admissible displacements are required to satisfy $\|u\|_\infty\le M$ for some fixed $M>0$. This condition is necessary to apply the compactness result of [19]. Although this condition is meaningful from a mechanical point of view (we can suppose without loss of generality to work in a e.g. 1000 km neighborhood of the earth), it has no mathematical justification at present. Lately, this condition has been dropped in [4] at the expense of working in a larger and more sophisticated space called $GSBD^2(\Omega)$ introduced in [55].

2.5. *Fracture, debonding and delamination.* We now arrive to our final goal of identifying the Γ-limit of the family of functionals, defined for $u\in SBD^2(\Omega)$, by

$$\begin{aligned}J_\varepsilon(u) &:= \frac12\int_{\Omega_f\setminus J_u}\mathbf{A}_f e^\varepsilon(u):e^\varepsilon(u)\,dx+\kappa_f\int_{J_u\cap\Omega_f}\big|\big((\nu_u)',\varepsilon^{-1}(\nu_u)_3\big)\big|\,d\mathcal{H}^2,\\ &\quad+\frac{\varepsilon^2}{2}\int_{\Omega_b\setminus J_u}\mathbf{A}_b e^\varepsilon(u):e^\varepsilon(u)\,dx+\kappa_b\varepsilon\int_{J_u\cap\Omega_b}\big|\big((\nu_u)',\varepsilon^{-1}(\nu_u)_3\big)\big|\,d\mathcal{H}^2.\end{aligned}$$

Unfortunately, the understanding of the limit behavior of this functional is still an open question at present in such a generality. We thus simplify the problem by considering a scalar version of this problem where, now, $u\in SBV^2(\Omega)$ is scalar valued, and the energy associated with u is given by

$$\begin{aligned}I_\varepsilon(u) &:= \frac{\mu_f}{2}\int_{\Omega_f\setminus J_u}(|\nabla' u|^2+\varepsilon^{-2}|\partial_3 u|^2)\,dx+\kappa_f\int_{J_u\cap\Omega_f}\big|\big((\nu_u)',\varepsilon^{-1}(\nu_u)_3\big)\big|\,d\mathcal{H}^2,\\ &\quad+\frac{\mu_b}{2}\int_{\Omega_b\setminus J_u}(\varepsilon^2|\nabla' u|^2+|\partial_3 u|^2)\,dx+\kappa_b\int_{J_u\cap\Omega_b}|(\varepsilon(\nu_u)',(\nu_u)_3)|\,d\mathcal{H}^2.\end{aligned}$$

The scalar nature of this new problem makes the analysis more tractable and we are able to identify the Γ-limit of the family $\{I_\varepsilon\}$. This is the object of the following result which has been proved in [164].

THEOREM 2.6. The functional I_ε Γ-converges in $SBV^2(\Omega)$, with respect to the strong $L^2(\Omega_f)$ topology, to the functional $I_0 : SBV^2(\Omega_f) \to [0,\infty]$ defined by

$$I_0(u) = \begin{cases} \dfrac{\mu_f}{2}\displaystyle\int_{\omega\setminus J_u} |\nabla' u|^2\,dx + \kappa_f \mathcal{H}^1(J_u) + \dfrac{\mu_b}{2}\int_{\omega\setminus\Delta_u} |u|^2\,dx' + \kappa_b\mathcal{L}^2(\Delta_u) & \text{if } u \in SBV^2(\omega), \\ \infty & \text{otherwise,} \end{cases}$$

where $\Delta_u := \{|u| > \sqrt{2\kappa_b/\mu_b}\}$ is the delamination set.

As expected, this result shows the interplay between transverse cracks characterized by the jump set J_u (which is still invariant with respect to the vertical direction) and delamination surfaces corresponding to the set Δ_u. There is a threshold criterion stipulating that, as long as the displacement is small (less than the material constant $\sqrt{2\kappa_b/\mu_b}$), it is energetically favorable to pay a cohesive energy penalizing the mismatch between the prescribed displacement in the substrate and the displacement in the film, while if the displacement overpasses this threshold, it is preferable to create a discontinuity surface leading a delamination zone.

The generalization of this result to the full vectorial case is still not entirely understood. However, we expect the following result to be true.

CONJECTURE 2.1. Under a uniform bound assumption, the functional J_ε Γ-converges in $SBD^2(\Omega)$, with respect to the strong $L^2(\Omega_f;\mathbb{R}^3)$ topology, to the functional $J_0 : SBD^2(\Omega_f) \to [0,\infty]$ defined by

$$\begin{aligned} J_0(u) \;=\; & \int_{\omega\setminus J_{\bar u}} \Big[\frac{\lambda_f\mu_f}{\lambda_f+2\mu_f} e_{\alpha\alpha}(\bar u)e_{\beta\beta}(\bar u) + \mu_f e_{\alpha\beta}(\bar u)e_{\alpha\beta}(\bar u)\Big]\,dx' \\ & + \frac{1}{12}\int_{\omega\setminus J_{\nabla u_3}} \Big[\frac{\lambda_f\mu_f}{\lambda_f+2\mu_f} e_{\alpha\alpha}(\nabla u_3)e_{\beta\beta}(\nabla u_3) + \mu_f e_{\alpha\beta}(\nabla u_3)e_{\alpha\beta}(\nabla u_3)\Big]\,dx' \\ & + \kappa_f\mathcal{H}^1(J_{\bar u}\cup J_{u_3}\cup J_{\nabla u_3}) + \frac{\mu_b}{2}\int_{\omega\setminus\Delta_u} |\bar u|^2\,dx' + \kappa_b\mathcal{L}^2(\Delta_u), \end{aligned}$$

if

$$\begin{cases} u_3 \in SBV(\omega), \quad \nabla u_3 \in SBD(\omega), \\ \bar u := \int_0^1 (u_1(\cdot,x_3), u_2(\cdot,x_3))\,dx_3 \in SBD(\omega), \\ u_\alpha(x) = \bar u_\alpha(x') + \Big(\frac{1}{2} - x_3\Big)\partial_\alpha u_3(x'), \\ J_u = (J_{\bar u}\cup J_{u_3}\cup J_{\nabla u_3})\times(0,1), \\ \Delta_u := \{|\bar u| > \sqrt{2\kappa_b/\mu_b}\}\cup\{u_3 \neq 0\}, \end{cases}$$

and $J_0(u) = \infty$ otherwise.

Right now, this conjecture is not proved. However, in [15] the validity of the upper bound is established while some insight into the proof of the lower bound is provided.

3. Geometry and morphogenesis of thin films (by Marta Lewicka). In this section, we present the author's choice of topics and results motivated by the mathematical study of curvature-driven morphogenesis. For brevity, we only include state-of-the-art analytical results concerning the dimension reduction for prestrained materials, while we refer the reader to [141] for a larger scope review and a list of open problems which are ripe for exploration through methods of Differential Equations, Mathematical Analysis and Geometry.

Prestrained materials arise in science and technology from a range of causes: inhomogeneous growth, plastic deformation, swelling or shrinkage by solvent absorption. In all these situations, the resulting shape is a consequence of the heterogeneous incompatibility of strains that leads to local elastic stresses. One approach towards understanding the coupling between residual stress and the ultimate shape of the body relies on the model of non-Euclidean elasticity, introduced below.

3.1. *The set-up of non-Euclidean elasticity.* Let g be a smooth Riemannian metric, given on an open, bounded domain $\Omega \subset \mathbb{R}^3$. Since $g(x)$ is symmetric and positive definite, it possesses a unique symmetric, positive definite square root $A(x) = g(x)^{1/2}$. Define:

$$\mathcal{E}(u) = \int_\Omega W\left((\nabla u)A^{-1}\right)\,\mathrm{d}x \qquad \forall u \in H^1(\Omega, \mathbb{R}^3), \tag{3.1}$$

where the energy density $W : \mathbb{R}^{3\times 3} \to [0, \infty]$ obeys the principles of material frame invariance (with respect to the special orthogonal group $SO(3)$), normalisation, non-degeneracy, and material consistency, valid for all $F \in \mathbb{R}^{3\times 3}$, $R \in SO(3)$:

$$\begin{aligned} &W(RF) = W(F), \qquad W(Id_3) = 0, \qquad W(F) \geq c\,\mathrm{dist}^2(F, SO(3)),\\ &W(F) \to +\infty \quad \text{as } \det F \to 0+, \quad \text{and:} \quad \forall \det F \leq 0 \quad W(F) = +\infty. \end{aligned} \tag{3.2}$$

The model (3.2) postulates that the body Ω seeks to realize a configuration with a prescribed metric g by means of an orientation preserving isometric immersion $u : \Omega \to \mathbb{R}^3$:

$$(\nabla u)^T \nabla u = g \quad \text{ and } \quad \det \nabla u > 0 \quad \text{in } \omega,$$

Although any $\mathcal{G}$ always has a Lipschitz u satisfying the first condition above, one can show that any such immersion changes its orientation in any neighbourhood of a point where the Riemann curvature $[R_{ij,kl}]_{i,j,k,l=1\ldots 3}$ of $\mathcal{G}$ is not zero. Excluding such nonphysical deformations leads to the energy $\mathcal{E}$ in (3.1), that quantifies the total pointwise deviation of the deformation gradient ∇u from $\mathcal{G}^{1/2}$, modulo rotations. The infimum of $\mathcal{E}$ in absence of forces or boundary conditions is then indeed strictly positive for a non-Euclidean $\mathcal{G}$:

THEOREM 3.1. [152] If $[R_{ij,kl}] \not\equiv 0$ in Ω, then $\inf\left\{\mathcal{E}(u);\ u \in H^1(\Omega, \mathbb{R}^3)\right\} > 0$.

The above statement points to the dichotomy: either g and $\mathcal{E}$ are, by a smooth change of variable equivalent to the scenario with $g = Id_3$ and $\min \mathcal{E} = 0$, or otherwise the zero energy level cannot be achieved even in the limit of weakly regular H^1 deformations. The latter case points to existence of residual stress at free equilibria.

3.2. *Thin prestrained films.* Consider now a family $(\Omega^\varepsilon, u^\varepsilon, g, A, \mathcal{E}^\varepsilon)_{\varepsilon>0}$ (or more generally $(\Omega^\varepsilon, u^\varepsilon, g^\varepsilon, A^\varepsilon, \mathcal{E}^\varepsilon)_{\varepsilon>0}$) given in function of the thickness parameter ε in:

$$\Omega^\varepsilon = \omega \times \big(-\frac{\varepsilon}{2}, \frac{\varepsilon}{2}\big).$$

The open, bounded set $\omega \subset \mathbb{R}^2$ with Lipschitz boundary is viewed as the midplate of the thin film Ω^ε, on which we pose the energy of elastic deformations:

$$\mathcal{E}^\varepsilon(u^\varepsilon) = \frac{1}{\varepsilon}\int_{\Omega^\varepsilon} W\big((\nabla u^\varepsilon)A^{-1}\big)\,\mathrm{d}x \qquad \forall u^\varepsilon \in H^1(\Omega^\varepsilon, \mathbb{R}^3). \tag{3.3}$$

The main objective of study is now to predict the scaling of $\inf \mathcal{E}^\varepsilon$ as $\varepsilon \to 0$ and to analyze the asymptotic behaviour of minimizing deformations u^ε in relation to the curvatures of the prestrain $A = g^{1/2}$. Similarly as in Theorem 3.1 there is a connection between $\inf \mathcal{E}^\varepsilon$ and existence of isometric immersions, which is now more subtle. In the context of dimension reduction, this connection relies on the isometric immersions of the metric $g(\cdot,0)_{2\times 2}$ on ω into $\mathbb{R}^3$, corresponding to parametrised surfaces $y : \omega \to \mathbb{R}^3$ satisfying:

$$(\nabla y)^T \nabla y = g(\cdot,0)_{2\times 2} \quad \text{in } \omega \tag{3.4}$$

The following result was proved first for $g = g(x')$ in [152] and was further generalized to the abstract setting of Riemannian manifolds in [131]:

THEOREM 3.2. [23] Let $\{u^\varepsilon \in H^1(\Omega^\varepsilon, \mathbb{R}^3)\}_{\varepsilon\to 0}$ satisfy $\mathcal{E}^\varepsilon(u^\varepsilon) \le C\varepsilon^2$. Then we have:

(i) (Compactness). There exist $\{c^\varepsilon \in \mathbb{R}^3, R^\varepsilon \in SO(3)\}_{\varepsilon\to 0}$ such that the rescaled deformations $\{y^\varepsilon(x', x_3) = R^\varepsilon u^\varepsilon(x', \varepsilon x_3) - c^\varepsilon\}_{\varepsilon\to 0}$ converge up to a subsequence in $H^1(\Omega^1, \mathbb{R}^3)$, to some $y \in H^2(\Omega^1, \mathbb{R}^3)$ depending only on x' and satisfying (3.4).

(ii) (Liminf inequality). There holds the lower bound:

$$\liminf_{\varepsilon\to 0} \frac{1}{\varepsilon^2}\mathcal{E}^\varepsilon(u^\varepsilon) \ge \mathcal{I}_{2,g}(y) = \frac{1}{24}\int_\omega \mathcal{Q}_2\big(x', (\nabla y)^T\nabla\vec{b} - \frac{1}{2}\partial_3 g(\cdot,0)_{2\times 2}\big)\,\mathrm{d}x', \tag{3.5}$$

where $\mathcal{Q}_2(x', \cdot)$ are nonnegative quadratic forms derived from $D^2W(Id_3)$, and where $\vec{b}$ satisfies: $\big[\partial_1 y, \partial_2 y, \vec{b}\big] \in SO(3)g(\cdot,0)^{1/2}$. Equivalently, $\vec{b}$ is the Cosserat vector comprising the nonzero shear, in addition to $\vec{N}$ that is normal to $y(\omega)$:

$$\vec{b} = (\nabla y) g_{2\times 2}^{-1} \begin{bmatrix} g_{13} \\ g_{23} \end{bmatrix} + \frac{\sqrt{\det g}}{\sqrt{\det g_{2\times 2}}}\vec{N}, \qquad \vec{N} = \frac{\partial_1 y \times \partial_2 y}{|\partial_1 y \times \partial_2 y|}. \tag{3.6}$$

Moreover, there holds:

(iii) (Limsup inequality). If $y \in H^2(\omega, \mathbb{R}^3)$ satisfies (3.4), then convergence as in (i) holds for some $\{u^\varepsilon \in H^1(\Omega^\varepsilon, \mathbb{R}^3)\}_{\varepsilon\to 0}$ with $c_\varepsilon = 0, R^\varepsilon = Id_3$, and:

$$\lim_{\varepsilon\to 0} \frac{1}{\varepsilon^2}\mathcal{E}^\varepsilon(u^\varepsilon) = \mathcal{I}_{2,g}(y).$$

Theorem 3.2 may be restated as the following Γ-convergence:

$$\frac{1}{\varepsilon^2}\mathcal{E}^\varepsilon\big(y(x', \varepsilon x_3)\big) \xrightarrow{\Gamma} \begin{cases} \mathcal{I}_{2,g}(y) & \text{if } y \in H^2(\omega, \mathbb{R}^3) \text{ and it satisfies (3.4)} \\ +\infty & \text{otherwise,} \end{cases}$$

with respect to convergence in $H^1(\Omega^1, \mathbb{R}^3)$. Consequently, there is a one-to-one correspondence between (global) approximate minimizers of $\mathcal{E}^\varepsilon$ and (global) minimizers of $\mathcal{I}_{2,g}$, provided that $g(\cdot,0)_{2\times 2}$ has a H^2-regular isometric immersion from ω to $\mathbb{R}^3$. We remark

that, in general, one cannot expect $\mathcal{E}^\varepsilon$ to have a minimizer. The lowersemicontinuity of $\mathcal{E}$ in (3.1) is tied to the quasiconvexity of the energy density, whereas it is known that the prototypical density $F \mapsto \mathrm{dist}^2(F, SO(3))$ is not even rank-one convex [217].

From Theorem 3.2, one can also deduce a counterpart of Theorem 3.1, in the context of thin prestrain films, stating equivalence of existence of a H^2 isometric immersion of a 2-dimensional metric $\bar{g}$ in $\mathbb{R}^3$, with the energy scaling $\inf \mathcal{E}^\varepsilon \leq C\varepsilon^2$ for some smooth (equivalently, for any) metric g on Ω^1 such that $g(\cdot,0)_{2\times 2} = \bar{g}$.

3.3. *Other energy scalings.* A separate energy bound may be obtained by constructing deformations u^h through the Kirchhoff-Love extension of isometric immersions of regularity $\mathcal{C}^{1,\alpha}$. Existence of such is guaranteed by techniques of convex integration [60] for all $\alpha < 1/5$, and this threshold implies the particular energy scaling bound in:

THEOREM 3.3. [141] If $\omega \subset \mathbb{R}^2$ is simply connected with $\mathcal{C}^{1,1}$-regular boundary, then:

$$\inf \mathcal{E}^\varepsilon \leq C\varepsilon^\beta \qquad \forall \beta < \frac{2}{3}.$$

Not much is known about the asymptotic behaviour of deformations with the energy scaling $\mathcal{E}^\varepsilon(u^\varepsilon) \leq C\varepsilon^\beta$ for $\beta < 2$. We refer the reader to the list of available results in [141], where we also point out the connection of the analytical results to experiments. On the other hand, in the opposite regime where $\beta > 2$, the complete information is available.

We start by observing that in view of Theorem 3.2, there holds:

$$\lim_{\varepsilon\to 0} \frac{1}{\varepsilon^2} \inf \mathcal{E}^\varepsilon = 0$$

iff there exists $y \in H^2(\omega, \mathbb{R}^3)$ and $\vec{b}$ in (3.6), with:

$$(\nabla y)^T \nabla y = g(\cdot,0)_{2\times 2} \quad \text{ and } \quad \mathrm{sym}\big((\nabla y)^T \nabla \vec{b}\big) = \frac{1}{2}\partial_3 g(\cdot,0)_{2\times 2} \quad \text{ in } \omega. \tag{3.7}$$

The above compatibility of tensors $g(\cdot,0)_{2\times 2}$ and $\partial_3 g(\cdot,0)_{2\times 2}$ is proved in [155, 23, 140] to be equivalent to the satisfaction of the Gauss-Codazzi-Mainardi equations for the first and second fundamental forms: $I = (\nabla y)^T \nabla y$, $II = (\nabla y)^T \nabla \vec{N} = \sqrt{g^{33}}\big(\mathrm{sym}((\nabla y)^T \nabla \vec{b}) - \frac{1}{2}\partial_3 g(\cdot,0)_{2\times 2}\big) - \frac{1}{\sqrt{g^{33}}}\big[\Gamma^3_{ij}(\cdot,0)\big]_{i,j=1\ldots 2}$. These turn out to be precisely expressed by:

$$R_{12,12}(\cdot,0) = R_{12,13}(\cdot,0) = R_{12,23}(\cdot,0) = 0 \quad \text{ in } \omega. \tag{3.8}$$

Moreover, if (3.8) holds, then $\mathrm{Ker}\, \mathcal{I}_{2,g} = \big\{Ry_0 + c;\ R \in SO(3),\ c \in \mathbb{R}^3\big\}$ where $y_0 : \bar{\omega} \to \mathbb{R}^3$ is the unique "compatible" smooth isometric immersion satisfying (3.7) together with its corresponding Cosserat vector $\vec{b} = \vec{b}_1$. Further, by a direct construction: $\inf \mathcal{E}^\varepsilon \leq C\varepsilon^4$.

These statements may be generalized beyond $\beta = 4$: the only viable scalings of $\inf \mathcal{E}^\varepsilon \sim \varepsilon^\beta$ in the regime $\beta \geq 2$ are the even powers $\beta = 2n$. Namely, we have:

THEOREM 3.4. [139] For every $n \geq 2$, if $\lim_{\varepsilon\to 0} \frac{1}{\varepsilon^{2n}} \inf \mathcal{E}^\varepsilon = 0$ then $\inf \mathcal{E}^\varepsilon \leq C\varepsilon^{2(n+1)}$. Moreover, the following three statements are equivalent:

(i) $\inf \mathcal{E}^\varepsilon \leq C\varepsilon^{2(n+1)}$.

(ii) $R_{12,12}(\cdot,0) = R_{12,13}(\cdot,0) = R_{12,23}(\cdot,0) = 0$ and $\partial_3^{(k)} R_{i3,j3}(\cdot,0) = 0$ in ω, for all $k = 0 \ldots n-2$ and all $i, j = 1 \ldots 2$.

(iii) There exist smooth fields $y_0, \{\vec{b}_k\}_{k=1}^{n+1} : \bar{\omega} \to \mathbb{R}^3$, frames $B_0 = \big[\partial_1 y_0,\ \partial_2 y_0,\ \vec{b}_1\big]$, $\big\{B_k = \big[\partial_1 \vec{b}_k,\ \partial_2 \vec{b}_k,\ \vec{b}_{k+1}\big]\big\}_{k=1}^{n} : \bar{\omega} \to \mathbb{R}^{3\times 3}$, such that: $\displaystyle\sum_{k=0}^{m} \binom{m}{k} B_k^T B_{m-k} - \partial_3^{(m)} g(\cdot,0) = 0$ for all $m = 0 \dots n$.

Equivalently: $\Big(\displaystyle\sum_{k=0}^{n} \frac{x_3^k}{k!} B_k\Big)^T \Big(\sum_{k=0}^{n} \frac{x_3^k}{k!} B_k\Big) = g(x', x_3) + \mathcal{O}(\varepsilon^{n+1})$ on Ω^ε as $\varepsilon \to 0$.

The field y_0 is the unique smooth isometric immersion of $g(\cdot,0)_{2\times 2}$ into $\mathbb{R}^3$ for which $\mathcal{I}_{2,g}(y_0) = 0$.

We note that if $R(\cdot,0) = 0$ and $\partial_3^{(m)}\big[R_{i3,j3}(\cdot,0)\big]_{i,j=1\dots 2} = 0$ on ω for all $m = 0 \dots n-2$, but $\partial_3^{(n-1)}\big[R_{i3,j3}(\cdot,0)\big]_{i,j=1\dots 2} \neq 0$, then: $c\varepsilon^{2(n+1)} \leq \inf \mathcal{E}^\varepsilon \leq C\varepsilon^{2(n+1)}$ for some $c, C > 0$. The conformal metrics $g(x', x_3) = e^{2\phi(x_3)} Id_3$ provide a class of examples for the viability of all scalings: $\inf \mathcal{E}^\varepsilon \sim \varepsilon^{2n}$ by choosing $\phi^{(k)}(0) = 0$ for $k = 1 \dots n-1$ and $\phi^{(n)}(0) \neq 0$.

A crucial ingredient in proving compactness of sequences of deformations that satisfy an energy bound in Theorem 3.4 (i), is the following approximation result:

THEOREM 3.5. [139, 155] Assume any of the equivalent conditions in Theorem 3.4, for some $n \geq 1$. Then, given $\{u^\varepsilon \in H^1(\Omega^\varepsilon, \mathbb{R}^3)\}_{\varepsilon\to 0}$ such that $\mathcal{E}^\varepsilon(u^\varepsilon) \leq C\varepsilon^{2(n+1)}$, there exists $\{R^\varepsilon \in H^1(\omega, SO(3))\}_{\varepsilon\to 0}$ with:

$$\frac{1}{\varepsilon}\int_{\Omega^\varepsilon} \big|\nabla u^\varepsilon - R^\varepsilon \sum_{k=0}^{n} \frac{x_3^k}{k!} B_k\big|^2 \,\mathrm{d}x \leq C\varepsilon^{2(n+1)} \quad \text{and} \quad \int_\omega |\nabla R^\varepsilon(x')|^2 \,\mathrm{d}x' \leq C\varepsilon^{2n}.$$

When $n = 0$, the above bounds are deduced from the celebrated geometric rigidity estimate in [91], which is the nonlinear version of Korn's inequality. Dependence of the optimal constants in these inequalities on the various geometric features of the domains where they are posed, has been addressed for example in [149, 150, 106, 216].

3.4. *The infinite hierarchy of* Γ*-limits.* To derive a counterpart of Theorem 3.2 for higher energy scalings, one observes the following compactness properties under the assumption $\mathcal{E}^\varepsilon(u^\varepsilon) \leq C\varepsilon^{2(n+1)}$. First [139], there exist $\{c^\varepsilon \in \mathbb{R}^3, R^\varepsilon \in SO(3)\}_{\varepsilon\to 0}$ with:

$$V^\varepsilon(x') = \frac{1}{\varepsilon^n} \fint_{-\varepsilon/2}^{\varepsilon/2} (\bar{R}^\varepsilon)^T \big(u^\varepsilon(x', x_3) - c^\varepsilon\big) - \Big(y_0(x') + \sum_{k=1}^{n} \frac{x_3^k}{k!} \vec{b}_k(x')\Big) \,\mathrm{d}x_3$$

converging as $\varepsilon \to 0$ in $H^1(\omega, \mathbb{R}^3)$, to a limit V that is an infinitesimal isometry:

$$V \in \mathcal{V}_{y_0} = \big\{V \in H^2(\omega, \mathbb{R}^3);\ \mathrm{sym}\big((\nabla y_0)^T \nabla V\big) = 0\big\}.$$

In particular, there exists $\vec{p} \in H^1(\omega, \mathbb{R}^3)$ with $\mathrm{sym}\big(B_0^T\big[\nabla V,\ \vec{p}\big]\big) = 0$. Second, the strains:

$$\frac{1}{\varepsilon}\mathrm{sym}\big((\nabla y_0)^T \nabla V^\varepsilon\big)$$

converge as $\varepsilon \to 0$, weakly in $L^2(\omega, \mathbb{R}^{2\times 2})$ to a limiting $\mathbb{S}$ in the finite strain space:

$$\mathbb{S} \in \mathcal{S}_{y_0} = \mathrm{closure}_{L^2}\big\{\mathrm{sym}((\nabla y_0)^T \nabla w);\ w \in H^1(\omega, \mathbb{R}^3)\big\}.$$

The space $\mathcal{S}_{y_0}$ can be identified, in particular, in the following two cases on ω simply connected. When $y_0 = id_2$, then $\mathcal{S}_{y_0} = \{\mathbb{S} \in L^2(\omega, \mathbb{R}^{2\times 2}_{sym});\ \operatorname{curl}\operatorname{curl}\mathbb{S} = 0\}$. When Gauss's curvature $\kappa((\nabla y_0)^T\nabla y_0) = \kappa\big(g(\cdot,0)_{2\times 2}\big) > 0$ in $\bar\omega$, then $\mathcal{S}_{y_0} = L^2(\omega, \mathbb{R}^{2\times 2}_{sym})$ [147].

We further have Γ-convergence with respect to the above compactness statements:

THEOREM 3.6. [140, 139] In the energy (3.3) scaling regimes in Theorem 3.4, there holds:
(i) For the von Kármán-like regime, we have for all $V \in \mathcal{V}_{y_0}$ and $\mathbb{S} \in \mathcal{S}_{y_0}$:

$$\begin{aligned}
&\frac{1}{\varepsilon^4}\mathcal{E}^\varepsilon \xrightarrow{\ \Gamma\ } \mathcal{I}_{4,g}(V,\mathbb{S}) = \\
&\frac{1}{2}\int_\omega \mathcal{Q}_2\Big(x', \underbrace{\mathbb{S}(x') + \frac{1}{2}\nabla V(x')^T\nabla V(x') + \frac{1}{24}\nabla\vec{b}_1(x')^T\nabla\vec{b}_1(x') - \frac{1}{48}\partial_{33}g(x',0)_{2\times 2}}_{\text{stretching}}\Big)\mathrm{d}x' \\
&\qquad + \frac{1}{24}\int_\omega \mathcal{Q}_2\Big(x', \underbrace{\nabla y_0(x')^T\nabla\vec{p}(x') + \nabla V(x')^T\nabla\vec{b}_1(x')}_{\text{bending}}\Big)\ \mathrm{d}x' \\
&\qquad\qquad + \frac{1}{1440}\int_\omega \mathcal{Q}_2\Big(x', \underbrace{\begin{bmatrix} R_{13,13} & R_{13,23} \\ R_{13,23} & R_{23,23}\end{bmatrix}}_{\text{curvature}}\Big)\ \mathrm{d}x'.
\end{aligned}$$

When $g = Id_3$ then $\mathcal{I}_{4,Id_3}(V,\mathbb{S})$ reduces to the classical von Kármán functional, given in terms of the out-of-plane scalar displacement v in $V = (\alpha x^\perp + \beta, v)$ for which $\vec{p} = (-\nabla v, 0)$, and the in-plane displacement w in $\mathbb{S} = \operatorname{sym}\nabla w$:

$$\mathcal{I}_4(v,w) = \frac{1}{2}\int_\omega \mathcal{Q}_2\big(\operatorname{sym}\nabla w + \frac{1}{2}\nabla v\otimes\nabla v\big)\ \mathrm{d}x' + \frac{1}{24}\int_\omega \mathcal{Q}_2(\nabla^2 v)\ \mathrm{d}x'. \tag{3.9}$$

(ii) For all $n \geq 2$ (which is the case parallel to linear elasticity), we have for all $V \in \mathcal{V}_{y_0}$:

$$\begin{aligned}
&\frac{1}{\varepsilon^{2(n+1)}}\mathcal{E}^\varepsilon \xrightarrow{\ \Gamma\ } \mathcal{I}_{2(n+1),g}(V) \\
&\quad = \frac{1}{24}\int_\omega \mathcal{Q}_2\Big(x', \underbrace{(\nabla y_0)^T\nabla\vec{p} + (\nabla V)^T\nabla\vec{b}_1 + \alpha_n\big[\partial_3^{(n-1)}R_{i3,j3}\big]_{i,j=1\ldots 2}}_{\text{bending}}\Big)\ \mathrm{d}x' \\
&\quad + \beta_n\int_\omega \mathcal{Q}_2\Big(x', \mathbb{P}_{\mathcal{S}^\perp_{y_0}}\big(\big[\partial_3^{(n-1)}R_{i3,j3}\big]_{i,j=1\ldots 2}\big)\Big)\ \mathrm{d}x' \\
&\quad + \gamma_n\int_\omega \mathcal{Q}_2\Big(x', \mathbb{P}_{\mathcal{S}_{y_0}}\big(\big[\partial_3^{(n-1)}R_{i3,j3}\big]_{i,j=1\ldots 2}\big)\Big)\ \mathrm{d}x'.
\end{aligned}$$

Above, $\mathbb{P}_{\mathcal{S}_{y_0}}$, $\mathbb{P}_{\mathcal{S}^\perp_{y_0}}$ denote orthogonal projections onto $\mathcal{S}_{y_0}$ and onto its L^2-orthogonal complement $\mathcal{S}^\perp_{y_0}$. Coefficients $\alpha_n, \beta_n, \gamma_n \geq 0$ are given explicitly and $\alpha_n \neq 0$ iff n is even. For $g = Id_3$, each $\mathcal{I}_{2(n+1),Id_3}$ reduces then to the classical linear elasticity:

$$\mathcal{I}_{2(n+1)}(v) = \frac{1}{24}\int_\omega \mathcal{Q}_2\big(\nabla^2 v\big)\ \mathrm{d}x'. \tag{3.10}$$

The functional $\mathcal{I}_{4,g}$ consists of stretching and bending (with respect to the unique isometric immersion y_0 that gives the zero energy in the prior Γ-limit (3.5)) plus a new term, which quantifies the remaining three Riemann curvatures. In the present geometric

context, the bending term $(\nabla y_0)^T\nabla\vec{p}+(\nabla V)^T\nabla\vec{b}_1$ in $\mathcal{I}_{2(n+1),g}$ is of order $\varepsilon^n x_3$ and it interacts with the curvature $\big[\partial_3^{(n-1)}R_{i3,j3}(\cdot,0)\big]_{i,j=1\dots2}$ which is of order x_3^{n+1}. The interaction occurs iff the two terms have the same parity in x_3, namely at even n. The two remaining terms measure the L^2 norm of $\big[\partial_3^{(n-1)}R_{i3,j3}(\cdot,0)\big]_{i,j=1\dots2}$, with distinct weights assigned to $\mathcal{S}_{y_0}$ and $\big(\mathcal{S}_{y_0}\big)^\perp$ projections, according to the parity of n.

COROLLARY 3.7. In the context of Theorem 3.6, there holds:

$$\inf_{\mathcal{V}_{y_0}}\mathcal{I}_{2(n+1),g}\sim\big\|\big[\partial_3^{(n-1)}R_{i3,j3}(\cdot,0)\big]_{i,j=1\dots2}\|^2_{L^2(\omega)}.$$

We gather the findings about the infinite hierarchy of limiting models in Figure 3.

β	asymptotic expansion	constraint / regularity	limiting energy $\mathcal{I}_{\beta,g}$
2	$y(x')$ $\big\{_{3d:\ y(x')+x_3\vec{b}(x')}\big\}$	$y\in W^{2,2}$ $(\nabla y)^T\nabla y=g(x',0)_{2\times2}$	$c\|(\nabla y)^T\nabla\vec{b}-\frac{1}{2}\partial_3 g(x',0)_{2\times2}\|^2_{\mathbb{Q}_2}$ $\big[\partial_3 y,\partial_2 y,\vec{b}\big]\in SO(3)g(x',0)^{1/2}$
4	$y_0(x')+\varepsilon V(x')$ $+\varepsilon^2 w^\varepsilon(x')$	$R_{12,12},R_{12,13},R_{12,23}(x',0)=0$ $\big((\nabla y_0)^T\nabla V\big)_{sym}=0,$ $\big((\nabla y_0)^T\nabla w^h\big)_{sym}\to\mathbb{S}$ $V\in W^{2,2}(\omega,\mathbb{R}),\ w^\varepsilon\in W^{1,2}(\omega,\mathbb{R}^3)$	$c_1\|\frac{1}{2}(\nabla V)^T\nabla V+\mathbb{S}+\frac{1}{24}(\nabla\vec{b}_1)^T\nabla\vec{b}_1$ $-\frac{1}{48}\partial_{33}g(x',0)_{2\times2}\|^2_{\mathbb{Q}_2}$ $+c_2\|(\nabla y_0)^T\nabla\vec{p}+(\nabla V)^T\nabla\vec{b}_1\|^2_{\mathbb{Q}_2}$ $+c_3\|\big[R_{i3,j3}(x',0)\big]_{i,j=1,2}\|^2_{\mathbb{Q}_2}$
6 $\vdots$	$y_0(x')+\varepsilon^2V(x')$	$R_{ab,cd}(x',0)=0$ $\big((\nabla y_0)^T\nabla V\big)_{sym}=0,\ V\in W^{2,2}$	$c_2\|(\nabla y_0)^T\nabla\vec{p}+(\nabla V)^T\nabla\vec{b}_1+\alpha\big[\partial_3 R\big]\|^2_{\mathbb{Q}_2}$ $+c_3\|\mathbb{P}_{\mathcal{S}_{y_0}^\perp}\big[\partial_3 R\big]\|^2_{\mathbb{Q}_2}+c_4\|\mathbb{P}_{\mathcal{S}_{y_0}}\big[\partial_3 R\big]\|^2_{\mathbb{Q}_2}$
$2n$ $\vdots$	$y_0(x')+\varepsilon^{n-1}V(x')$ $\big\{_{3d:\ y_0+\sum_{k=1}^{n-1}\frac{x_3^k}{k!}\vec{b}_k(x')}$ $+\varepsilon^{n-1}V(x')$ $+\varepsilon^{n-1}x_3\vec{p}(x')\big\}$	$R_{ab,cd}(x',0)=0$ $\big[\partial_3^{(k)}R\big](x',0)=0\ \forall k\le n-3$ $\big((\nabla y_0)^T\nabla V\big)_{sym}=0,\ V\in W^{2,2}$	$c_2\|(\nabla y_0)^T\nabla\vec{p}+(\nabla V)^T\nabla\vec{b}_1+\alpha\big[\partial_3^{(n-2)}R\big]\|^2_{\mathbb{Q}_2}$ $+c_3\|\mathbb{P}_{\mathcal{S}_{y_0}^\perp}\big[\partial_3^{(n-2)}R\big]\|^2_{\mathbb{Q}_2}$ $+c_4\|\mathbb{P}_{\mathcal{S}_{y_0}}\big[\partial_3^{(n-2)}R\big]\|^2_{\mathbb{Q}_2}$

FIG. 3. The infinite hierarchy of Γ-limits for prestrained films ($\beta\ge2$).

3.5. *The weak prestrain.* Assume now that the given prestrain $A^\varepsilon=(g^\varepsilon)^{1/2}$ on Ω^ε is incompatible only through smooth perturbations $S,B:\bar\omega\to\mathbb{R}^{3\times3}_{sym}$ of higher order in:

$$A^\varepsilon(x',x_3)=Id_3+\varepsilon^\gamma S(x')+\varepsilon^{\gamma/2}x_3B(x'). \tag{3.11}$$

The correlation of stretching and bending exponents γ, $\gamma/2$ may be relaxed [121]. In this context, the counterpart of Theorem 3.2 is as follows:

THEOREM 3.8. [151] Assume that a family deformations $\{u^\varepsilon\in H^1(\Omega^\varepsilon,\mathbb{R}^3)\}_{\varepsilon\to0}$ satisfies the energy bound: $\mathcal{E}^\varepsilon(u^\varepsilon)\le C\varepsilon^{\gamma+2}$, for some $\gamma\in(1,2)$. Then we have:

(i) (Compactness). There exist $\{R^\varepsilon\in SO(3),c^\varepsilon\in\mathbb{R}^3\}_{\varepsilon\to0}$ such that for $\{y^\varepsilon(x',x_3)=R^\varepsilon u^\varepsilon(x',\varepsilon x_3)-c^\varepsilon\}_{\varepsilon\to0}$ the following holds. First, $\{y^\varepsilon\}$ converge to x' in $H^1(\Omega^1,\mathbb{R}^3)$.

Second, the fields $\{V^\varepsilon(x') = \frac{1}{\varepsilon^{\gamma/2}} \fint_{-1/2}^{1/2} y^\varepsilon(x',t) - x' \, \mathrm{d}t\}_{h\to 0}$ converge in $H^1(\omega,\mathbb{R}^3)$, up to a subsequence, to some V of the form $V = (0,0,v)^T$, and satisfying:

$$v \in H^2(\omega,\mathbb{R}), \qquad \det \nabla^2 v = -\mathrm{curl}\,\mathrm{curl}\, S_{2\times 2}. \tag{3.12}$$

(ii) (Γ-convergence). If ω is simply connected with $\mathcal{C}^{1,1}$ boundary, then we have:

$$\frac{1}{\varepsilon^{\gamma+2}}\mathcal{E}^\varepsilon(u^h) \xrightarrow{\Gamma} \mathcal{I}_{S,B}(v) = \frac{1}{12}\int_\omega \mathcal{Q}_2\big(x', \nabla^2 v + B_{2\times 2}\big)\, \mathrm{d}x'. \tag{3.13}$$

As before, one can further deduce that the Monge-Ampére problem (3.12) has a H^2-regular solution iff $\inf \mathcal{E}^\varepsilon \le C\varepsilon^{\gamma+2}$. Moreover, $c\varepsilon^{\gamma+2} \le \inf \mathcal{E}^\varepsilon \le C\varepsilon^{\gamma+2}$ for some $c, C > 0$ is equivalent to the solvability of (3.12) and the simultaneous non-vanishing of the lowest order terms (i.e. terms of order γ and $\frac{\gamma}{2}$, respectively) in curvatures $R_{12,12}(\cdot,0)$ and $[R_{12,i3}(\cdot,0)]_{i=1,2}$. This last condition is equivalent to:

$$\mathrm{curl}\,\mathrm{curl}\, S_{2\times 2} + \det B_{2\times 2} \not\equiv 0 \quad \text{ or } \quad \mathrm{curl}\, B_{2\times 2} \not\equiv 0 \quad \text{ in } \omega.$$

We mention that a parallel analysis of the weak prestrain as in (3.11), but imposed on a shell rather than a plate Ω^ε, has been carried out in [144]. When the mid-surface curvature are of order given by a power of ε and hence compete with the order of the prestrain, the resulting Γ-limit involves a further Monge-Ampère-type constraint.

Construction of the recovery sequence in the proof of Theorem 3.8 suggests to view the Monge-Ampére equation $\det \nabla^2 v = f$ through its very weak form, well defined for all $v \in H^1_{loc}(\omega,\mathbb{R})$, in the sense of distributions:

$$\mathcal{D}et\, \nabla^2 v \doteq -\frac{1}{2}\mathrm{curl}\,\mathrm{curl}(\nabla v \otimes \nabla v) = f \qquad \text{in } \omega. \tag{3.14}$$

An application of techniques of convex integration [154, 60] assure that for any smooth $f : \bar\omega \to \mathbb{R}$ and $\alpha < \frac{1}{5}$, the set of $\mathcal{C}^{1,\alpha}(\bar\omega)$ solutions to (3.14) is dense in $\mathcal{C}^0(\bar\omega)$. One consequence of this result is that the operator $\mathcal{D}et\nabla^2$ is weakly discontinuous everywhere in $H^1(\omega)$. By an explicit construction, there follows a counterpart of Lemma 3.3:

THEOREM 3.9. [121] Assume that $\omega \subset \mathbb{R}^2$ is simply connected with $\mathcal{C}^{1,1}$ boundary. Then:

$$\inf \mathcal{E}^\varepsilon \le C\varepsilon^\beta \qquad \text{for all } \ \gamma \in \big[\frac{2}{7}, 2\big] \ \text{ and } \ \beta < \frac{5}{3}\gamma + \frac{2}{3},$$
$$\inf \mathcal{E}^\varepsilon \le C\varepsilon^\gamma \qquad \text{for all } \ \gamma \in \big(0, \frac{2}{7}\big).$$

We point out [104], that one can consider the generalization of (3.14) to problems posed on higher-dimensional domains $\omega \subset \mathbb{R}^N$, in the context of dimension reduction and isometry matching. The set $\{\mathrm{sym}\nabla w;\ H^1(\omega,\mathbb{R}^N)\}$ can be shown to coincide with the kernel of the operator $Curl^2$, where

$$Curl^2(A) = \big[Curl^2(A)_{ab,cd}\big]_{a,b,c,d=1\ldots N},$$

defined for $A \in L^2(\omega,\mathbb{R}^{N\times N})$, is given as the application of two exterior derivatives in:

$$Curl^2(A)_{ab,cd} = \big[\partial_a\partial_c A_{bd} + \partial_b\partial_d A_{ac} - \partial_a\partial_d A_{bc} - \partial_b\partial_c A_{ad}\big]_{a,b,c,d=1\ldots N}.$$

Then: $R_{ab,cd}(Id_N + \delta^2 A) = -\frac{\delta^2}{2} Curl^2(A)_{ab,cd} + o(\delta^2)$. Taking $A = \nabla v \otimes \nabla v$, one can see that a scalar displacement field v on ω can be matched by a higher order perturbation

vector field w, so that defining $\bar{\phi}^\varepsilon(x') = x' + \left(\varepsilon^2 w(x'), \varepsilon v(x')\right)^T : \omega \to \mathbb{R}^N$, the metric is matched in $(\nabla\bar{\phi})^T\nabla\bar{\phi} = Id_N + \varepsilon^2 A + \mathcal{O}(\varepsilon^4)$ iff $\left[\det(\nabla^2 v)_{ab,cd}\right]_{ab,cd} = -Curl^2(A)$.

3.6. *Classical nonlinear elasticity: case of no prestrain.* We now list results concerning the dimension reduction of thin elastic shells, where instead of the imposed prestrain, the stored energy is due to the presence of external loads. Consider a family $\{S^\varepsilon\}_{\varepsilon\to 0}$ of thin shells around an oriented 2d midsurface S with the unit normal vector $\vec{n}$:

$$S^\varepsilon = \{x + t\vec{n}(x);\ x \in S,\ -\varepsilon/2 < t < \varepsilon/2\} \subset \mathbb{R}^3$$

The elastic energy (with density W that satisfies (1.1)) of deformations and the total energy in presence of the applied force $f^\varepsilon \in L^2(S^\varepsilon, \mathbb{R}^3)$ are given, respectively, by:

$$\mathcal{E}^\varepsilon(u^\varepsilon) = \frac{1}{\varepsilon}\int_{S^\varepsilon} W(\nabla u^\varepsilon), \quad J^\varepsilon(u^\varepsilon) = \mathcal{E}^\varepsilon(u^\varepsilon) - \frac{1}{\varepsilon}\int_{S^\varepsilon} f^\varepsilon u^\varepsilon \qquad \forall u^\varepsilon \in W^{1,2}(S^\varepsilon, \mathbb{R}^3).$$

It has been shown [92] that if $\{f^\varepsilon\}_{\varepsilon\to 0}$ scale like ε^α, then $\mathcal{E}^\varepsilon(u^\varepsilon)$ at approximate minimizers u^ε of J^ε scale like ε^β, with $\beta = \alpha$ for $0 \le \alpha \le 2$ and $\beta = 2\alpha - 2$ for $\alpha > 2$. The dimension reduction question in this context consists thus of identifying the Γ-limits $\mathcal{I}_{\beta,S}$ of the rescaled energies $\{\frac{1}{\varepsilon^\beta}\mathcal{E}^\varepsilon\}_{\varepsilon\to 0}$. Contrary to the curvature-driven shape formation, there is no energy quantization and any scaling exponent $\beta > 0$ is viable.

In case of $S \subset \mathbb{R}^2$ i.e. when $\{S^\varepsilon\}_{\varepsilon\to 0}$ is a family of thin plates, such Γ-convergence was first established for $\beta = 0$ [136], and later [92] for all $\beta \ge 2$. This last regime corresponds to a rigid behavior since the limiting deformations are isometries if $\beta = 2$ (in accordance with the general result in Theorem 3.2), or infinitesimal isometries if $\beta > 2$ (see the compactness analysis in subsection 3.4). One particular case is $\beta = 4$, where the derivation yields the von Kármán theory (3.9), then $\beta > 4$ with the Γ-limit as in (3.10), and $\beta \in (2, 4)$ where the result is effectively included in Theorem 3.8. We gather these results in Figure 4, which should be compared with Figure 3.

3.7. *The infinite hierarchy of shell theories and the matching properties.* The first result for the case when S is a surface of arbitrary geometry was given in [136] as the membrane theory ($\beta = 0$) where the limit $\mathcal{I}_{0,S}$ depends only on the stretching and shearing. The case $\beta = 2$ was analyzed in [90] and proved to reduce to the flexural shell model, i.e. a geometrically nonlinear pure bending, constrained to isometric immersions of S. The energy $\mathcal{I}_{2,S}$ depends then on the change of curvature as in Theorem 3.2.

For $\beta = 4$ the Γ-limit $\mathcal{I}_{4,S}$, as shown in [145, 146, 147], acts on the first order isometries:

$$V \in \mathcal{V}_1 = \mathcal{V}_{id_2} = \left\{V \in H^2(S, \mathbb{R}^3);\ \mathrm{sym}\nabla V = 0\right\}$$

i.e. displacements of S whose covariant derivative is skew-symmetric, and finite strains:

$$B \in \mathcal{S} = \mathcal{S}_{id_2} = \mathrm{closure}_{L^2}\{\mathrm{sym}\nabla w;\ w \in H^1(S, \mathbb{R}^3)\}$$

(compare the definitions of $\mathcal{V}_{y_0}, \mathcal{S}_{y_0}$ in section 3.4). The limiting energy consists of two terms corresponding to the stretching (second order change in metric) and bending (first order change in the second fundamental form $II = \nabla\vec{N}$ on S) of a family of deformations:

$$\{\phi^\eta = \mathrm{id} + \eta V + \eta^2 w^\eta\}_{\eta\to 0}$$

scaling exponent β	asymptotic expansion of minimizing $u^\varepsilon_{\lfloor\omega}$	constraint / regularity	$\Gamma-$limit $\mathcal{I}_{\beta,S}$
$\beta=2$ Kirchhoff	$y(x')$ $\left\{3d\text{: } y(x')+x_3\vec{n}(x')\right\}$	$y\in W^{2,2}(\omega,\mathbb{R}^3)$ $(\nabla y)^T\nabla y = Id_2$	$c\|(\nabla y)^T\nabla\vec{N}\|^2_{\mathcal{Q}_2}$
$2<\beta<4$ linearised Kirchhoff	$x'+\varepsilon^{\beta/2-1}v(x')x_3$	$v\in W^{2,2}(\omega,\mathbb{R})$ $\det\nabla^2 v=0$	$c\|\nabla^2 v\|^2_{\mathcal{Q}_2}$
$\beta=4$ von Kármán	$x'+\varepsilon v(x')x_3$ $+\varepsilon^2 w(x')$	$v\in W^{2,2}(\omega,\mathbb{R})$ $w\in W^{1,2}(\omega,\mathbb{R}^2)$	$c_1\|\frac{1}{2}\nabla v^{\otimes 2}+(\nabla w)_{sym}\|^2_{\mathcal{Q}_2}$ $+c_2\|\nabla^2 v\|^2_{\mathcal{Q}_2}$
$\beta>4$ linear elasticity	$x'+\varepsilon^{\beta/2-1}v(x')x_3$	$v\in W^{2,2}(\omega,\mathbb{R})$	$c\|\nabla^2 v\|^2_{\mathcal{Q}_2}$

FIG. 4. The finite hierarchy of Γ-limits for plates ($\beta\geq 2$)

of S, induced by displacements $V\in\mathcal{V}_1$ and w^η satisfying $\lim_{\eta\to 0}\mathrm{sym}\nabla w^\eta = B$. The out-of-plane displacements v present in (3.9) are therefore replaced by the vector fields in $\mathcal{V}_1$, preserving the metric on S up to first order. For $\beta>4$ the limiting energy consists [145, 146] only of the bending term and it coincides with the linear elasticity.

The form of $\mathcal{I}_{\beta,S}$ for any $\beta>2$ and arbitrary S has been conjectured in [153]. Namely, $\mathcal{I}_{\beta,S}$ acts on the space of k-th order infinitesimal isometries $\mathcal{V}_k$, where k is such that:

$$\beta\in[\beta_{k+1},\beta_k)\quad\text{ where }\quad\beta_n=2+2/n\quad\text{ for all } n\geq 1.$$

The space $\mathcal{V}_k$ consists of k-tuples $(V_1,\dots,V_k)$ of displacements $V_i: S\to\mathbb{R}^3$, such that the deformations $\{\phi^\eta = id_S+\sum_{i=1}^k\eta^i V_i\}_{\eta\to 0}$ preserve the metric on S up to order η^k, i.e. $(\nabla\phi^\eta)^T\nabla\phi^\eta-\mathrm{Id}_2=\mathcal{O}(\eta^{k+1})$. Further, setting $\eta=\varepsilon^{\beta/2-1}$, we have:

(i) When $\beta=\beta_{k+1}$ then $\mathcal{I}_{\beta,S}\simeq\int_S\mathcal{Q}_2\left(x,\delta_{k+1}I_S\right)+\int_S\mathcal{Q}_2\left(x,\delta_1 II_S\right)$, where $\delta_{k+1}I_S$ is the change of metric on S of the order η^{k+1}, generated by the family of deformations $\{\phi^\eta\}_{\eta\to 0}$ and $\delta_1 II_S$ is the first order (i.e. order η) change in the second fundamental form II_S of S.

(ii) When $\beta\in(\beta_{k+1},\beta_k)$ then $\mathcal{I}_{\beta,S}=\int_S\mathcal{Q}_2\left(x,\delta_1 II_S\right)$.

(iii) The constraint of k-th order isometry $\mathcal{V}_k$ may be relaxed to that of $\mathcal{V}_m$, $m<k$, if S has the following $m\mapsto k$ matching property. For every $(V_1,\dots V_m)\in\mathcal{V}_m$ there exist sequences of corrections $V^\eta_{m+1},\dots,V^\eta_k$, equibounded in η, such that: $\tilde{\phi}^\eta=\mathrm{id}+\sum_{i=1}^m\eta^i V_i+\sum_{i=m+1}^k\eta^i V_i^\eta$ preserve the metric on S up to order η^k.

The above is supported by all the rigorously derived models. In particular, plates enjoy the $2\mapsto\infty$ matching property [92], i.e. every $W^{1,\infty}\cap H^2$ element of $\mathcal{V}_2$ may be matched to an exact isometry in the sense of (iii) above. Hence all theories for $\beta\in(2,4)$ collapse to a single theory (linearized Kirchhoff model, see Figure 4). Further, elliptic (i.e. strictly convex up to the boundary) surfaces enjoy [147] a matching property of

$1 \mapsto \infty$, which is stronger than that in case of plates. Namely, on S elliptic and $\mathcal{C}^{4,\alpha}$, every $V \in \mathcal{V}_1 \cap \mathcal{C}^{2,\alpha}$, possesses a sequence $\{w_\eta\}_{\eta\to 0}$, equibounded in $\mathcal{C}^{2,\alpha}(\bar{S}, \mathbb{R}^3)$, and such that $\phi^\eta = id_S + \eta V + \eta^2 w_\eta$ is an (exact) isometry for all $\eta \ll 1$. As a consequence, for elliptic surfaces with sufficient regularity the Γ-limit of the nonlinear elastic energies $\varepsilon^{-\beta}\mathcal{E}^\varepsilon$ for any scaling regime $\beta > 2$ is given by the bending functional constrained to the first order isometries, as in the case $\beta > 4$.

In [111] a further matching property of isometries on developable surfaces without affine regions, has been proved. Namely, on such S of regularity $\mathcal{C}^{2k,1}$, every $V \in \mathcal{V}_1 \cap \mathcal{C}^{2k-1,1}$ enjoys $1 \mapsto k$ matching property. The implication for elasticity of thin shells with smooth developable mid-surface is that, again, the only small slope theory is the linear theory; a developable shell transitions directly from the linear regime to fully nonlinear bending if the applied forces are adequately increased. While the von Kármán theory describes buckling of thin plates, the equivalent variationally correct theory for developable shells is the purely nonlinear bending.

3.8. *Remarks.* The related problem of dynamical viscoelasticity in presence of prestrain has not been satisfactorily addressed, to date. To understand how growth patterns change in response to shape, one must turn to experiments. The simple developmental feedback from shape to growth has been studied in [148], where we initiated this analysis by showing the local and global in time existence of the classical solutions to a general class of stress-assisted diffusion systems. As a follow-up, it would be interesting to tackle the questions of stability of viscoelastic prestrained shock profiles, using the Evans function-based analysis as in [17]. The inverse design problems in morphogenesis require a separate attention, for a handful of simple analytical observations see [3]. Finally, we point out a plethora of parallel discrete problems (e.g. origami, kirigami) both in the static description as well as in the shape evolution through singular prestrain.

4. Micromagnetics of curved thin films (By Giovanni Di Fratta). The analysis of micromagnetic thin films is a subject with a long history. It dates back to the seminal papers [101, 40], where the authors show that in *planar* thin films, the effect of the demagnetizing field operator drops down to an easy-surface anisotropy term. In the last decade, magnetic systems with the shape of a curved thin film have been subject to extensive experimental and theoretical research (nanotubes, 3d helices, thin spherical shells). The wide range of magnetic properties emerging in curved geometries makes them well-suited for spintronic applications, from racetrack memory devices to spin-wave filters (see [204, 205] for topical reviews). The embedding of two-dimensional structures in the three-dimensional space permits altering the system's magnetic properties by tailoring its local curvature. It turns out that even in the absence of *Dzyaloshinskii-Moriya interaction* (DMI) [81, 175], *curved* geometries can induce an effective antisymmetric interaction that supports the emergence of *magnetic skyrmions*, i.e., of topologically protected states to which a topological degree can be assigned.

In the next section, we define magnetic skyrmions in the mathematical framework of the variational theory of micromagnetism, which is also quickly recalled in the same section. After a brief review of magnetic thin films in planar structures, we present the recent developments about curved thin films, which are the geometric structures where magnetic skyrmions naturally emerge. For that, we focus on the general setting of a bounded C^2-surface $S \subseteq \mathbb{R}^3$. Then, we concentrate on the analysis of magnetic skyrmions in spherical thin films ($S = \mathbb{S}^2$), and we describe the challenges still open. We conclude with a section on the analysis of magnetic skyrmions in cylindrical surfaces that highlights how simpler geometries can be the source of valuable techniques for the analysis of more complex scenarios.

4.1. *Magnetic skyrmions in curved geometries.* Skyrmions are a class of solitons, topologically stable and with quasiparticle properties: they behave like particles, but they are inherently more complex structures due to their collective nature. They owe their name to the nuclear physicist Tony Skyrme, who, in 1962, proposed a description of elementary subatomic particles as geometric twists in a continuous quantum field [199].

From the mathematical perspective, magnetic skyrmions emerge as topologically protected magnetization textures that carry a specific topological charge, referred to as the *skyrmion number*. If $\mathcal{M}$ is a compact and smooth hypersurface of $\mathbb{R}^{n+1}$, and $\boldsymbol{m} : \mathcal{M} \to \mathbb{S}^n$ is a sufficiently smooth vector field on $\mathcal{M}$, the skyrmion number of $\boldsymbol{m}$ is defined by the Kronecker integral [190]

$$N_{\mathrm{sk}}(\boldsymbol{m}) := \frac{1}{|\mathbb{S}^n|} \int_{\mathcal{M}} \boldsymbol{m}^* \omega_n, \tag{4.1}$$

with $\omega_n(x) := \sum_{j=1}^{n} (-1)^{j-1} x_j \mathrm{d}x_1 \wedge \ldots \wedge \widehat{\mathrm{d}x_j} \wedge \ldots \wedge \mathrm{d}x_n$ the volume form on $\mathbb{S}^n$, and $\boldsymbol{m}^* \omega_n$ the pull-back of ω_n by $\boldsymbol{m}$ on $\mathcal{M}$. According to Hadamard, $N_{\mathrm{sk}}(\boldsymbol{m})$ is always an integer number and coincides with the topological degree of $\boldsymbol{m}$. Also, by Hopf's theorem [171], skyrmions with different topological charges belong to different homotopy classes; therefore, from the physical point of view, skyrmions are expected to be topologically protected against external perturbations and thermal fluctuations.

Since their discovery, magnetic skyrmions have been the object of intense research work in condensed matter physics. Their stability, reduced size, and the small current densities sufficient to control them, make magnetic skyrmions extremely attractive for applications in modern spintronics [85]. An in-depth understanding of their rich structure (e.g., chirality, topological charge, stability) leads to challenging problems in a subject area where geometry and continuum mechanics meet topology and analysis, and this has raised interest in magnetic skyrmions also from a mathematical perspective [11, 21, 57, 72, 74, 76, 82, 83, 115, 117, 132, 156, 157, 166, 169, 170, 179].

4.2. *The variational theory of micromagnetism.* The appropriate theoretical model for magnetic phenomena depends on the length scale of interest. Models at the level of individual atoms are necessarily quantum mechanical. However, for length scales down to tens of nanometers, there is a well-established *continuum theory of micromagnetism* [34, 113], which dates back to the seminal work of Landau–Lifshitz on fine ferromagnetic particles [134]. In this theory, the observable states of a rigid ferromagnetic particle, occupying a region $\Omega \subseteq \mathbb{R}^3$, are described by its magnetization $\mathcal{M}$, a vector field verifying the fundamental constraint of micromagnetism: there is a material-dependent constant M_s such that $|\mathcal{M}| = M_s$ in Ω. The *spontaneous magnetization* $M_s := M_s(T)$ depends only on the temperature T and vanishes above a critical value T_c, characteristic of each crystal type, known as the *Curie temperature*. When the specimen is at a fixed temperature well below T_c, the function M_s is constant in Ω, and the magnetization takes the form $\mathcal{M} := M_s \boldsymbol{m}$, where $\boldsymbol{m} : \Omega \to \mathbb{S}^2$ is a vector field with values in the unit sphere of $\mathbb{R}^3$ (cf. [34, 75, 113]).

Although the length of $\boldsymbol{m}$ is constant in space, this is generally not the case for its direction. For single crystal ferromagnets (cf. [1, 5, 57]), the observable states of the magnetization are the local minimizers of the micromagnetic energy functional which, after normalization, reads as

$$\mathcal{F}_\Omega(\boldsymbol{m}) := \underbrace{\frac{1}{2}\int_\Omega |\nabla \boldsymbol{m}|^2}_{=:\mathcal{E}_\Omega(\boldsymbol{m})} + \underbrace{\int_\Omega \varphi_{\mathrm{an}}(\boldsymbol{m})}_{=:\mathcal{A}_\Omega(\boldsymbol{m})} + \underbrace{\frac{1}{2}\int_{\mathbb{R}^3} |\boldsymbol{h}_{\mathsf{d}}[\boldsymbol{m}\chi_\Omega]|^2}_{=:\mathcal{W}_\Omega(\boldsymbol{m})} - \underbrace{\int_\Omega \boldsymbol{h}_{\mathsf{a}} \cdot \boldsymbol{m}}_{=:\mathcal{Z}_\Omega(\boldsymbol{m})}. \tag{4.2}$$

Here, $\boldsymbol{m} \in H^1(\Omega, \mathbb{S}^2)$, and $\boldsymbol{m}\chi_\Omega$ is the extension by zero of $\boldsymbol{m}$ to $\mathbb{R}^3$. The *exchange energy* $\mathcal{E}_\Omega$ penalizes nonuniformities in the orientation of the magnetization. The *magnetocrystalline anisotropy energy* $\mathcal{A}_\Omega$ accounts to the existence of preferred directions of the magnetization: its energy density $\varphi_{\mathrm{an}} : \mathbb{S}^2 \to \mathbb{R}^+$ vanishes only on a finite set of directions (the so-called *easy directions*). The *magnetostatic self-energy* $\mathcal{W}_\Omega$ is the energy due to the demagnetizing field $\boldsymbol{h}_{\mathsf{d}}$ generated by $\boldsymbol{m}$. From the mathematical point of view, for every $\boldsymbol{m} \in L^2(\mathbb{R}^3, \mathbb{R}^3)$, $\boldsymbol{h}_{\mathsf{d}}[\boldsymbol{m}]$ is the unique solution in $L^2(\mathbb{R}^3, \mathbb{R}^3)$ of the Maxwell-Ampére equations of magnetostatics:

$$\mathbf{curl}\, \boldsymbol{h}_{\mathsf{d}} = \mathbf{0}, \quad \operatorname{div} \boldsymbol{b} = 0, \quad \boldsymbol{b} = \mu_0 (\boldsymbol{h}_{\mathsf{d}} + \boldsymbol{m}) \,. \tag{4.3}$$

Here, $\boldsymbol{b}$ denotes the magnetic flux density, and μ_0 is the magnetic permeability of the vacuum. The *Zeeman energy* $\mathcal{Z}_\Omega$ models the tendency of a specimen to have the magnetization aligned with the applied field $\boldsymbol{h}_{\mathsf{a}}$ (cf. Figure 5). The energy contributions $\mathcal{A}_\Omega$ and $\mathcal{Z}_\Omega$ are of fundamental importance in ferromagnetism. However, from the variational point of view, they typically behave like continuous perturbations, and their

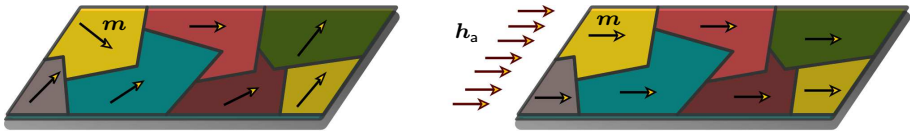

FIG. 5. Below the Curie temperature ($T \ll T_c$), the modulus of $\boldsymbol{M} = M_s \boldsymbol{m}$ is constant in Ω (but not the direction). The direction of $\boldsymbol{M}$ can be modified/controlled by an external magnetic field $\boldsymbol{h}_{\mathsf{a}}$.

analysis is usually straightforward. To streamline the presentation, we will often neglect these terms.

The variational problem (4.2) is non-convex, non-local, and contains multiple length scales. The four terms in the energy functional (4.2) consider effects originating from different spatial scales, such as short-range exchange forces and long-range magnetostatic interactions. The competition among the four contributions in (4.2) explains most of the striking pictures of the magnetization observable in ferromagnetic materials; in particular, the domain structure suggested by Weiss, i.e., regions of uniform or slowly varying magnetization (*magnetic domains*) separated by thin transition layers (*domain walls*) (see, e.g., [62, 63, 118, 119, 120, 174, 188], and the references therein).

Recent advances in nanotechnology have led to the fabrication of ultrathin films (and multilayers) with a thickness down to several atomic layers and a lateral extent down to tens of nanometers. These structures often display unusual magnetic properties connected to a prominent influence of interfacial effects; first and foremost, the emergence of magnetic skyrmions originating from the *Dzyaloshinskii-Moriya interaction* (DMI) [81, 175]. In thin films, DMI is closely related to reflection symmetry breaking, whereas a lack of inversion symmetry is the primary cause in bulk magnetic materials. The bulk DMI corresponds to the trace of the chirality tensor, which leads to the energy contribution

$$\mathcal{D}_\Omega(\boldsymbol{m}) := \gamma \int_\Omega \mathbf{curl}\, \boldsymbol{m} \cdot \boldsymbol{m}. \tag{4.4}$$

The normalized constant $\gamma \in \mathbb{R}$ is the bulk DMI constant, and its sign affects the chirality of the ferromagnetic system [25, 181].

However, the main interest in curved geometry relies on the observation that they can host magnetic skyrmions even when no spin-orbit coupling mechanism (in the guise of DMI) is considered (cf. [94, 130]). The evidence of these spontaneous states sheds light on the role of the geometry in magnetism: chiral spin-textures can be stabilized by curvature effects only, in contrast to the planar case where DMI is required [81, 175]. For that reason, from now on, we will focus on the micromagnetic energy functional

$$\mathcal{G}_\Omega(\boldsymbol{m}) := \frac{1}{2}\int_\Omega |\nabla \boldsymbol{m}|^2 + \frac{1}{2}\int_{\mathbb{R}^3} |\boldsymbol{h}_{\mathsf{d}}[\boldsymbol{m}\chi_\Omega]|^2 + \int_\Omega \varphi_{\mathrm{an}}(\boldsymbol{m}), \tag{4.5}$$

and we will be interested in the asymptotic regime of curved thin films.

REMARK 4.1. Although we will focus on the variational theory of micromagnetism, we will need to refer to magnetization dynamics from time to time. We recall that the motion of non-equilibrium magnetizations is governed by the Landau–Lifshitz–Gilbert

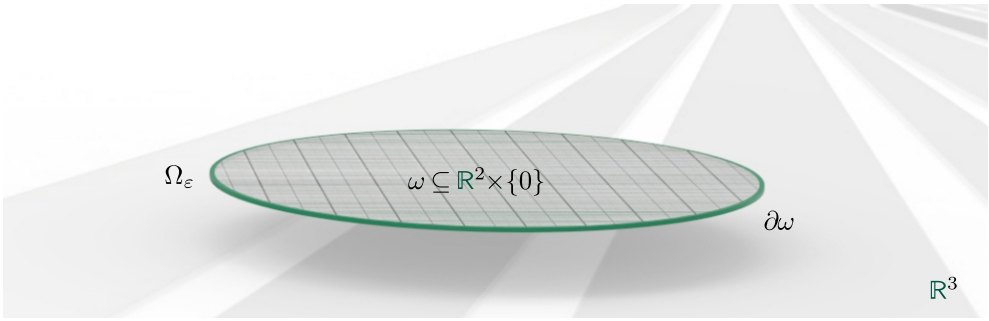

FIG. 6. The thin shell Ω_ε is generated by extruding, along the e_3 axis, a planar surface $\omega \subseteq \mathbb{R}^2 \times \{0\}$.

(LLG) equation [99, 134]

$$\frac{\partial \boldsymbol{m}}{\partial t} - \alpha \boldsymbol{m} \times \frac{\partial \boldsymbol{m}}{\partial t} = -\boldsymbol{m} \times \boldsymbol{h}_{\mathsf{eff}}[\boldsymbol{m}] \quad \text{in } \Omega \times \mathbb{R}_+. \tag{4.6}$$

The LLG equation is driven by the *effective field* $\boldsymbol{h}_{\mathsf{eff}}[\boldsymbol{m}] := -\partial_{\boldsymbol{m}} \mathcal{G}_\Omega(\boldsymbol{m})$ and includes both conservative precessional and dissipative contributions; the constant α is the so-called Gilbert damping constant.

4.3. *The planar thin-film regime.* Let ω be a smooth domain in $\mathbb{R}^2$. For any $\varepsilon > 0$ the tubular neighborhood Ω_ε is defined by (cf. Figure 6)

$$\Omega_\varepsilon := \left\{ x \in \mathbb{R}^3 : x = \xi + \varepsilon e_3, \xi \in \omega \right\}.$$

The micromagnetic energy functional on $H^1(\Omega_\varepsilon, \mathbb{S}^2)$ reads as (cf. (4.5))

$$\mathcal{G}_\varepsilon(\boldsymbol{m}_\varepsilon) := \frac{1}{2} \int_{\Omega_\varepsilon} |\nabla \boldsymbol{m}_\varepsilon|^2 - \frac{1}{2} \int_{\Omega_\varepsilon} \boldsymbol{h}_{\mathsf{d}}[\boldsymbol{m}_\varepsilon \chi_{\Omega_\varepsilon}] \cdot \boldsymbol{m}_\varepsilon + \int_{\Omega_\varepsilon} \varphi_{\mathrm{an}}(\boldsymbol{m}_\varepsilon). \tag{4.7}$$

Here, ω is the planar surface generating the cylindrical surface $\Omega_\varepsilon := \omega \times (0, \varepsilon)$, and $e_3 = (0, 0, 1)$ is the normal to the planar surface ω (cf. Figure 6). The existence for any $\varepsilon > 0$ of at least a minimizer for $\mathcal{G}_\varepsilon$ in $H^1(\Omega_\varepsilon, \mathbb{S}^2)$ is easily obtained by the direct method of the calculus of variations. The interest is in the asymptotic behavior of the energies $(\varepsilon^{-1}\mathcal{G}_\varepsilon)$ as $\varepsilon \to 0$, i.e., on the identification of the empty slots in the following typical Γ-convergence diagram

$$\operatorname*{argmin}_{\boldsymbol{m}_\varepsilon \in H^1(\Omega_\varepsilon, \mathbb{S}^2)} \varepsilon^{-1} \mathcal{G}_\varepsilon(\boldsymbol{m}_\varepsilon) \quad \overset{\varepsilon \to 0}{\longrightarrow} \quad \operatorname*{argmin}_{\square} \square. \tag{4.8}$$

For planar thin films, it is well-known that the demagnetizing field behaves like the projection of the magnetization onto the plane of the film. The first mathematical justification of this observation in micromagnetics is in the work of Gioia and James [101], where it is shown that the role of the demagnetizing field operator reduces to an easy-surface anisotropy term. Their theory generalizes Stoner and Wohlfarth's results for flat ellipsoids [202] to arbitrary-shaped planar thin films. In the language of the scheme in (4.8), they proved that

$$\operatorname*{argmin}_{\boldsymbol{m}_\varepsilon \in H^1(\Omega_\varepsilon, \mathbb{S}^2)} \frac{1}{\varepsilon} \mathcal{G}_\varepsilon(\boldsymbol{m}_\varepsilon) \quad \overset{\varepsilon \to 0}{\longrightarrow} \quad \operatorname*{argmin}_{\boldsymbol{m} \in H^1(\omega, \mathbb{S}^2)} \mathcal{G}_0(\boldsymbol{m}), \tag{4.9}$$

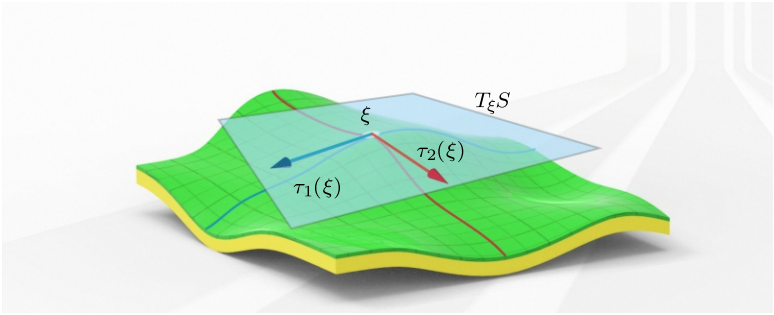

FIG. 7. The thin shell Ω_ε is generated by extruding, along the normal direction $\boldsymbol{n}$, a surface S embedded in $\mathbb{R}^3$.

with

$$\mathcal{G}_0(\boldsymbol{m}) := \frac{1}{2}\int_\omega |\nabla \boldsymbol{m}|^2 + \frac{1}{2}\int_\omega (\boldsymbol{m}\cdot e_3)^2 + \int_\omega \varphi_{\rm an}(\boldsymbol{m}). \tag{4.10}$$

Note that when the magnetocrystalline anisotropy is in-plane, i.e., when $\varphi_{\rm an}(\xi) = 0$ for every $\xi \in \mathbb{S}^1 \times \{0\}$, every constant and in-plane magnetization minimizes $\mathcal{G}_0$. However, it is understandable from the Maxwell–Ampére equations of magnetostatics (4.3) that when ε is sufficiently small, not every constant in-plane configuration is equally favored. In fact, the direction of the limiting minimizer will depend on the shape anisotropy of $\partial\omega$. In order to get mathematical evidence of this fact, one can use the methods of potential theory to obtain higher-order correctors in the energy expansion. This has been done by Carbou in [40], where it is shown that

$$\min \varepsilon^{-1}\mathcal{G}_\varepsilon = \min \mathcal{G}_0 - \frac{1}{2}\varepsilon \ln \varepsilon \min \mathcal{G}_0'' + o(\varepsilon \ln \varepsilon)$$

with

$$\mathcal{G}_0''(\xi) := \int_{\partial\omega} (\xi\cdot\nu)^2, \quad \xi \in \mathbb{S}^1 \times \{0\}.$$

Here, ν is the normal to $\partial\omega$, and the result has the following interpretation. When the magnetocrystalline anisotropy is in-plane, among all constant and in-plane magnetization $\xi \in \mathbb{S}^1 \times \{0\}$ that minimize $\mathcal{G}_0$, the limiting magnetization tends to align along the direction that minimizes $\mathcal{G}_0''(\xi)$. The same result can be obtained using harmonic analysis, and we refer the reader to [124], which also considers other attractive geometric regimes. Finally, we mention the results in [58], where the contribution of DMI is taken into account, again in the geometric setting of planar thin films. It is shown that, in the limiting thin-film model, part of the DMI behaves like the projection of the magnetic moment onto the normal to the film, contributing this way to an increase in the shape anisotropy arising from the magnetostatic self-energy.

4.4. *The curved thin film regime.* To discuss results about curved thin films, we need to introduce the proper setup. Let S be a smooth surface admitting a tubular neighborhood of thickness $\delta > 0$. For any $\varepsilon \in I_\delta := (0,\delta)$ the tubular neighborhood Ω_ε is defined by $\Omega_\varepsilon := \{x \in \mathbb{R}^3 : x = \xi + \varepsilon \boldsymbol{n}(\xi), \xi \in S\}$, where $\boldsymbol{n}(\xi)$ denotes the normal at $\xi \in S$ (cf. Figure 7).

The micromagnetic energy functional defined on $H^1(\Omega_\varepsilon, \mathbb{S}^2)$ reads as (cf. (4.5))

$$\mathcal{G}_\varepsilon(\boldsymbol{m}_\varepsilon) := \frac{1}{2}\int_{\Omega_\varepsilon} |\nabla \boldsymbol{m}_\varepsilon|^2 - \frac{1}{2}\int_{\Omega_\varepsilon} \boldsymbol{h}_{\mathrm{d}}\left[\boldsymbol{m}_\varepsilon \chi_{\Omega_\varepsilon}\right] \cdot \boldsymbol{m}_\varepsilon. \tag{4.11}$$

The existence of at least a minimizer for $\mathcal{G}_\varepsilon$ in $H^1(\Omega_\varepsilon, \mathbb{S}^2)$ is easily obtained by the direct method of the calculus of variations.

For every $\varepsilon \in I_\delta := (0, \delta)$ we denote by ψ_ε the diffeomorphism of $\mathcal{M} := S \times (0,1)$ onto Ω_ε given by

$$\psi_\varepsilon : (\xi, s) \in \mathcal{M} \mapsto \xi + \varepsilon s \boldsymbol{n}(\xi) \in \Omega_\varepsilon.$$

For every $\xi \in S$ the symbols $\tau_1(\xi), \tau_2(\xi)$ denote an orthonormal basis of $T_\xi S$ made by its principal directions, i.e., an orthonormal basis consisting of eigenvectors of the shape operator of S (cf. [79]). We then write $\kappa_1(\xi), \kappa_2(\xi)$ for the principal curvatures at $\xi \in S$. Note that, for any $x \in \Omega_\delta$ the trihedron

$$(\tau_1(\xi), \tau_2(\xi), \boldsymbol{n}(\xi)) \quad \text{with} \quad \xi := \pi(x)\,, \tag{4.12}$$

constitutes an orthonormal basis of $T_{\pi(x)}\Omega_\delta$ that depends only on S. Also, we denote by $\sqrt{\mathfrak{g}_\varepsilon}$ the metric factor which relates the volume form on Ω_ε to the volume form on $\mathcal{M}$, by $\mathfrak{h}_{1,\varepsilon}, \mathfrak{h}_{2,\varepsilon}$ the metric coefficients which link the gradient on Ω_ε to the gradient on $\mathcal{M}$. A direct computation shows that (cf., e.g., [182])

$$\sqrt{\mathfrak{g}_\varepsilon(\xi, s)} := |1 + 2\varepsilon s H(\xi) + (\varepsilon s)^2 G(\xi)| \quad , \quad \mathfrak{h}_{i,\varepsilon}(\xi, s) := \frac{1}{1 + \varepsilon s \kappa_i(\xi)} \quad (i = 1, 2).$$

where $H(\xi)$ and $G(\xi)$ are the mean and Gaussian curvature at $\xi \in S$. Also, we denote by $H^1(\mathcal{M}, \mathbb{R}^3)$ the Sobolev space of vector-valued functions defined on $\mathcal{M}$ and endowed with the norm

$$\|\boldsymbol{u}\|^2_{H^1(\mathcal{M})} := \int_{\mathcal{M}} |\boldsymbol{u}(\xi, s)|^2 \mathrm{d}\xi \mathrm{d}s + \int_{\mathcal{M}} |\nabla^*_\xi \boldsymbol{u}(\xi, s)|^2 + |\partial_s \boldsymbol{u}(\xi, s)|^2 \mathrm{d}\xi \mathrm{d}s. \tag{4.13}$$

Here, $\nabla^*_\xi \boldsymbol{u}$ is the tangential gradient of $\boldsymbol{u}$ on S, and we write $H^1(\mathcal{M}, \mathbb{S}^2)$ for the subset of $H^1(\mathcal{M}, \mathbb{R}^3)$ consisting of vector-valued functions with values in $\mathbb{S}^2$.

With $\mathcal{M} = S \times I$, we introduce the following functionals on $H^1(\mathcal{M}, \mathbb{S}^2)$. The exchange energy on $\mathcal{M}$ is defined by

$$\mathcal{E}^\varepsilon_{\mathcal{M}}(\boldsymbol{u}) := \frac{1}{2}\sum_{i=1}^{2} \int_{\mathcal{M}} |\mathfrak{h}_{i,\varepsilon} \partial_{\tau_i(\xi)} \boldsymbol{u}|^2 \sqrt{\mathfrak{g}_\varepsilon} \mathrm{d}\xi \mathrm{d}s + \frac{1}{2}\frac{1}{\varepsilon^2} \int_{\mathcal{M}} |\partial_s \boldsymbol{u}|^2 \sqrt{\mathfrak{g}_\varepsilon} \mathrm{d}\xi \mathrm{d}s. \tag{4.14}$$

The magnetostatic self-energy on $\mathcal{M}$ is defined by

$$\mathcal{W}^\varepsilon_{\mathcal{M}}(\boldsymbol{u}) := -\frac{1}{2}\sum_{i=1}^{2} \int_{\mathcal{M}} \boldsymbol{h}_\varepsilon[\boldsymbol{u}](\xi, s) \cdot \boldsymbol{u}(\xi, s) \sqrt{\mathfrak{g}_\varepsilon(\xi, s)} \mathrm{d}\xi \mathrm{d}s. \tag{4.15}$$

Here, $\boldsymbol{h}_\varepsilon[\boldsymbol{u}] \in L^2(\mathcal{M}, \mathbb{R}^3)$ is the demagnetizing filed on $\mathcal{M}$ defined by $\boldsymbol{h}_\varepsilon[\boldsymbol{u}](\xi, s) := \boldsymbol{h}_{\mathrm{d}}[(\boldsymbol{u}\chi_I) \circ \psi_\varepsilon^{-1}] \circ \psi_\varepsilon$.

It is imperative to observe that for any $\varepsilon \in I_\delta$, the minimization problem for $\mathcal{G}_\varepsilon$ in $H^1(\Omega_\varepsilon, \mathbb{S}^2)$ is equivalent to the minimization in $H^1(\mathcal{M}, \mathbb{S})$ of the functional $\mathcal{F}_\varepsilon$ defined by

$$\mathcal{F}_\varepsilon(\boldsymbol{u}) := \mathcal{E}^\varepsilon_{\mathcal{M}}(\boldsymbol{u}) + \mathcal{W}^\varepsilon_{\mathcal{M}}(\boldsymbol{u}),$$

in the sense that the configuration $\boldsymbol{m}_\varepsilon \in H^1(\Omega_\varepsilon, \mathbb{S}^2)$ minimizes $\mathcal{G}_\varepsilon$ if and only if $\boldsymbol{u}_\varepsilon := \boldsymbol{m} \circ \psi_\varepsilon \in H^1(\mathcal{M}, \mathbb{S})$ minimizes $\varepsilon \mathcal{F}_\varepsilon$.

We can now state a proper generalization of the results in [101] (cf. (4.9)) to the curved setting.

THEOREM 4.2 ([40, 75, 72]). The family $(\mathcal{F}_\varepsilon)$ is equicoercive in the weak $H^1(\mathcal{M}, \mathbb{S}^2)$ and $(\mathcal{F}_\varepsilon) \xrightarrow{\Gamma} \mathcal{F}'_0$ in the sense of Γ-convergence, with $\mathcal{F}'_0$ given by

$$\mathcal{F}'_0(\boldsymbol{u}) := \frac{1}{2} \int_S |\nabla^*_\xi \boldsymbol{u}|^2 \mathrm{d}\xi + \frac{1}{2} \int_S (\boldsymbol{u} \cdot \boldsymbol{n})^2 \, \mathrm{d}\xi \tag{4.16}$$

if $\partial_s \boldsymbol{u} = 0$, and $\mathcal{F}'_0(\boldsymbol{u}) = +\infty$ otherwise. Here, $\nabla^*_\xi \boldsymbol{u}$ is the tangential gradient of $\boldsymbol{u}$ on S.

Also, by the fundamental theorem of Γ-convergence

$$\min_{H^1(\Omega_\varepsilon, \mathbb{S}^2)} \varepsilon^{-1} \mathcal{G}_\varepsilon = \min_{H^1(\mathcal{M}, \mathbb{S}^2)} \mathcal{F}'_0 + o(\varepsilon),$$

and if $(\boldsymbol{u}_\varepsilon)_{\varepsilon \in I_\delta}$ is a minimizing family for $(\mathcal{F}_\varepsilon)_{\varepsilon \in I_\delta}$, there exists a subsequence of $(\boldsymbol{u}_\varepsilon)_{\varepsilon \in I_\delta}$ which *strongly* converges in $H^1(\mathcal{M}, \mathbb{S}^2)$ to a minimum point of $\mathcal{F}'_0$.

REMARK 4.3. Theorem 4.2 applies to bounded surfaces that admit a tubular neighborhood. The range of such surfaces is broad. Indeed, any compact and smooth surface is orientable and admits a tubular neighborhood (of uniform thickness) [79]. In particular, the analysis holds for bounded convex surfaces (e.g., planar surfaces, the sphere, the ellipsoid) and non-convex ones (e.g., the torus). Also, it covers the class of bounded surfaces that are diffeomorphic to an open subset of a compact surface (e.g., the finite cylinder or the graph of a C^2-function).

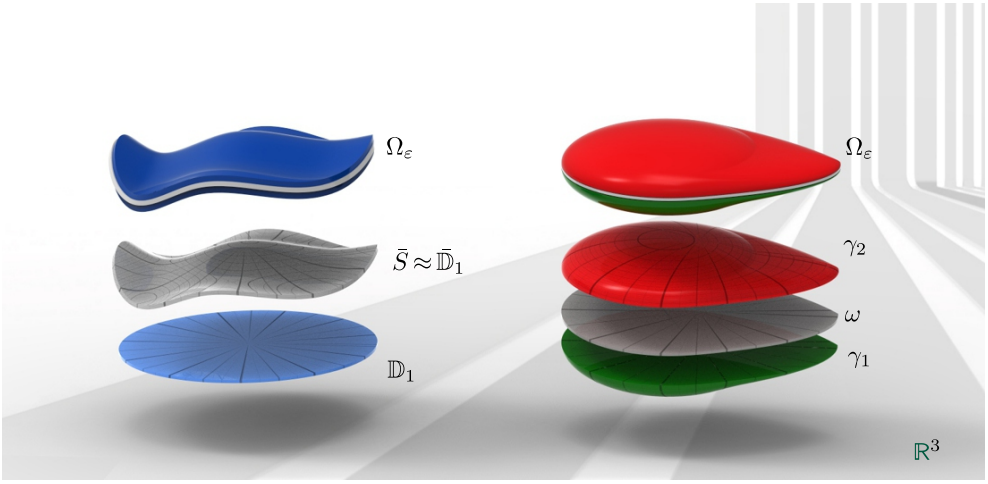

FIG. 8. • (Left) The thin shell Ω_ϵ is generated by extruding, along the normal direction ν, a surface S whose closure is diffeomorphic to the closed unit disk $\mathbb{D}_1$ of $\mathbb{R}^2$. • (Right) A pillow-like thin shell: $\Omega_\varepsilon := \{(x, z) \in \omega \times \mathbb{R}^2 : \varepsilon\gamma_1(x) \leqslant z \leqslant \varepsilon\gamma_2(x)\}$ where $\omega \subseteq \mathbb{R}^2$ is a planar surface and γ_1, γ_2 functions vanishing on the boundary of ω.

Theorem 4.2 states that in the curved thin-film regime, the magnetostatic self-energy tends to favor tangential vector fields. The first analysis of the curved thin-film limit is addressed in Carbou [40], where Theorem 4.2 is established under the assumption that the thin geometry is generated by a surface diffeomorphic to the closed unit disk of $\mathbb{R}^2$ (cf. Figure 8). Also, in [200], a Γ-convergence analysis is performed on pillow-like shells, i.e., on shells of small thickness $\varepsilon > 0$ having the form

$$\Omega_\varepsilon := \{(x, z) \in \omega \times \mathbb{R} : \varepsilon\gamma_1(x) \leqslant z \leqslant \varepsilon\gamma_2(x)\}$$

with $\omega \subseteq \mathbb{R}^2$ and γ_1, γ_2 functions vanishing on the boundary of ω.

The inherent local character of the results in [40] and [200] does not cover significant scenarios like the one of a spherical thin film [198, 201, 76]. After all, it is on compact surfaces that topological protection can be exploited through the mathematical concept of degree. The lack of mathematical justifications in this context motivated the results in [75], where three distinct variational principles for the magnetostatic self-energy are introduced. Through them and the explicit construction of suitable families of scalar and vector potentials, one can circumvent the technical difficulties in [40], at least in the stationary case. Indeed, the approach in [75], dealing with energy estimates rather than with the asymptotic behavior of the demagnetizing field operator, is not suitable for analyzing the time-dependent case governed by the LLG. The results in [72] hold in the more general framework of smooth (C^2 is sufficient) and bounded orientable surfaces in $\mathbb{R}^3$ (in particular, they cover the class of compact surfaces). The proofs in [40] and [72] cover both the stationary case, which is governed by the micromagnetic energy functional, and the time-dependent case driven by the LLG. They are based on a characterization of the limiting demagnetizing field operator on curved thin films, which states that the demagnetizing field behaves like the projection of the magnetization on the normal to the film. In other words, one has strong L^2-convergence of $\boldsymbol{h}_\varepsilon[\boldsymbol{u}](\xi, s)$ to $[\boldsymbol{n}(\xi) \otimes \boldsymbol{n}(\xi)]\, \boldsymbol{u}(\xi)$. Strong convergence in L^2 is crucial for extending these results to the LLG equation (see [72]).

In the curved setting, the problem of identifying higher-order correctors in the energy expansion of the magnetostatic energy is still open. For a compact surface with boundary, the question is whether the next order term in the expansion $\mathcal{W}^\varepsilon_{\mathcal{M}}(\boldsymbol{u})$ reduces to a shape anisotropy term on the boundary of the surface (of the order $(\varepsilon|\ln\varepsilon|)^{-1}$ if ε is the thickness of the thin film). For compact surfaces *without* a boundary (e.g., $\mathbb{S}^2$), the analysis should benefit from the absence of a lateral surface in the curved thin shell, which is what contributes at the $(\varepsilon|\ln\varepsilon|)^{-1}$ order in the planar case; yet, even for $\mathbb{S}^2$ the question has not been investigated.

4.5. *Topologically protected states in spherical thin films.* Spherical thin films are currently of interest due to their capability to host *spontaneous* skyrmion solutions [94, 130] even when no spin-orbit coupling mechanism (DMI) is considered. In addition to fundamental reasons, the interest in these geometries is triggered by recent advances in the fabrication of magnetic spherical hollow nanoparticles, which lead to artificial materials with unexpected characteristics and numerous applications ranging from logic devices to biomedicine (cf. [197]).

From Theorem 4.2, we know that for a spherical magnetic thin film, the energy functional reads as:

$$\mathcal{F}_\kappa : \boldsymbol{m} \in H^1(\mathbb{S}^2, \mathbb{S}^2) \mapsto \int_{\mathbb{S}^2} \left|\nabla^*_\xi \boldsymbol{m}(\xi)\right|^2 + \kappa \left(\boldsymbol{m}(\xi) \cdot \boldsymbol{n}(\xi)\right)^2 \mathrm{d}\xi. \tag{4.17}$$

Here, $\boldsymbol{n}(\xi) \equiv \xi$ and, as before, ∇^*_ξ is the surface gradient at $\xi \in \mathbb{S}^2$. The parameter $\kappa \in \mathbb{R}$ summarizes the contribution of *crystal* and *shape* anisotropy. The role of $\kappa \in \mathbb{R}$ is easily understood. Uniform states are the only local minimizers of $\mathcal{F}_\kappa$ when $\kappa = 0$. For $\kappa > 0$, tangential vector fields are energetically favored, and this corresponds to the case of *in-plane* crystal anisotropy in planar thin films. When $\kappa < 0$, energy minimization prefers normal vector fields, which compares to the case of *perpendicular* crystal anisotropy in planar thin films, or, to be more precise, to the situation where shape anisotropy prevails over perpendicular crystal anisotropy.

An exact characterization of the minimizers of $\mathcal{F}_\kappa$ is a challenging task with far-reaching consequences in modern storage technologies [198]. Recently, a partial answer has been given for the case $\kappa < 0$. In [76], the following result is proved.

PROPOSITION 1 ([76]). For every $\kappa \in \mathbb{R}$, the normal vector fields $\pm\boldsymbol{n}(\xi)$ are stationary points of the micromagnetic energy functional $\mathcal{F}_\kappa$ on the space $H^1(\mathbb{S}^2, \mathbb{S}^2)$. Moreover, they are strict local minimizers for every $\kappa < 0$ and are unstable for $\kappa > 0$. If $\kappa \leqslant -4$, the normal vector fields are the only global minimizers of $\mathcal{F}_\kappa$.

Also, in [170], it is shown that for $\kappa \ll 0$, skyrmionic solutions topologically distinct from the ground state emerge as excited states.

The interest in results of this type is in the topological remark that $\pm\boldsymbol{n}$ carry different *skyrmion numbers*. Indeed, since $\deg(\pm\boldsymbol{n}) = \pm 1$, by Hopf theorem, these two configurations cannot be homotopically mapped one into the other and are, therefore, topologically protected against external perturbations and thermal fluctuations. These considerations make the two ground states $\pm\boldsymbol{n}$ promising in view of novel spintronic devices [85].

REMARK 4.4. It is worth pointing out a correspondence between Proposition 1 and Brown's fundamental theorem on small ferromagnetic particles, which states the existence of a critical value of the radius of a spherical particle below which all local minimizers are constant in space [36, 70, 71, 6]. Indeed, a simple scaling argument shows that the constant κ in (4.17) can also be interpreted as a measure of the size of the particle.

The proof of Proposition 1 is based on the derivation of sharp Poincaré inequalities arising when the pointwise constraint $\boldsymbol{m} \in \mathbb{S}^2$ is relaxed to the energy constraint

$$\frac{1}{4\pi} \int_{\mathbb{S}^2} |\boldsymbol{m}(\xi)|^2 \mathrm{d}\xi = 1. \tag{4.18}$$

Depending on the value of κ, minimizers of the relaxed problem may turn out to be minimizers of the original problem (i.e., $\mathbb{S}^2$-valued). This is indeed the case for the normal vector fields $\pm\boldsymbol{n}$ when $\kappa \leqslant -4$.

THEOREM 4.5 (Sharp Poincaré-type inequality on $\mathbb{S}^2$, [76]). Let $\kappa \in \mathbb{R}$. For every $\boldsymbol{u} \in H^1(\mathbb{S}^2, \mathbb{R}^3)$ the following inequality holds

$$\int_{\mathbb{S}} |\nabla^*_\xi \boldsymbol{u}(\xi)|^2 \mathrm{d}\xi + |\kappa| \int_{\mathbb{S}} |\boldsymbol{u}(\xi) \times \boldsymbol{n}(\xi)|^2 \mathrm{d}\xi \geqslant (|\kappa| + \gamma(\kappa)) \int_{\mathbb{S}} |\boldsymbol{u}(\xi)|^2 \mathrm{d}\xi. \tag{4.19}$$

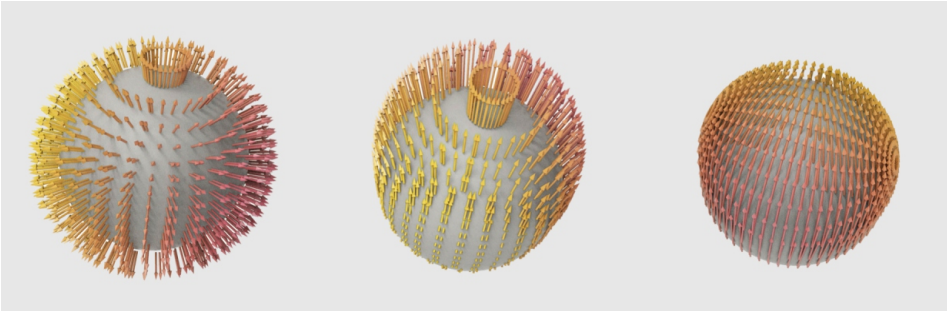

FIG. 9. Examples of vector fields for which the equality sign is reached in the Poincaré inequality (4.19). Minimizers for κ negative. • (Left) $\kappa = -8$ • (Center) $\kappa = -4$ • (Right) $\kappa = -2$.

with best constant $\gamma(\kappa)$ given by

$$\gamma(\kappa) := \begin{cases} \kappa + 2 & \text{if} \quad \kappa \leqslant -4, \\ \frac{1}{2}\left((\kappa+6) - \sqrt{\kappa^2 + 4\kappa + 36}\right) & \text{if} \quad \kappa > -4. \end{cases}$$

Moreover, for any $\kappa \in \mathbb{R}$, the equality sign is reached if, and only if,

$$\boldsymbol{u}(\xi) = c_0 \boldsymbol{y}^{(1)}_{0,0}(\xi) + \sum_{j=-1}^{1} \eta_j \boldsymbol{y}^{(1)}_{1,j} + \sigma_j \boldsymbol{y}^{(2)}_{1,j}.$$

Here, $\boldsymbol{y}^{(i)}_{n,j}$ are the vector spherical harmonics of degree n and order j, with $|j| \leqslant n$ (cf. [18, 76]) while the coefficients $c_0, (\eta, \sigma) := (\eta_j, \sigma_j)_{|j|\leqslant 1}$ are defined as follows. If $\kappa < -4$ then $c_0 = \pm\sqrt{4\pi}$, and $\eta = \sigma = 0$; in particular, $\pm\boldsymbol{n}$ are the unique minimizers. If $\kappa > -4$ then

$$c_0 = 0, \quad \sigma = \frac{-2\sqrt{2}}{(\gamma(\kappa) - 2)}\eta, \quad |\eta|^2 = 2\pi \frac{-(\kappa+2) + \sqrt{\kappa^2 + 4\kappa + 36}}{\sqrt{\kappa^2 + 4\kappa + 36}}.$$

If $\kappa = -4$ then

$$\sigma = \frac{\sqrt{2}}{2}\eta, \quad 2c_0^2 + 3|\eta|^2 = 8\pi.$$

REMARK 4.6. Recall that, $\boldsymbol{y}^{(1)}_{n,j}$ are normal vector fields, while $\boldsymbol{y}^{(2)}_{n,j}$ and $\boldsymbol{y}^{(3)}_{n,j}$ are tangential vector fields (cf. [18, 76]). Also, note that for $\kappa \to 0^-$ the minimizers tend to be constant. A plot of vector fields $\boldsymbol{u} \in H^1(\mathbb{S}^2, \mathbb{R}^3)$ for which the equality sign is reached in the Poincaré inequality (4.19) is reported in Figure 9.

For $\kappa > 0$, the energy landscape of $\mathcal{F}_\kappa$ is hard to describe analytically and is still an open question. Although tangential vector fields are energetically favored when $\kappa > 0$, topological obstructions (hairy ball theorem) prevent the existence of purely tangential vector fields in $H^1(\mathbb{S}^2, \mathbb{S}^2)$. The primary interest here is in the study of energy minimizers within prescribed homotopy classes. More specifically, on the characterizations of the global minimizers of $\mathcal{F}_\kappa$ in $H^1(\mathbb{S}^2, \mathbb{S}^2)$ under the constraint (cf. (4.1))

$$\frac{1}{4\pi}\int_{\mathbb{S}^2} \boldsymbol{m} \cdot (\partial_{\tau_1}\boldsymbol{m} \times \partial_{\tau_2}\boldsymbol{m}) = n \in \mathbb{Z}, \tag{4.20}$$

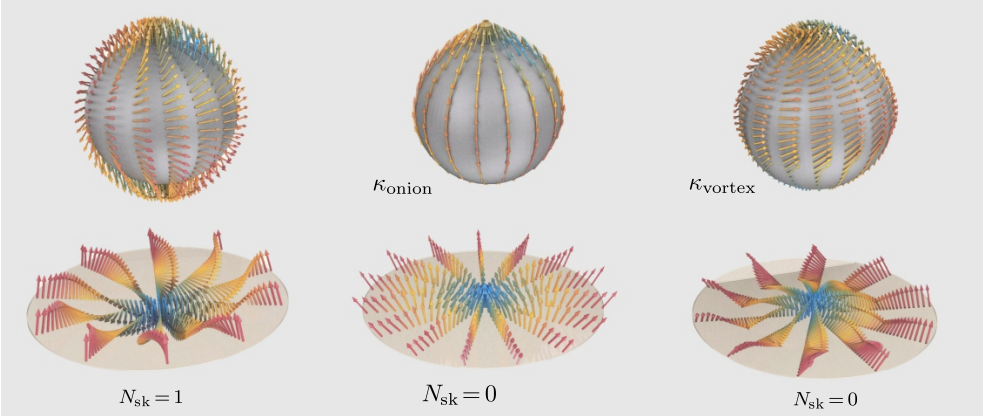

FIG. 10. Numerics suggest that when $\kappa > 0$, the energy $\mathcal{F}_\kappa$ can exhibit magnetic states with skyrmion number 0 or ± 1. Also, within the homotopy class $\{N_{\text{sk}} = 0\}$, the energy $\mathcal{F}_\kappa$ favors the so-called *onion* state if κ is sufficiently small and the *vortex* state otherwise.

for some prescribed integer n, which uniquely identifies the homotopy class of $\boldsymbol{m}$. Numerics suggest that when $\kappa > 0$, the energy $\mathcal{F}_\kappa$ can exhibit magnetic states with skyrmion number 0 or ± 1 (cf. Figure 10, and [130, 198, 201]). Also, within the homotopy class $\{N_{\text{sk}} = 0\}$, the energy $\mathcal{F}_\kappa$ favors the so-called *onion* state if κ is sufficiently small, and the *vortex* state otherwise (cf. Figure 10). Moreover, in analogy with well-known results for harmonic maps into spheres, the minimizers of $\mathcal{F}$ appear axially symmetric. However, to turn these observations into quantitative statements can be particularly tricky because of the complete rotational symmetry of the underlying Euler-Lagrange equations, which requires capturing the emergence of breaking symmetry phenomena in the energy minimizers.

4.6. *Conclusions and further outlook.* In the previous sections, we reviewed some of the main results in the theory of magnetic curved thin films and stressed how these achievements allow further investigations on the profile of energy minimizers in specific geometries. We presented a characterization of the ground states in spherical thin films when the anisotropy constant κ is negative (see (4.17)), and we also pointed out that the situation appears more involved when $\kappa > 0$. However, careful consideration reveals that similar symmetry-breaking phenomena already emerge in the analysis of the ground states for a more tractable geometry like the one of a cylinder. This led to the developments in [73], where different strategies are introduced that seem promising to tackle similar questions in more complex geometries.

Consider the *circular* cylinder $\mathcal{C} = I \times \mathbb{S}^1$, $I := [-1, 1]$ and the energy functional

$$\mathcal{E}_\alpha(\boldsymbol{m}) := \int_{\mathcal{C}} |\nabla_\xi \boldsymbol{m}|^2 \, \mathrm{d}\xi + \alpha^2 \int_{\mathcal{C}} |\boldsymbol{m} \times \boldsymbol{n}|^2 \, \mathrm{d}\xi, \qquad \boldsymbol{m} \in H^1(\mathcal{C}, \mathbb{S}^2). \tag{4.21}$$

First, it is possible to show that for any $\alpha^2 > 0$, minimizers of the energy $\mathcal{E}_\alpha$ are z-invariant, i.e., if $\boldsymbol{m}$ minimizes $\mathcal{E}_\alpha$ then $\boldsymbol{m}(z, \zeta) = \boldsymbol{m}(\zeta)$ for every $(z, \zeta) \in \mathcal{C}$. Actually, z-invariance of the minimizers holds under the more general assumption of cylindrical surfaces of the type $\mathcal{C} := I \times \Gamma$ where $I := [-1, 1]$ and $\Gamma \subseteq \mathbb{R}^2$ is the image of a smooth

Jordan curve $\zeta : [0, 2\pi] \to \Gamma$. Then, one realizes that when $\mathcal{C} = I \times \mathbb{S}^1$, special attention must be deserved to *weakly* axially symmetric configurations. These are defined by the condition that

$$\int_{\mathbb{S}^1} \boldsymbol{m}_\perp(z, \gamma) \mathrm{d}\gamma = 0 \quad \forall z \in I, \tag{4.22}$$

where $\boldsymbol{m}_\perp := \boldsymbol{m} - (\boldsymbol{m} \cdot e_3)\, e_3$. It is simple to prove that every axially symmetric configuration satisfies (4.22). The relevant observation here is that every minimizer of $\mathcal{E}$ in the class of *weakly* axially symmetric competitors is, in fact, axially symmetric. The proof is based on a symmetrization argument in conjunction with the classical Poincaré-Wirtinger inequality for null average and periodic functions. We believe that these results can be transposed to the context of spherical thin films to prove similar results for the energy functional (4.17) in the unexplored regime $\kappa > 0$.

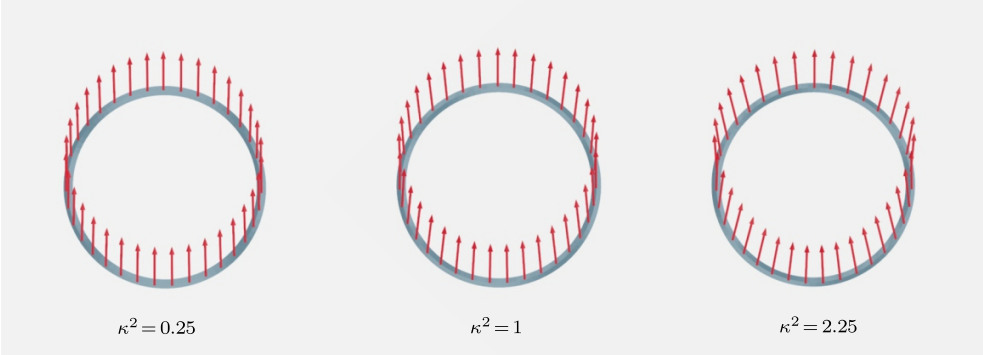

FIG. 11. A plot of the vector fields minimizing the energy (4.21) in $H^1(\mathbb{S}^1, \mathbb{S}^1)$. There is a critical value κ_*^2 of the anisotropy parameter, $\kappa_*^2 \approx 2.31742$, below which the global minimizers of (4.21) have degree zero, and above which the only two global minimizers are the normal vector fields $\pm\boldsymbol{n}$ (and have degree one). From left to right, we plot the minimizers for $\kappa^2 = 0.25$, $\kappa^2 = 1$, and $\kappa^2 = 2.25$.

One can further analyze global minimizers of the energy $\mathcal{E}$ in the unrestricted class $H^1(\mathcal{C}, \mathbb{S}^2)$, i.e., when no *weak* axial symmetry is assumed on the competitors. Then, by deriving a family of sharp Poincaré-type inequalities, one obtains that for $\alpha^2 \geqslant 3$, the normal vector fields $\pm\boldsymbol{n}$ are the only global minimizers of the energy functional $\mathcal{E}$ in $H^1(\mathcal{C}, \mathbb{S}^2)$. Precisely, the following result holds.

PROPOSITION 2 (see [73]). For every value $\alpha^2 > 0$ of the anisotropy, the normal vector fields $\pm\boldsymbol{n}$ are stationary points of the micromagnetic energy functional $\mathcal{E}_\alpha$. If $\alpha^2 \geqslant 3$, the normal vector fields $\pm\boldsymbol{n}$ are the only global minimizers of the energy functional $\mathcal{E}_\alpha$ in $H^1(\mathcal{C}, \mathbb{S}^2)$. Also, they are locally stable for every $\alpha^2 \geqslant 1$ and unstable for $0 < \alpha^2 < 1$. Moreover, when $\alpha^2 > 1$, the normal vector fields $\pm\boldsymbol{n}$ are local minimizers of the energy $\mathcal{E}_\alpha$.

REMARK 4.7. It is simple to show that the constant vector fields $\pm e_3$ are stationary points of the micromagnetic energy functional and they are unstable for all $\kappa^2 > 0$. Despite this, one can prove that they are stable in the class of axially symmetric minimizers.

Finally, motivated by their importance in numerical simulations, one is interested in global minimizers of $\mathcal{E}_\alpha$ in the class of in-plane configurations. In [73] it is shown that if $\boldsymbol{m}_\perp \in H^1(\mathbb{S}^1, \mathbb{S}^1)$ is the *profile* of a minimizer of $\mathcal{E}_\alpha$, then either $\deg \boldsymbol{m}_\perp = 0$ or $\deg \boldsymbol{m}_\perp = 1$ (cf. Figure 11). Indeed, there exists a threshold value α_*^2 of the anisotropy parameter such that the normal vector fields $\pm\boldsymbol{n}$ are the only two in-plane energy minimizers when $\kappa^2 > \kappa_*^2$ and the common minimum value of the energy is 2π. Instead, when $\kappa^2 < \kappa_*^2$, the minimal energy depends on κ^2. The precise minimal values and the analytic expressions of the minimizers can be written in terms of elliptic integrals.

There are several analogies in the behavior of the minimizers of the micromagnetic energy in cylindrical and spherical surfaces. However, there are also remarkable exceptions. Indeed, in both cases, the normal vector fields turn out to be the unique global minimizers of the energy functional in a wide range of the parameters [76]. Nevertheless, the topological implications are different. On the one hand, the normal vector fields to $\mathbb{S}^2$ carry a different skyrmion number because $\deg(\pm\boldsymbol{n}_{\mathbb{S}^2}) = \pm 1$, and, by Hopf's theorem, they cannot be homotopically mapped one into the other (this translates into the so-called topological protection of the ground states). On the other hand, due to the odd dimension, the two normal vector fields to $\mathbb{S}^1$ have the same degree, and therefore, they can be easily switched one to the other through suitable external perturbation.

5. One-dimensional domain walls in thin film ferromagnets: an overview (by C. Muratov).

5.1. *Introduction.* Magnetism is a physical phenomenon that has been known to mankind for at least two millennia. In nature, it manifests itself in the ability of the naturally magnetized mineral magnetite to exert an attractive force on objects made of iron. Importantly, this interaction represents one of the basic examples of *actio ad distans*, since a piece of iron feels the force of a magnet separated from it by a macroscopically large distance. The latter is due to the nonlocal character of the interaction that is mediated by the magnetic field.

Despite its long history, magnetism remained a poorly understood phenomenon until the early 20th century. The 1907 work of Weiss was the first to explain the macroscopic alignment of the individual magnetic moments of atoms in a ferromagnet through the concept of the *molecular field* [211]. Yet it took another 20 years with the works of Pauli, Dirac and Heisenberg during the "golden age" of quantum mechanics to identify the microscopic origin of ferromagnetism as a manifestation of the Pauli exclusion principle and spin – a purely quantum-mechanical degree of freedom of a particle [191, 77, 108, 109, 78]. The exclusion principle gives rise to the Heisenberg exchange interaction between electrons, which, in turn, leads to the emergence of a macroscopic magnetic moment in ferromagnets due to the alignment of the electron spins.

Heisenberg exchange favors alignment of spins of the neighboring electrons in a ferromagnetic material, creating a non-zero magnetization that would ideally be uniform in space. However, such a uniform magnetization generates a magnetic field that does not always favor alignment of the spins at large distances. The competition of Heisenberg exchange with the magnetostatic interaction gives rise to the notion of *magnetic domains*, introduced in the 1926 book of Weiss and Foëx, whereby the magnetization in a ferromagnet consists of extended regions of space in which the spins are aligned, separated by sharp transition regions [212]. These types of configurations can lower the magnetostatic interaction energy via fine scale oscillations of the magnetization between different domains, which results in a vast variety of the observed magnetic domain patterns [112].

The theory of magnetic domains was put on a solid theoretical footing in 1935 through the work of Landau and Lifshitz, who formulated what is now known as the *micromagnetic modeling framework* [134]. Landau and Lifshitz interpreted the observed magnetization patterns as the result of the minimization of the micromagnetic energy functional, defined on three-dimensional vector fields of constant length. Their ideas were further extended in the works of Néel, Kittel and Brown [183, 184, 122, 33, 34]. Furthermore, the dynamics of the magnetization in response to external influences may be studied with the help of the Landau-Lifshitz-Gilbert equation and its extensions [134, 100, 32, 93]. Stochastic effects may also be added to study the effect of thermal noise on the magnetization, as pioneered by Brown [35]. Today these formulations find their implementations in the form of efficient numerical algorithms that allow to explore the complexity of the magnetic systems computationally [97, 138, 187, 86].

From the mathematical point of view, micromagnetics pose a great number of challenging problems, from calculus of variations, to nonlinear dynamics, to stochastic analysis.

This field caught the attention of mathematicians fairly recently, but has already generated a large and growing body of literature (for an excellent review from 2006, see [68]). In the calculus of variations, one is faced with highly nonlinear, nonlocal, often topologically constrained minimization problems that involve multiple spatial scales. It is only very recently that the basic ideas of the theories of magnetic domains began to receive rigorous mathematical treatment, with the methods of asymptotic analysis in the calculus of variations playing a significant role (see, e.g., [43, 44, 49, 189, 125, 66, 126], this list is certainly not exhaustive).

The basic ingredient in the analysis of the domain structure of ferromagnets is the domain wall solution, which represents a one-dimensional transition layer profile that connects different values of the magnetization at the opposite sides. This note aims at giving a brief overview of the state of the art and some open questions in the modeling and analysis of domain wall solutions in thin ferromagnetic films with the magnetization lying mostly in the film plane.

5.2. *Micromagnetic energy functional.* The starting point of micromagnetic modeling is the micromagnetic energy functional $E(\mathbf{M})$ defined on a vector field $\mathbf{M}:\Omega\to\mathbb{R}^3$ that represents the *magnetization vector*, i.e., the vector-valued magnetic dipole moment per unit volume, in a ferromagnetic body occupying a bounded three-dimensional domain Ω in free space. The length of the magnetization vector is fixed to be equal to the saturation magnetization, i.e., $|\mathbf{M}(\mathbf{r})|=M_s$ for all $\mathbf{r}=(x,y,z)\in\Omega$, but the direction of $\mathbf{M}(\mathbf{r})$ is allowed to be arbitrary. If Ω is occupied by a bulk uniaxial ferromagnetic single crystal with the easy axis along the y-axis, the micromagnetic energy takes the form (in the SI units) [135]

$$E(\mathbf{M})=\frac{A}{M_s^2}\int_\Omega|\nabla\mathbf{M}|^2\,d^3r+\frac{K}{M_s^2}\int_\Omega(M_1^2+M_3^2)\,d^3r \\ -\mu_0\int_\Omega\mathbf{M}\cdot\mathbf{H}\,d^3r+\mu_0\int_{\mathbb{R}^3}\int_{\mathbb{R}^3}\frac{\nabla\cdot\mathbf{M}(\mathbf{r})\,\nabla\cdot\mathbf{M}(\mathbf{r}')}{8\pi|\mathbf{r}-\mathbf{r}'|}\,d^3r\,d^3r'. \tag{5.1}$$

Here $\mathbf{M}=(M_1,M_2,M_3)$, and the terms, in order of appearance, are the exchange, the magnetocrystalline anisotropy, the Zeeman and the magnetostatic energy, also referred to as the stray field energy, respectively. The constants A,K,μ_0 are, respectively, the exchange stiffness, the anisotropy constant and the permeability of vacuum, and $\mathbf{H}$ is the applied external magnetic field. In the last term in (5.1), the magnetization vector $\mathbf{M}$ is extended by zero outside Ω and $\nabla\cdot\mathbf{M}$ is understood distributionally. In writing (5.1), the effects of magnetostrsiction and other, more exotic interactions have been neglected [135].

The exchange energy in (5.1) forces the magnetization to be spatially uniform, while the anisotropy energy forces the magnetization to align with $\pm\hat{\mathbf{y}}$. The Zeeman term favors alignment of the magnetization along the applied field $\mathbf{H}$. The stray field energy, in contrast, is a non-negative term that can be viewed as the Coulombic energy of the "magnetic charges" with density $\rho=-\nabla\cdot\mathbf{M}$ and, therefore, forcing the distributional divergence of the magnetization to be zero.

When $\Omega=\mathbb{R}^3$ and $\mathbf{H}=0$, the energy in (5.1) is explicitly minimized by $\mathbf{M}=\pm M_s\hat{\mathbf{y}}$, illustrating the fundamental bistability of the magnetization in a uniaxial ferromagnetic crystal. It was quickly recognized, however, that in a large but finite sample $\Omega\subset\mathbb{R}^3$ a

spatially uniform magnetization would result in a high stray field due to the jumps of the magnetization to zero at $\partial\Omega$, leading to a large magnetostatic energy term. Instead, the energy is reduced by dividing Ω into subdomains in which $\mathbf{M}$ alternates between the two preferred orientations, thus creating a domain structure. The first step in understanding the latter is to understand the structure of the transition layer between the two preferred orientations of $\mathbf{M}$.

5.3. *Domain walls in bulk materials.* Domain walls are the basic building blocks of the magnetic domains. The concept of a domain wall as a narrow transition region separating the two distinct orientations of the magnetization was first proposed by Bloch [24], but within the micromagnetic modeling framework it was formulated by Landau and Lifshitz [134] and further developed by Néel [185]. We can conveniently rewrite the stray field energy with the help of the magnetostatic potential U solving

$$\Delta U = \nabla \cdot \mathbf{M} \qquad \text{in} \quad \mathcal{D}'(\mathbb{R}^3) \tag{5.2}$$

and vanishing at infinity. In the absence of the applied field the energy is then [33, 135, 75]

$$E(\mathbf{M}) = \frac{A}{M_s^2}\int_\Omega |\nabla \mathbf{M}|^2\, d^3r + \frac{K}{M_s^2}\int_\Omega (M_1^2 + M_3^2)\, d^3r + \frac{\mu_0}{2}\int_\Omega |\nabla U|^2\, d^3r. \tag{5.3}$$

We next extend the above discussion to the case $\Omega = \mathbb{R}^3$ and assume that $\mathbf{M} = \mathbf{M}(x)$, i.e., that $\mathbf{M}$ varies only along $\hat{\mathbf{x}}$. We further assume that $\mathbf{M}$ satisfies

$$\lim_{x\to\pm\infty} \mathbf{M}(x) = \pm M_s \hat{\mathbf{y}}, \tag{5.4}$$

and that the gradient of U vanishes as $x \to \pm\infty$. Then the energy per unit area in the yz-plane is

$$E_{1\mathrm{d}}(\mathbf{M}) = \int_{-\infty}^{\infty} \left(\frac{A}{M_s^2}|\mathbf{M}'|^2 + \frac{K}{M_s^2}(M_1^2 + M_3^2) + \frac{\mu_0}{2} M_1^2 \right) dx, \tag{5.5}$$

where we took into account that the solution of (5.2) in this case yields $\nabla U = M_1 \hat{\mathbf{x}}$.

Landau and Lifshitz approached the problem of determining the domain wall profile by assuming that $M_1 = 0$ to make the stray field contribution to the energy vanish. This *ansatz* then implies that we can write $\mathbf{M} = \mathbf{M}_0$, where

$$\mathbf{M}_0 = M_s(0, \cos\theta, \sin\theta), \tag{5.6}$$

for some rotation angle $\theta = \theta(x)$ to be determined. Assuming that $\mathbf{M}_0$ from (5.6) minimizes the energy in (5.5) among the profiles satisfying (5.4), one obtains

$$A\theta'' - K\sin\theta\cos\theta = 0, \qquad \theta(-\infty) = \pm\pi, \qquad \theta(+\infty) = 0, \tag{5.7}$$

whose unique solution, up to translations, is

$$\theta = \pm \arccos(\tanh(x/L)), \tag{5.8}$$

where $L = \sqrt{K/A}$ is the wall width [134]. This solution is referred to as the *Bloch wall* solution. The corresponding wall energy per unit area is $E_{1\mathrm{d}}(\mathbf{M}_0) = 4\sqrt{AK}$. Thus, the domain wall is expected to give a net contribution proportional to the domain wall area to the energy of the magnetic domains.

One may wonder to which extent this logic is mathematically sound. At the level of the one-dimensional energy $E_{1\mathrm{d}}$, why should the magnetization $\mathbf{M}$ admit the representation in

(5.6), and even if it does, why should it satisfy the conditions at infinity in (5.7), namely, not exhibit *winding*, which would correspond to adding integer multiples of 2π to one of the limits? Going to higher dimensions, would the obtained profile also minimize the energy in (5.3) when, say, $\Omega = \mathbb{R} \times [0, l)^2$, for $l > 0$, and periodicity in y and z? More broadly, is the obtained profile the unique, up to translations, critical point of $E_{1\mathrm{d}}$ or E among profiles with suitable behavior at infinity? What if $\Omega = \mathbb{R}^3$?

These questions bear a striking similarity with another problem arising in the context of phase field models of phase transitions [103] that has received considerable attention in the mathematical community under the name of the *De Giorgi conjecture* (for a review, see [61]). In its canonical form, De Giorgi conjecture states that the only bounded solutions $u : \mathbb{R}^n \to \mathbb{R}$ of the Euler-Lagrange equation

$$\Delta u + u - u^3 = 0 \tag{5.9}$$

associated with the Ginzburg-Landau energy

$$E_{\mathrm{GL}}(u) = \int_\Omega \left(\frac{1}{2} |\nabla u|^2 + \frac{1}{4}(1 - u^2)^2 \right) d^n r \tag{5.10}$$

for every $\Omega \subset \mathbb{R}^n$ bounded, which are monotone in one spatial variable are one-dimensional, i.e., $u(x_1, \dots, x_n) = \tanh(x_1/\sqrt{2})$ after a rotation and a translation [59]. In the physical dimensions, $n = 2, 3$, the conjecture was proved by Ghoussoub and Gui [98] and Ambrosio and Cabré [7], respectively. A simpler version of this conjecture additionally assumes that the solution approaches $u = \pm 1$ along the direction of monotonicity, and when this limit is uniform, the solution is known to be one-dimensional without the need of a rotation or monotonicity assumption (see [61] and references therein). In particular, the latter result applies when $\Omega = \mathbb{R} \times [0, l)^2$, for any $l > 0$, to any finite energy solution of (5.9) connecting $u = \pm 1$ as $x \to \pm\infty$.

The corresponding problem associated with (5.3) represents a vectorial and nonlocal extension of the above problem, and is in general considerably more challenging, even with additional assumptions on the behavior of the solution "at infinity". One may naturally ask whether, say, the solution given by (5.6) and (5.8) is the unique, up to translations, minimizer of (5.3) satisfying (5.4) for $\Omega = \mathbb{R} \times [0, l)^2$ and periodic boundary conditions, for any $l > 0$. The answer to this question may be rather easily seen to be positive, but in fact it does not involve the solution of the very complicated Euler-Lagrange equation associated with (5.3). Instead, one can proceed with the help of the vectorial version of the Modica-Mortola trick [172], which is available for the problems of micromagnetics [128]. For example, setting $\mathbf{m} = \mathbf{M}/M_s$, in one space dimension we have (see also [96])

$$\begin{aligned} E_{1\mathrm{d}}(\mathbf{M}) &\geq \int_{\mathbb{R}} \big(A|\nabla \mathbf{m}|^2 + K(m_1^2 + m_3^2) \big) dx \\ &\geq \int_{\mathbb{R}} \left(A \frac{|m_2'|^2}{1 - m_2^2} + K(1 - m_2^2) \right) dx \\ &\geq 2\sqrt{AK} \int_{\mathbb{R}} |m_2'| dx \\ &\geq 4\sqrt{AK} = E_{1\mathrm{d}}(\mathbf{M}_0), \end{aligned} \tag{5.11}$$

and, therefore, $E(\mathbf{M}) \geq l^2 E_{1\mathrm{d}}(\mathbf{M}_0)$, with equality if and only if $\mathbf{M} = \mathbf{M}_0$ in $\Omega = \mathbb{R} \times [0, l)^2$, up to a translation.

However, things get more complicated if one only requires that $\mathbf{M}$ be a local minimizer, or even a critical point of E. Even in one dimension, the question as to whether $\mathbf{M}_0$ is the only critical point of $E_{1\mathrm{d}}$ satisfying (5.4) would require solving a system of nonlinear ordinary differential equations associated with (5.5) and includes a possibility of winding solutions. Things come to the next level of complexity in higher dimensions due to the nonlocality introduced by (5.2), and even further complexity arises due to severe lack of compactness when $\Omega = \mathbb{R}^3$. In particular, in contrast to the scalar problem in (5.9) the vectorial problem associated with (5.3) lacks rotational symmetry. Furthermore, simply changing the orientation of the wall, e.g., taking $\mathbf{M} = \mathbf{M}_0(y)$ immediately results in an infinite wall energy per unit area, since the wall becomes *charged* and, therefore, the magnetostatic potential U solving (5.2) exhibits an asymptotically linear behavior far away from the wall.

5.4. *Micromagnetics of thin films.* We now turn to the situation in which Ω is a domain in the form of an extended film, i.e., $\Omega = \mathbb{R}^2 \times (0, d)$, where d is the film thickness. Notice that in this case the uniform magnetization configurations $\mathbf{M} = \pm M_s \hat{\mathbf{y}}$ do not produce any stray field and, therefore, are still the global minimizers of the energy in (5.3) for $\mathbf{H} = 0$. At the same time, the one-dimensional domain wall profile given by (5.6) and (5.8) is no longer a minimizer of (5.3) per unit length in the y-direction, since it generates a stray field due to the jump of the magnetization at the top and bottom surfaces of the film, $z = 0$ and $z = d$. For sufficiently thick films, this stray field modifies the wall profile only in the small vicinity of the surfaces by creating the Néel caps [196], unless the material is magnetically sufficiently soft [133, 80]. At the same time, as was pointed out in 1955 by Néel, as the thickness of the film becomes sufficiently small it becomes energetically favorable for the magnetization to rotate in the film plane, giving rise to a *Néel wall* [186]. This is due to the appearance of a *shape anisotropy*, whereby to the leading order the stray field energy behaves as a local penalty term for the out-of-plane component of the magnetization [214, 101]. It can be most easily seen from the solution of (5.2) for a spatially uniform magnetization, in which case $\nabla U = M_3 \hat{\mathbf{z}} \chi_{(0,d)}(z)$, where here and everywhere below χ_D denotes the characteristic function of the set D, generating an additional anisotropy-like term in (5.3). When the film thickness decreases, a transition from the Bloch to the Néel wall occurs [186, 69, 209].

For *thin films*, i.e., films whose thickness is smaller than the exchange length $\ell_{\mathrm{ex}} = \sqrt{2A/(\mu_0 M_s^2)}$, which is the characteristic length scale at which the exchange and the magnetostatic interactions balance each other, the magnetization vector becomes nearly independent of z, and due to the strong shape anisotropy the magnetization is forced to lie almost entirely in the film plane in magnetically soft materials. There are many possible combinations of the material and geometric parameters that lead to a whole hierarchy of thin film regimes [66, 129, 176, 177, 116, 126, 114, 173] (this list is not meant to be exhaustive). For Néel walls in extended films with moderate magnetocrystalline anisotropy, an appropriate model that balances the exchange, anisotropy and the magnetostatic energy as the film thickness vanishes was introduced in [177] (see also [65, 39]). Assuming that $\Omega = D \times (0, d)$ for some $D \subseteq \mathbb{R}^2$ and that $\mathbf{M}(x, y, z) = M_s(\mathbf{m}(x, y)\chi_{(0,d)}(z), 0)$ for

some $\mathbf{m} : \mathbb{R}^2 \to \mathbb{S}^1 \cup \{0\}$ with $|\mathbf{m}| = \chi_D$, we can compute the energy of the magnetization configuration explicitly (below we follow the presentation in [160]). Measuring the lengths in the units of the Bloch wall width $L = \sqrt{A/K}$, the energy in the units of $2Ad$, and introducing the dimensionless *thin film parameter*

$$\nu = \frac{\mu_0 M_s^2 d}{2\sqrt{AK}}, \tag{5.12}$$

we arrive at the following expression for the energy [95]:

$$E(\mathbf{m}) = \frac{1}{2}\int_D \left(|\nabla \mathbf{m}|^2 + m_1^2 - 2\mathbf{h}\cdot\mathbf{m}\right) d^2r + \frac{\nu}{2}\int_{\mathbb{R}^2}\int_{\mathbb{R}^2} K_\delta(|\mathbf{r}-\mathbf{r}'|)\nabla\cdot\mathbf{m}(\mathbf{r})\,\nabla\cdot\mathbf{m}(\mathbf{r})\,d^2r\,d^2r', \tag{5.13}$$

where

$$K_\delta(r) = \frac{1}{2\pi\delta}\left\{\ln\left(\frac{\delta+\sqrt{\delta^2+r^2}}{r}\right) - \sqrt{1+\frac{r^2}{\delta^2}} + \frac{r}{\delta}\right\}, \tag{5.14}$$

$\delta = d/L$ is the dimensionless film thickness, and we set $\mathbf{H} = K/(\mu_0 M_s)(\mathbf{h}, 0)$ for $\mathbf{h} : \mathbb{R}^2 \to \mathbb{R}^2$, assuming that the applied field lies in the film plane.

Observe that when δ is small, we have

$$K_\delta(r) \simeq \frac{1}{4\pi r} \qquad \text{and} \qquad \int_{\partial D} K_\delta(|\mathbf{r}-\mathbf{r}'|)\,d\mathcal{H}^1(\mathbf{r}') \simeq \frac{1}{2\pi}\ln\delta^{-1}. \tag{5.15}$$

Therefore, to the leading order as $\delta \to 0$ we have $E(\mathbf{m}) \simeq E_\delta(\mathbf{m})$, where

$$E_\delta(\mathbf{m}) = \frac{1}{2}\int_D \left(|\nabla\mathbf{m}|^2 + m_1^2 - 2\mathbf{h}\cdot\mathbf{m}\right) d^2r + \frac{\nu}{8\pi}\int_D\int_D \frac{\nabla\cdot\mathbf{m}(\mathbf{r})\,\nabla\cdot\mathbf{m}(\mathbf{r})}{|\mathbf{r}-\mathbf{r}'|}\,d^2r\,d^2r' - \frac{\nu}{4\pi}\int_D\int_{\partial D}\frac{\nabla\cdot\mathbf{m}(\mathbf{r})(\mathbf{m}(\mathbf{r}')\cdot\mathbf{n}(\mathbf{r}'))}{|\mathbf{r}-\mathbf{r}'|}\,d\mathcal{H}^1(\mathbf{r}')\,d^2r + \frac{\nu\ln\delta^{-1}}{4\pi}\int_{\partial D}(\mathbf{m}(\mathbf{r})\cdot\mathbf{n}(\mathbf{r}))^2\,d\mathcal{H}^1(\mathbf{r}), \tag{5.16}$$

where $\mathbf{n}(\mathbf{r})$ denotes the outward unit normal at $\mathbf{r} \in \partial D$. As the last term in (5.16) forces $\mathbf{m}\cdot\mathbf{n} = 0$, in the limit we arrive at

$$E_0(\mathbf{m}) = \frac{1}{2}\int_D \left(|\nabla\mathbf{m}|^2 + m_1^2 - 2\mathbf{h}\cdot\mathbf{m}\right) d^2r + \frac{\nu}{8\pi}\int_D\int_D \frac{\nabla\cdot\mathbf{m}(\mathbf{r})\,\nabla\cdot\mathbf{m}(\mathbf{r})}{|\mathbf{r}-\mathbf{r}'|}\,d^2r\,d^2r', \tag{5.17}$$

with admissible configurations $\mathbf{m} \in H^1(D;\mathbb{S}^1)$ satisfying Dirichlet boundary condition $\mathbf{m} = s\mathbf{t}$ on ∂D, where $\mathbf{t}$ is the positively oriented unit tangent vector to ∂D and $s : \partial D \to \{-1, 1\}$ is constant on each connected component of ∂D.

The reduced thin film energy in (5.17) may be rigorously justified via a uniform Γ-expansion in the limit of vanishing film thickness [126], provided that the anisotropy constant K and the applied field $\mathbf{h}$ scale as $O(d^2)$, which is appropriate for moderately soft ferromagnetic materials of a few nanometer thickness [107, 177]. Notice that it represents a different regime from the thin film limits considered by De Simone, Kohn, Müller and Otto in [66], which are relevant to extremely soft ferromagnetic materials such as permalloy and in which the magnetostatic energy dominates. The connection

of the energy in (5.17) with the latter is obtained by considering the regime of $\nu \gg 1$. Similarly, the regime that leads to (5.17) is different from the one studied by Kohn and Slastikov in [129], which corresponds to specimens of small lateral extent (see also [173]). Also notice that the energy in (5.16) does not support boundary vortices, which appear in the regime studied by Moser [176].

5.5. *Domain walls in thin films.* The analysis of domain wall profiles in thin films requires to extend (5.17) to the cases in which the film domain D is unbounded. Therefore, we first modify the functional to make the energy of the ferromagnetic state zero in the presence of the applied field $\mathbf{h} = (h_1, h_2)$ for either $0 \leq h_1 < 1$ and $h_2 = 0$, or $h_1 = 0$ and $h_2 > 0$, corresponding to two cases of interest, namely, the field applied in the direction perpendicular to the easy axis and the field applied along the easy axis:

$$E(\mathbf{m}) = \frac{1}{2}\int_{\mathbb{R}^2} \Big(|\nabla \mathbf{m}|^2 + (m_1 - h_1)^2 + 2h_2(1 - m_2)\Big) d^2r + \frac{\nu}{8\pi}\int_{\mathbb{R}^2}\int_{\mathbb{R}^2} \frac{\nabla \cdot \mathbf{m}(\mathbf{r})\, \nabla \cdot \mathbf{m}(\mathbf{r})}{|\mathbf{r} - \mathbf{r}'|}\, d^2r\, d^2r', \tag{5.18}$$

where we dropped the subscript zero from the energy to simplify notations. In the first case, the ground states of the energy are $\mathbf{m} = (h_1, \pm\sqrt{1 - h_1^2})$, while in the second case the ground state is $\mathbf{m} = (0, 1)$. The case of zero applied field is included in the first case, and the case $h_1 \geq 1$ and $h_2 = 0$ is analogous to the second case.

We also need to derive a one-dimensional analog of the energy in (5.18). To that end, we assume that $\mathbf{m} = \mathbf{m}(\xi)$, where $\xi = x\cos\beta + y\sin\beta$ for some $\beta \in [0, \frac{\pi}{2}]$, i.e., that $\mathbf{m}$ varies only along the direction $(\cos\beta, \sin\beta)$ in the xy-plane. Writing $\mathbf{m} = (-\sin\theta, \cos\theta)$, where θ is the angle between the magnetization vector and the easy axis measured counterclockwise, we then have that the energy per unit length normal to the $(\cos\beta, \sin\beta)$ direction is [160]

$$E_\beta(\theta) = \frac{1}{2}\int_{-\infty}^{\infty} \big(|\theta'|^2 + (\sin\theta - h_1)^2 + 2h_2(1 - \cos\theta)\big)\, d\xi + \frac{\nu}{8\pi}\int_{-\infty}^{\infty}\int_{-\infty}^{\infty} \frac{(\sin(\theta(\xi) - \beta) - \sin(\theta(\xi') - \beta))^2}{(\xi - \xi')^2}\, d\xi\, d\xi'. \tag{5.19}$$

The associated Euler-Lagrange equation is

$$0 = \frac{d^2\theta}{d\xi^2} + h_1\cos\theta - (h_2 + \cos\theta)\sin\theta - \frac{\nu}{2}\cos(\theta - \beta)\left(-\frac{d^2}{d\xi^2}\right)^{1/2}\sin(\theta - \beta), \tag{5.20}$$

where

$$\left(-\frac{d^2}{d\xi^2}\right)^{1/2} u(\xi) = \frac{1}{\pi}⨍_{-\infty}^{\infty} \frac{u(\xi) - u(\xi')}{(\xi - \xi')^2}\, d\xi', \tag{5.21}$$

and $⨍$ denotes the principal value of the integral.

Before discussing the results and open questions for solutions of (5.20), let us recall what happens in the local case $\nu = 0$. In this case an elementary phase plane analysis shows that the only solutions that connect distinct equilibria at infinity are those that connect the adjacent minima of the potential energy term in (5.19). In particular, when $h_1 = h_2 = 0$, we must have $\theta(+\infty) - \theta(-\infty) = \pm\pi$, resulting in a 180-degree wall, while for $h_1 = 0$

and $h_2 > 0$ we must have $\theta(+\infty) - \theta(-\infty) = \pm 2\pi$, resulting in a 360-degree wall. When $h_2 = 0$ and $0 < h_1 < 1$, the solutions satisfy either $\theta(+\infty) - \theta(-\infty) = \pm(\pi - 2\arcsin h_1)$ or $\theta(+\infty) - \theta(-\infty) = \pm(\pi + 2\arcsin h_1)$. These solutions remain the only monotone solutions connecting the respective equilibria, up to rotations, in two space dimensions by the results of [98]. For $h_1 = 0$ they are energy minimizing, and when $0 < h_1 < 1$ the solution with the smaller variation is energy minimizing. Finally, their profiles may be computed by an explicit integration, just like in the case of the Bloch wall profile.

5.5.1. *180-degree uncharged walls.* As soon as $\nu > 0$, the analysis of (5.20) becomes much more complicated than in the case $\nu = 0$, as the problem becomes nonlocal and its solution can no longer be written down in closed form. In fact, this gave rise to a significant controversy about the structure of the 180-degree Néel wall profile in the physics literature (for a discussion, see [2] and [112]). Note that the 180-degree Néel walls are routinely observed experimentally in sufficiently thin, magnetically soft films [112, 20].

Early studies of 180-degree Néel walls relied on either ansatz-based, or numerical, or perturbative minimizations of the analog of (5.19) with $h_1 = h_2 = 0$ and $\beta = 0$ that is obtained from (5.13) [69, 48, 193, 95, 96]. The first rigorous analysis of existence and qualitative properties of the wall profiles, still in the context of (5.13), was carried out by Melcher [168] (see also [39] for a discussion of (5.19)). A comprehensive study of the energy minimizing profiles connecting distinct equilibria within the context of (5.19) with $0 \leq h_1 < 1$, $h_2 = 0$, and $\beta = 0$ was carried out by Chermisi and Muratov, in which existence, monotonicity, asymptotic decay and uniqueness of minimizers connecting the equilibrium $\theta = \arcsin h_1$ with $\theta = \pi - \arcsin h_1$ were established [41]. Furthermore, uniqueness of monotone solutions connecting these equilibria was established by Muratov and Yan, taking advantage of the hidden convexity of the one-dimensional energy [180]. Notice that such a result is non-trivial even in one space dimension, as in the nonlocal setting it is not a priori clear whether the solutions of (5.20) must necessarily be monotone. While it is known that the energy minimizing solution is monotone and vice versa, it is not known whether non-monotone domain wall solutions to (5.20) with $\beta = 0$ might also exist.

It would be interesting to see whether the monotone one-dimensional solutions to (5.20) with $\beta = 0$ also remain the unique monotone critical points of (5.17) with $D = \{(x, y) \in \mathbb{R}^2 : -l/2 < y < l/2\}$, a strip with width $l > 0$ and subject to periodicity in y. The vectorial nature of the problem prevents the use of monotone rearrangements to show that the minimizers are still monotone in this setting, contrary to the one-dimensional case. The only available result concerning the one-dimensionality of the minimizers that is currently available in this context is that of De Simone, Knüpfer and Otto, who studied a similar problem on a strip, but with clamped magnetization away from the origin and neglecting the magnetocrystalline anisotropy [64]. Introducing a small parameter in front of the exchange term, they showed that as this parameter tends to zero, the domain wall energy is *asymptotically* minimized by a one-dimensional profile. It is not known if the asymptotic profile is, in fact, one-dimensional for small but finite value of the parameter, nor is it known that the profile of the minimizer converges to a suitable discontinuous one-dimensional profile.

In connection with (5.18) and in the spirit of [64], one could also consider the following version of the energy

$$E_\varepsilon(\mathbf{m}) = \frac{1}{2}\int_{\mathbb{R}\times(-l/2,l/2)} \left(\varepsilon|\nabla\mathbf{m}|^2 + \frac{1}{\varepsilon}m_1^2\right) d^2r + \frac{\nu}{8\pi}\int_{\mathbb{R}\times(-l/2,l/2)}\int_{\mathbb{R}^2} \frac{\nabla\cdot\mathbf{m}(\mathbf{r})\,\nabla\cdot\mathbf{m}(\mathbf{r})}{|\mathbf{r}-\mathbf{r}'|}\, d^2r\, d^2r', \tag{5.22}$$

obtained by rescaling all lengths by ε, as in the Modica-Mortola rescaling and fixing the domain to be a strip after the rescaling. In one dimension the minimizer of this problem, which is simply a rescaling of the minimizer of (5.19) with $\beta = 0$, clearly converges to $\boldsymbol{m}(x) = \operatorname{sgn}(x)\hat{\mathbf{y}}$ as $\varepsilon \to 0$, after suitable translations. Whether the same conclusion holds on the strip remains to be seen, even if it seems to be plausible, as the energy minimizing magnetizations must converge to a function in $BV(\mathbb{R}\times(-l/2,l/2);\mathbb{R}^2)$ taking values $\pm\hat{\mathbf{y}}$ due to the Modica-Mortola estimate on the first two terms in the energy. Also, any deviations of the jump set of the limit function from a vertical line would create large stray field contributions that would be heavily penalized by the last term in (5.22). In fact, if ε is the width of the transition region between $\mathbf{m} = \hat{\mathbf{y}}$ and $\mathbf{m} = -\hat{\mathbf{y}}$ which makes an angle α with the vertical, then the last term can be seen to yield a contribution of order $|\ln\varepsilon|\sin^2\alpha$. It is then also natural to ask if one recovers the total variation of m_1 as the Γ-limit of E_ε in (5.22) as $\varepsilon \to 0$ if ν is replaced by $\nu_\varepsilon = \gamma|\ln\varepsilon|^{-1}$ for $\gamma > 0$ fixed. Surprisingly, the latter seems to be false, as the recovery sequence of the Modica-Mortola theory would generate a strictly positive magnetostatic contribution on the parts of the jump set where the distributional gradient of m_1 is not aligned with the x-axis. Lastly, we would like to mention that studying a version of (5.22) defined on $\mathbf{m} = (-\sin\theta, \cos\theta)$ as a functional of θ is, in turn, more subtle, as the latter keeps track of the winding of the magnetization, while the one in (5.22) does not. In particular, the energy in (5.22) would not be able to capture 360-degree walls in the limit (see also section 5.5.3).

5.5.2. *180-degree charged walls.* The domain walls considered so far do not carry a net "magnetic charge" [112]. More precisely, integrating the non-dimensionalized bulk magnetic charge density $\rho = -\nabla\cdot\mathbf{m}$ per unit length over these profiles yields the jump of the component of the magnetization along the wall, which is zero when $\beta = 0$. However, for $\beta \neq 0$ the magnitude of the jump of the magnetization is equal to $2\sin\beta \neq 0$ when $\mathbf{m}(\pm\infty) = \pm\hat{\mathbf{y}}$. This immediately makes the magnetostatic energy infinite:

$$\begin{aligned}\int_{-\infty}^{\infty}\int_{-\infty}^{\infty} \frac{(\sin(\theta(\xi)-\beta) - \sin(\theta(\xi')-\beta))^2}{(\xi-\xi')^2}\, d\xi\, d\xi' &\geq \int_R^\infty\int_{-\infty}^0 \frac{\sin^2(\theta(\xi')-\beta)}{(\xi-\xi')^2}\, d\xi\, d\xi' \\ &\geq \int_R^\infty \frac{\sin^2(\theta(\xi')-\beta)}{\xi'}\, d\xi' \geq \frac{1}{2}\sin^2\beta\int_R^\infty \frac{d\xi'}{\xi'} = +\infty,\end{aligned} \tag{5.23}$$

where we assumed without loss of generality that $\beta < \theta(\xi) < \beta + \pi$ for $\xi < 0$ and chose a sufficiently large $R > 0$ such that $\sin^2(\theta(\xi')-\beta) \geq \frac{1}{2}\sin^2\beta > 0$ for all $\xi' > R$. Thus, paradoxically there are no finite energy solutions to (5.20) for any $\beta \in (0, \frac{\pi}{2}]$. Nevertheless, one may wonder if (5.20) does have solutions with $\theta(+\infty) = 0$ and $\theta(-\infty) = \pm\pi$, as is the case when $\nu = 0$. At present, this question is completely open.

A closely related question was recently addressed by Lund, Muratov and Slastikov in a slightly different context [160]. They considered the situation in which the ferromagnetic film occupies a half-plane instead of the whole plane, and *edge domain walls* are expected due to the boundary penalty term forcing the magnetization to be tangential to the boundary [110, 210, 195, 167]. These magnetization configurations would solve a Dirichlet problem for (5.20) with $\xi > 0$ and the boundary condition $\theta(0) = \beta$, provided that $\sin(\theta - \beta)$ is set to zero in the nonlocal term for $\xi < 0$. Clearly, such a wall is bound to be charged if $\theta(+\infty) \in \pi\mathbb{Z}$ in order for the anisotropy energy to remain finite.

Lund, Muratov and Slastikov proved existence of solutions for the above problem by minimizing the *renormalized energy* obtained from (5.19) by subtracting the leading order divergent term at infinity from the nonlocal term. This leads to considering

$$E_\beta(\theta) = \int_0^\infty \left(\frac{1}{2}|\theta'|^2 + \frac{1}{2}\sin^2\theta + \frac{\nu}{4\pi} \cdot \frac{\sin^2(\theta-\beta) - \sin^2(\eta_\beta - \beta)}{\xi} \right) d\xi + \frac{\nu}{8\pi} \int_0^\infty \int_0^\infty \frac{(\sin(\theta(\xi)-\beta) - \sin(\theta(\xi')-\beta))^2}{(\xi-\xi')^2}\, d\xi\, d\xi' - \frac{\nu}{8\pi} \int_0^\infty \int_0^\infty \frac{(\sin(\eta_\beta(\xi)-\beta) - \sin(\eta_\beta(\xi')-\beta))^2}{(\xi-\xi')^2}\, d\xi\, d\xi', \quad (5.24)$$

where $\eta_\beta(\xi)$ is a fixed smooth non-increasing cutoff function such that $\eta_\beta(\xi) = \beta$ for all $\xi < 0$ and $\eta_\beta(\xi) = 0$ for all $\xi > 1$, and the minimization is carried out over all $\theta - \beta \in \mathring{H}^1_0(\mathbb{R}^+)$. Formally, it is not difficult to see that minimizers of (5.24) should satisfy (5.20) for $\xi > 0$.

In [160], it was shown that minimizers of (5.24) in the considered class indeed exist, are sufficiently regular and solve (5.20) classically for each $\beta \in (0, \frac{\pi}{2}]$ and each $\nu > 0$. Minimizers approach a limit $\theta(+\infty) \in \pi\mathbb{Z}$ and satisfy $|\theta'(0)| = \sin\beta$, but develop a singularity in $\theta''(\xi)$ as $\xi \to 0^+$. Not much else can be said a priori. In particular, minimizers are not guaranteed to be monotone or not to exhibit winding. In fact, numerical solution of the Dirichlet problem for (5.20) shows that both possibilities do occur. Also, minimizers do not have to be unique. Nevertheless, one can exclude winding when either ν or β is sufficiently small, and there is uniqueness in the small β case. Whether the obtained profiles are also minimizers for the two-dimensional problem is also not clear. However, in a closely related setting such a symmetry result was recently established by the same authors in [159].

To conclude this section, we would like to mention a recent paper by Knüpfer and Shi, who considered a two-dimensional problem related to head-to-head domain walls that in one dimension would correspond to the case of $\beta = \frac{\pi}{2}$ [127]. They considered a Modica-Mortola rescaling of the energy as in (5.22), except ν is again replaced by $\nu_\varepsilon = \gamma|\ln\varepsilon|^{-1}$, and considered clamped magnetization configurations as in [64]. However, as the stray field energy would still be infinite on the considered class of magnetizations, they modify the stray field term by subtracting a reference configuration from the magnetization. This amounts to introducing an additional external magnetic field that precisely cancels the divergence of the energy, thus modifying the nature of the problem in a rather significant way. Nevertheless, Knüpfer and Shi were able to establish several asymptotic results for the considered energy. In particular, for γ below some threshold the limit energy is given

by an *anisotropic perimeter* of the jump set of the limit magnetization configuration. We conjecture that such a result should also hold for a suitably renormalized version of the energy in (5.22) with the above choice of $\nu = \nu_\varepsilon$. It is also expected that while for small enough values of γ the minimizers are one-dimensional, for large enough values of γ they would develop a microstructure in the form of zig-zag walls [112].

5.5.3. *360-degree and other winding walls.* A qualitatively different type of a domain wall is the 360-degree wall. In contrast to the cases considered in the preceding sections, this wall, in which the magnetization rotates exactly once over the unit circle, connects the *same* limit magnetization on either side of the wall. Thus, a 360-degree wall represents an example of a *topological defect*, as such a wall is characterized by a non-trivial topological degree:

$$\deg(\mathbf{m}) = \frac{1}{2\pi}\int_{\mathbb{R}} (m_1 m_2' - m_2 m_1')d\xi = \frac{1}{2\pi}\int_{\mathbb{R}} \theta'\, d\xi = \frac{1}{2\pi}(\theta(+\infty) - \theta(-\infty)) = \pm 1, \tag{5.25}$$

where, as before, $\mathbf{m} = (-\sin\theta, \cos\theta)$ for $\theta = \theta(\xi)$. The 360-degree walls are also frequently observed in magnetically soft thin ferromagnetic films [84, 210, 42, 192, 112].

As was already mentioned, when $\nu = 0$ the 360-degree walls exist if and only if $h_1 = 0$ and $h_2 \neq 0$. This is in contrast with the experimental observations, in which these walls can be observed in the absence of any applied fields. In [178], Muratov and Osipov carried out an ansatz-based minimization and a computational study of 360-degree walls as a function of their orientation angle β for different $\nu > 0$. They found numerically that the solutions of (5.20) in the form of 360-degree walls exist for all $\beta \in (0, \frac{\pi}{2}]$, while they cease to exist for $\beta = 0$. Also, the wall energy was found to depend strongly on the wall orientation angle β. The existence of solutions was explained by the magnetostatic interaction between the two 180-degree cores inside a 360-degree wall, which is logarithmically attractive for $\beta \neq 0$, as the cores carry opposite charges. At the same time, for $\beta = 0$ the 180-degree cores only carry net dipole moments oriented opposite to each other. This results in an algebraic repulsion between the cores (see also [67]).

Ignat and Knüpfer studied the structure of 360-degree transition layers under clamping away from the origin in a model in which the energy consists of only exchange and stray field terms, and a small parameter balancing the two terms in the energy to yield a non-trivial limit [116]. Although these are not 360-degree walls per se, they exhibit many of the characteristics of the 360-degree wall solutions from [178]. In particular, Ignat and Knüpfer show the asymptotic behavior of the energy of the 360-degree wall solutions obtained in [178] for $\nu \gg 1$.

Ignat and Moser carried out an analysis of winding domain wall structures, which include 360-degree walls, via minimization of (5.19) (or its natural modification for $h_1 > 1$) [120]. Only the case $\beta = 0$ and $h_2 = 0$ was considered (the value of ν was also fixed, which is less essential). They proved that for $h_1 > 1$ there is a minimizer for any value of the degree. Note that in the case $\nu = 0$ such an existence result could be obtained only when $\deg(\mathbf{m}) = \pm 1$. The existence of minimizers with degrees strictly greater than 1 may be explained by the attractive interaction of the 360-degree cores, which are now dipoles

with the same orientation along the line and, therefore, attract each other. They also showed non-existence of minimizers with degree 1 for $\beta = 0$ and $h_1 \in [0, 1)$, confirming the numerics-based conclusion of [178]. Nevertheless, they also showed existence of a domain wall with a non-trivial winding in a range of positive values of h_1.

In the absence of the applied field, the analysis of existence of 360-degree walls for general orientations was carried out by Capella, Knüpfer and Muratov [38]. They proved existence of 360-degree walls for all $\nu > 0$ in the case $\beta = \frac{\pi}{2}$, i.e., when the wall direction is along the easy axis. The proof is enabled by a symmetric decreasing rearrangement of m_2, which lowers the energy and reduces the minimization to the analysis of monotone profiles. In particular, the obtained wall profile is monotone and satisfies (5.20).

Capella, Knüpfer and Muratov also proved existence of minimizers of (5.19) for all $\beta \in (0, \frac{\pi}{2}]$, provided the value of ν is sufficiently small depending on β [38]. Here the difficulty is due to the fact that one does not know any more if the wall profile is monotone. Instead, the proof relies on a perturbative argument, by which the deviation of the profile from the minimizer of the Modica-Mortola energy from the exchange and anisotropy contributions is quantified. As a by-product, Capella, Knüpfer and Muratov also characterize the width of the wall as a function of β and ν and obtain the asymptotic expression for the wall energy for either β or ν small.

It would be interesting to see if the one-dimensional minimizers obtained for $\nu > 0$ and no applied field remain as minimizers in the two-dimensional setting. For example, are minimizers of (5.19) for $\beta = \frac{\pi}{2}$ with $\deg(\mathbf{m}) = 1$ still minimizers of (5.18) with $D = \{(x, y) : -l/2 < x < l/2\}$ subject to periodicity and limit behavior at infinity? Notice that the answer to this question could turn out to be negative, depending on how the wall energy depends on its orientation angle. It is conceivable that tilting the wall may result in an energy decrease due to the orientation dependence of the wall energy, even if the length of the wall would otherwise increase. Further studies into this question are definitely needed. A closely related question comes up in the study of the Modica-Mortola rescaling of the energy given in (5.22), written in terms of the θ variable to retain the information about the magnetization winding. We conjecture that the Γ-limit of the latter energy should be given by an anisotropic perimeter type functional that takes into account winding multiplicity. For zero applied field the situation is complicated by the presence of 180-degree walls oriented along the easy axis, but those can be eliminated by assuming $h_2 > 0$.

5.5.4. *90-degree and 180-degree walls in biaxial materials.* We conclude by briefly mentioning a class of materials in which the magnetocrystalline anisotropy exhibits a four-fold symmetry, which is common for materials with cubic crystalline structure [135, 107]. The corresponding energy analogous to (5.18) with the applied field set equal to zero reads

$$E(\mathbf{m}) = \frac{1}{2}\int_{\mathbb{R}^2} \Big(|\nabla \mathbf{m}|^2 + m_1^2 m_2^2\Big) d^2 r + \frac{\nu}{8\pi}\int_{\mathbb{R}^2}\int_{\mathbb{R}^2} \frac{\nabla\cdot\mathbf{m}(\mathbf{r})\,\nabla\cdot\mathbf{m}(\mathbf{r})}{|\mathbf{r}-\mathbf{r}'|}\, d^2 r\, d^2 r', \quad (5.26)$$

with the easy directions along either $\pm\hat{\mathbf{x}}$ or $\pm\hat{\mathbf{y}}$. Thus, in addition to the usual types of domain walls, a 90-degree wall is also possible.

Lund and Muratov studied existence of 90-degree and 180-degree domain wall solutions by minimizing the one-dimensional version of (5.26) analogous to (5.19) [158]. They

found existence of 90-degree walls for $\beta = \frac{\pi}{4}$ (and all their possible $\frac{\pi}{2}$ rotations). This choice of β corresponds to the orientation that makes the wall charge-free for $\theta(+\infty) = 0$ and $\theta(-\infty) = \frac{\pi}{2}$. The analysis of this case follow the lines of that of 180-degree walls in uniaxial materials [41], with similar conclusions. In contrast, existence of 180-degree wall solutions was found for $\beta = 0$ (and all their possible $\frac{\pi}{2}$ rotations), using the techniques of the analysis of 360-degree walls in uniaxial materials for $\beta = \frac{\pi}{2}$ [38]. The issue here is to show that a 180-degree walls does not split into two 90-degree walls, and this does not happen because the latter would be charged for $\theta(+\infty) = 0$, $\theta(-\infty) = \pi$ and $\beta = 0$.

All the open questions that were discussed in the preceding sections are similarly relevant to biaxial materials. However, these materials may possess a richer domain structure due to the four possible equilibria of the magnetization, as well as a richer set of charge-free domain walls.

5.6. *Conclusion.* In summary, in recent years there have been a number of developments in modeling and analysis of the domain walls arising in thin ferromagnetic films in which the magnetization rotates in the film plane, pushing forward our understanding of the classical questions in physics that began to be formulated in the 1920s. Some of the domain wall solutions are by now fairly well understood in one space dimension. Nevertheless, there are more open questions than answers, especially in two-dimensional and vectorial settings, that will hopefully inspire the next generation of researchers in the calculus of variations and analysis of PDEs to further advance this exciting area at the intersection of mathematics and materials science.

Acknowledgements. Irene Fonseca acknowledges the Center for Nonlinear Analysis, where part of this work was carried out. Her research was partially funded by the NSF grant DMS-1906238. Gilles Francfort acknowledges the Flatiron Institute where part of this work was carried out. His research is partially funded by the NSF Grant DMREF-1921969. Marta Lewicka was partially supported by the NSF award DMS-2006439. Giovanni Di Fratta acknowledges the support of the Austrian Science Fund (FWF) through the project *Analysis and Modeling of Magnetic Skyrmions* (grant P-34609). Giovanni Di Fratta also thanks MedUni Wien for support and hospitality. The work of Cyrill Muratov was supported, in part, by NSF via grants DMS-0908279, DMS-1313687, DMS-1614948 and DMS-1908709. He gratefully acknowledges multiple valuable discussions with A. Bernand-Mantel and V. V. Slastikov.

References

[1] E. Acerbi, I. Fonseca, and G. Mingione. Existence and regularity for mixtures of micromagnetic materials. *Proceedings of the Royal Society A: Mathematical, Physical and Engineering Sciences*, 462(2072):2225–2243, 2006. Doi: 10.1098/rspa.2006.1655.

[2] A. Aharoni. *Introduction to the Theory of Ferromagnetism*, volume 109 of *International Series of Monographs on Physics*. Oxford University Press, New York, 2nd edition, 2001.

[3] A. Acharya, M. Lewicka and R. Pakzad, *A note on the metric-restricted inverse design problem*, Nonlinearity, **29**, pp. 1769-1797, (2016).

[4] S. Almi, E. Tasso: Brittle fracture in linearly elastic plates, Preprint 2020.

[5] F. Alouges and G. Di Fratta. Homogenization of composite ferromagnetic materials. *Proceedings of the Royal Society A: Mathematical, Physical and Engineering Science*, 471(2182):20150365, oct 2015. Doi: 10.1098/rspa.2015.0365.

[6] F. Alouges, G. Di Fratta, and B. Merlet. Liouville type results for local minimizers of the micromagnetic energy. *Calculus of Variations and Partial Differential Equations*, 53(3-4):525–560, jul 2015. Doi: 10.1007/s00526-014-0757-2.

[7] L. Ambrosio and X. Cabré. Entire solutions of semilinear elliptic equations in $\mathbb{R}^3$ and a conjecture of De Giorgi. *J. Amer. Math. Soc.*, 13:725–739, 2000.

[8] L. Ambrosio, A. Coscia, G. Dal Maso: Fine properties of functions with bounded deformation, *Arch. Rational Mech. Anal.* **139** (1997) 201–238.

[9] N. Ansini: The nonlinear sieve problem and applications to thin films, *Asympt. Anal.* **39** (2004) 113–145.

[10] N. Ansini, J.-F. Babadjian, C. I. Zeppieri: The Neumann sieve problem and dimensional reduction: a multiscale approach, *M3AS* **17** (2007) 681–735.

[11] M. F. Atiyah and N. S. Manton. Geometry and kinematics of two skyrmions. *Communications in Mathematical Physics*, 153(2):391–422, 1993.

[12] J.-F. Babadjian: Quasi-static evolution of a brittle thin film, *Calc. Var. Partial Differential Equations* **26** (2006) 69–118.

[13] J.-F. Babadjian: Lower semicontinuity of quasiconvex bulk energies in SBV and integral representation in dimension reduction, *SIAM J. Math. Anal.* **39** (2008) 1921–1950.

[14] J.-F. Babadjian: Traces of functions of bounded deformation, *Indiana Univ. Math. J.* **64** (2015) 1271–1290.

[15] J.-F. Babadjian, D. Henao: Reduced models for linearly elastic thin films allowing for fracture, debonding or delamination, *Interfaces Free Bound.* **18** (2016), 545–578.

[16] J.M. Ball: Convexity conditions and existence theorems in nonlinear elasticity, *Arch. Rat. Mech. Anal.*, **63**, 1976, 337–403.

[17] B. Barker, M. Lewicka and K. Zumbrun, Existence and stability of viscoelastic shock profiles, *Arch. Rational Mech. Anal.* **200(2)**, pp. 491-532, (2011).

[18] R. G. Barrera, G. A. Estevez, and J. Giraldo. Vector spherical harmonics and their application to magnetostatics. *European Journal of Physics*, 6(4):287–294, oct 1985.

[19] G. Bellettini, A. Coscia, G. Dal Maso: Compactness and lower semicontinuity properties in $SBD(\Omega)$, *Math. Z.* **228** (1998) 337–351.

[20] A. Berger and H. P. Oepen. Magnetic domain walls in ultrathin fcc cobalt films. *Phys. Rev. B*, 45:12596–12599, 1992.
[21] A. Bernand-Mantel, C. B. Muratov, and Thilo. M. Simon. A quantitative description of skyrmions in ultrathin ferromagnetic films and rigidity of degree ± 1 harmonic maps from $\mathbb{R}^2$ to $\mathbb{S}^2$. *ArXiv preprint arXiv:1912.09854*, 2019.
[22] K. Bhattacharya, I. Fonseca, G. A. Francfort: An asymptotic study of the debonding of thin films, *Arch. Rational Mech. Anal.* **161** (2002) 205–229.
[23] K. Bhattacharya, M. Lewicka, and M. Schaffner, Plates with incompatible prestrain, *Arch. Rational Mech. Anal.* **221(1)**, pp. 143-181, (2016).
[24] F. Bloch. Zur Theorie des Austauschproblems und der Remanenzerscheinung der Ferromagnetika. *Z. Physik*, 74:295–335, 1932.
[25] A. Bogdanov and A. Hubert. Thermodynamically stable magnetic vortex states in magnetic crystals. *Journal of Magnetism and Magnetic Materials*, 138(3):255–269, 1994. Doi: 10.1016/0304-8853(94)90046-9.
[26] G. Bouchitté, I. Fonseca, G. Leoni, L. Mascarenhas: A global method for relaxation in $W^{1,p}$ and in SBV_p, *Arch. Rational Mech. Anal.* **165** (2002) 187–242.
[27] G. Bouchitté, I. Fonseca, M.L. Mascarenhas, The Cosserat vector in membrane theory: a variational approach *J. Convex Anal.*, **16**-2, 2009, 351–365.
[28] B. Bourdin, G. A. Francfort, J.-J. Marigo: The variational approach to fracture, *J. Elasticity* **91** (2008) 5–148.
[29] F. Bourquin, P. G. Ciarlet, G. Geymonat, A. Raoult: Γ-convergence et analyse asymptotique des plaques minces, *C. R. Acad. Sci. Paris, Série I*, **315**, 1017–1024.
[30] A. Braides, I. Fonseca: Brittle thin films, *Appl. Math. Optim.* **44** (2001) 299–323.
[31] A. Braides, A. Defranceschi, *Homogenization of multiple integrals*, Oxford Lecture Series in Mathematics and its Applications, 12, Clarendon Press, Oxford, 1998.
[32] A. Brataas, A. D. Kent, and H. Ohno. Current-induced torques in magnetic materials. *Nature Mat.*, 11:372–381, 2012.
[33] W. F. Brown. *Magnetostatic Principles in Ferromagnetism*. North-Holland, Amsterdam, 1962.
[34] W. F. Brown. *Micromagnetics*. Interscience Publishers, London, 1963.
[35] W. F. Brown. Thermal fluctuations of a single-domain particle. *Phys. Rev.*, 130:1677–1686, 1963.
[36] W. F. Brown. The Fundamental Theorem of the Theory of Fine Ferromagnetic Particles. *Annals of the New York Academy of Sciences*, 147(12 The Fundamen):463–488, jun 1969. Doi: 10.1111/j.1749-6632.1969.tb41269.x.
[37] W. Cao and L. Szekelyhidi, Very weak solutions to the two-dimensional Monge-Ampere equation, *Science China Mathematics*, **62**, pp. 1041-1056, (2019).
[38] A. Capella, H. Knüpfer, and C. B. Muratov. Existence and structure of 360° walls in thin uniaxial ferromagnetic films. Preprint, 2021.
[39] A. Capella, C. Melcher, and F. Otto. Wave-type dynamics in ferromagnetic thin films and the motion of Néel walls. *Nonlinearity*, 20:2519–2537, 2007.
[40] G. Carbou. Thin layers in micromagnetism. *Mathematical Models and Methods in Applied Sciences*, 11(09):1529–1546, 2002. Doi: 10.1142/s0218202501001458.
[41] M. Chermisi and C. B. Muratov. One-dimensional Néel walls under applied external fields. *Nonlinearity*, 26:2935–2950, 2013.
[42] H. S. Cho, C. Hou, M. Sun, and H. Fujiwara. Characteristics of 360°-domain walls observed by magnetic force microscope in exchange-biased NiFe films. *J. Appl. Phys.*, 85:5160–5162, 1999.
[43] R. Choksi and R. V. Kohn. Bounds on the micromagnetic energy of a uniaxial ferromagnet. *Comm. Pure Appl. Math.*, 51:259–289, 1998.
[44] R. Choksi, R. V. Kohn, and F. Otto. Domain branching in uniaxial ferromagnets: a scaling law for the minimum energy. *Commun. Math. Phys.*, 201:61–79, 1999.
[45] P. G. Ciarlet: *Mathematical elasticity. Vol. II,* **27**, Studies in Mathematics and its Applications. North-Holland Publishing Co., Amsterdam (1997).
[46] P.G. Ciarlet and P. Destuynder, A justification of the two-dimensional linear plate model, *J. Mécanique*, **18**, 1979, 315–344.
[47] S. Conti, C. De Lellis and L. Szekelyhidi, *h-principle and rigidity for $C^{1,\alpha}$ isometric embeddings*, Proceedings of the Abel Symposium (2010).
[48] R. Collette. Shape and energy of n[e-acute]el walls in very thin ferromagnetic films. *J. Appl. Phys.*, 35:3294–3301, 1964.

[49] S. Conti. Branched microstructures: scaling and asymptotic self-similarity. *Comm. Pure Appl. Math.*, 53:1448–1474, 2000.
[50] S. Conti, G. Dolzmann, Derivation of Elastic Theories for Thin Sheets and the Constraint of Incompressibility. In: *Analysis, Modeling and Simulation of Multiscale Problems*, Mielke A. (ed.) Springer, Berlin, Heidelberg, 2006.
[51] S. Conti, M. Focardi, F. Iurlano: Phase field approximation of cohesive fracture models, *Ann. Inst. H. Poincaré Anal. Non Linéaire* **33** (2016) 1033–1067.
[52] S. Conti, F. Maggi, Confining thin elastic sheets and folding paper, *Arch. Rat. Mech. Anal.*, **187**, 2008, 1–48.
[53] S. Conti, F. Maggi, S. Müller, Rigorous derivation of Föppl's theory for clamped elastic membranes leads to relaxation, *SIAM J. Math. Anal.*, **38**, 2006, 657–680.
[54] G. Dal Maso, *An introduction to* Γ*-convergence*, Birkhäuser, Boston, 1993.
[55] G. Dal Maso: Generalised functions of bounded deformation, *J. Eur. Math. Soc. (JEMS)* **15** (2013) 1943–1997.
[56] G. Dal Maso, F. Iurlano: Fracture models as Γ-limits of damage models, *Comm. Pure Appl. Anal.* **12** (2013) 1657–1686.
[57] E. Davoli and G. Di Fratta. Homogenization of Chiral Magnetic Materials: A Mathematical Evidence of Dzyaloshinskii's Predictions on Helical Structures. *Journal of Nonlinear Science*, Jan 2020. Doi: 10.1007/s00332-019-09606-8.
[58] E. Davoli, G. Di Fratta, D. Praetorius, and M. Ruggeri. Micromagnetics of thin films in the presence of Dzyaloshinskii-Moriya interaction. *Mathematical Models and Methods in Applied Sciences*, (forthcoming).
[59] E. De Giorgi. Convergence problems for functionals and operators. In *Proceedings of the International Meeting on Recent Methods in Nonlinear Analysis (Rome, 1978)*, pages 131–188, Bologna, Italy, 1979. Pitagora.
[60] C. De Lellis, D. Inauen D. and L. Szekelyhidi, *A Nash-Kuiper theorem for* $C^{1,1/5-\delta}$ *immersions of surfaces in* 3 *dimensions*, Revista matematica iberoamericana, **34**, pp. 1119-1152, (2018).
[61] M. Del Pino, M. Kowalczyk, and J. C. Wei. On De Giorgi's conjecture and beyond. *Proc. Natl. Acad. Sci. USA*, 109:6845–6850, 2012.
[62] A. DeSimone. Energy minimizers for large ferromagnetic bodies. *Archive for Rational Mechanics and Analysis*, 125(2):99–143, 1993. Doi: 10.1007/BF00376811.
[63] A. DeSimone. Hysteresis and imperfection sensitivity in small ferromagnetic particles. *Meccanica*, 30(5):591–603, 1995. Doi: 10.1007/BF01557087.
[64] A. DeSimone, H. Knüpfer, and F. Otto. 2-d stability of the Néel wall. *Calc. Var. PDE*, 27:233–253, 2006.
[65] A. DeSimone, R. V. Kohn, S. Müller, and F. Otto. Magnetic microstructures—a paradigm of multiscale problems. In *ICIAM 99 (Edinburgh)*, pages 175–190. Oxford Univ. Press, 2000.
[66] A. Desimone, R. V. Kohn, S. Müller, and F. Otto. A reduced theory for thin-film micromagnetics. *Comm. Pure Appl. Math.*, 55:1408–1460, 2002.
[67] A. Desimone, R. V. Kohn, S. Müller, and F. Otto. Repulsive interaction of Néel walls, and the internal length scale of the cross-tie wall. *Multiscale Model. Simul.*, 1:57–104, 2003.
[68] A. DeSimone, R. V. Kohn, S. Müller, and F. Otto. Recent analytical developments in micromagnetics. In G. Bertotti and I. D. Mayergoyz, editors, *The Science of Hysteresis*, volume 2 of *Physical Modelling, Micromagnetics, and Magnetization Dynamics*, pages 269–381. Academic Press, Oxford, 2006.
[69] H.-D. Dietze and H. Thomas. Bloch- und Néel-Wände in dünnen ferromagnetischen Schichten. *Z. Physik*, 163:523–534, 1961.
[70] G. Di Fratta, C. Serpico, and M. d'Aquino. A generalization of the fundamental theorem of Brown for fine ferromagnetic particles. *Physica B: Condensed Matter*, 407(9):1368–1371, 2012. Doi: 10.1016/j.physb.2011.10.010.
[71] G. Di Fratta. The Newtonian potential and the demagnetizing factors of the general ellipsoid. *Proceedings of the Royal Society A: Mathematical, Physical and Engineering Sciences*, 4472.2190:20160197, 2016. Doi: 10.1098/rspa.2016.0197.
[72] G. Di Fratta. Micromagnetics of curved thin films. *Zeitschrift für angewandte Mathematik und Physik*, 71(4), jun 2020. Doi: 10.1007/s00033-020-01336-2.
[73] G. Di Fratta, A. Fiorenza, and V. Slastikov. On symmetry of energy minimizing harmonic-type maps on cylindrical surfaces. *ArXiv:2110.08755*, 2021.

[74] G. Di Fratta, A. Monteil, and V. Slastikov. Symmetry properties of minimizers of a perturbed dirichlet energy with a boundary penalization. *ArXiv preprint 2106.15830, CVGMT preprint 5110*, 2021.
[75] G. Di Fratta, C. B. Muratov, G. Di Fratta, C. B. Muratov, F. N. Rybakov, and V. V. Slastikov. Variational principles of micromagnetics revisited. *SIAM J. Math. Anal.*, 52:3580–3599, 2020.
[76] G. Di Fratta, V. Slastikov, and A. Zarnescu. On a sharp Poincaré-type inequality on the 2-sphere and its application in micromagnetics. *SIAM Journal on Mathematical Analysis (SIMA), 2019, 51.4: 3373-3387. Doi:10.1137/19M1238757*, 2(1):1–13, jan 2019.
[77] P. A. M. Dirac. On the theory of quantum mechanics. *Proc. R. Soc. Lond. Ser. A*, 112:661–677, 1926.
[78] P. A. M. Dirac. The quantum theory of the electron. *Proc. R. Soc. Lond. Ser. A*, 117:610–624, 1928.
[79] M. Do Carmo. *Differential Geometry of Curves and Surfaces, Second Edition*. Prentice-hall, Englewood Cliffs, 2018. Doi: 10.1201/b18913.
[80] L. Döring, R. Ignat, and F. Otto. A reduced model for domain walls in a reduced model for domain walls in soft ferromagnetic films at the cross-over from symmetric to asymmetric wall types. *J. Eur. Math. Soc.*, 16:1377–1422, 2014.
[81] I. Dzyaloshinsky. A thermodynamic theory of "weak" ferromagnetism of antiferromagnetics. *Journal of Physics and Chemistry of Solids*, 4(4):241–255, 1958. Doi: 10.1016/0022-3697(58)90076-3.
[82] M. J. Esteban. Existence of 3-d skyrmions. *Communications in Mathematical Physics*, 251(math-ph/0401042):209–210, 2004. Doi: 10.1007/s00220-004-1139-y.
[83] M. J. Esteban and P.-L. Lions. Skyrmions and symmetry. *Asymptotic Analysis*, 1(3):187–192, 1988.
[84] E. Feldtkeller and W. Liesk. 360°-Wände in magnetischen Schichten. *Z. Angew. Phys.*, 14:195–199, 1962.
[85] A. Fert, V. Cros, and J. Sampaio. Skyrmions on the track. *Nature Nanotechnology*, 8(3):152–156, 2013. Doi: 10.1038/nnano.2013.29.
[86] J. Fidler and T. Schrefl. Micromagnetic modelling—the current state of the art. *J. Phys. D: Appl. Phys.*, 33:R135–R156, 2000.
[87] M. Focardi, F. Iurlano: Asymptotic analysis of Ambrosio-Tortorelli energies in linearized elasticity, *SIAM J. Math. Anal.* **46** (2014) 2936–2955.
[88] G. A. Francfort, J.-J. Marigo: Revisiting brittle fracture as an energy minimization problem, *J. Mech. Phys. Solids* **46** (1998) 1319–1342.
[89] L. Freddi, R. Paroni, C. Zanini: Dimension reduction of a crack evolution problem in a linearly elastic plate, *Asympt. Anal.* **70** (2010) 101–123.
[90] G. Friesecke, R.D. James, M. Mora and S. Müller, *Derivation of nonlinear bending theory for shells from three-dimensional nonlinear elasticity by Gamma-convergence*, C. R. Math. Acad. Sci. Paris, **336(8)**, pp. 697-702, (2003).
[91] G. Friesecke, R.D. james and S. Müller, A Theorem on Geometric Rigidity and the Derivation of Nonlinear Plate Theory from Three-Dimensional Elasticity, *Com. Pure Appl. Math.*, **LV**, 2002, 1461–1506.
[92] G. Friesecke, R.D. james and S. Müller, A Hierarchy of Plate Models Derived from Nonlinear Elasticity by Gamma-Convergence, *Arch. Rat. Mech. Anal.*, **180**, 2006, 183–236.
[93] P. Gambardella and I. M. Miron. Current-induced spin-orbit torques. *Phil. Trans. Roy. Soc. London, Ser. A*, 369:3175–3197, 2011.
[94] Y. Gaididei, V. P. Kravchuk, and D. D. Sheka. Curvature effects in thin magnetic shells. *Physical Review Letters*, 112(25):257203, 2014. Doi: 10.1103/PhysRevLett.112.257203.
[95] C. J. García-Cervera. *Magnetic Domains and Magnetic Domain Walls*. PhD thesis, New York University, 1999.
[96] C. J. García-Cervera. One-dimensional magnetic domain walls. *Euro. J. Appl. Math.*, 15:451–486, 2004.
[97] C. J. García-Cervera. Numerical micromagnetics: A review. *Bol. Soc. Esp. Mat. Apl.*, 39:103—135, 2007.
[98] N. Ghoussoub and C. Gui. On a conjecture of De Giorgi and some related problems. *Math. Ann.*, 311:481–491, 1998.
[99] T. L. Gilbert. A Lagrangian formulation of the gyromagnetic equation of the magnetisation field. *Phys. Rev.*, 100:1243, 1955. Doi: 10.1103/PhysRev.100.1243.

[100] T.L. Gilbert. A phenomenological theory of damping in ferromagnetic materials. *IEEE Trans. Magn.*, 40:3443–3449, 2004.
[101] G. Gioia and R. D. James. Micromagnetics of very thin films. *Proceedings of the Royal Society A: Mathematical, Physical and Engineering Sciences*, 453(1956):213–223, 1997. Doi: 10.1098/rspa.1997.0013.
[102] A. A. Griffith: The phenomena of rupture and flow in solids, *Philos. Trans. R. Soc. Lond.* **221A** (1920) 163–198.
[103] M. E. Gurtin. *Thermomechanics of evolving phase boundaries in the plane*. Oxford Mathematical Monographs. Oxford University Press, New York, 1993.
[104] Q. Han and M. Lewicka, *Convex integration for the Monge-Ampère systems*, in preparation, (2021).
[105] Q. Han, M. Lewicka, and L. Mahadevan, *Geodesics and isometric immersions in kirigami*, (2021).
[106] D. Harutyunyan, *Gaussian curvature as an identifier of shell rigidity*, Archive for Rational Mechanics and Analysis, **226(2)**, pp. 743-766, (2017).
[107] B. Heinrich and J. F. Cochran. Ultrathin metallic magnetic films: magnetic anisotropies and exchange interactions. *Adv. Phys.*, 42:523–639, 1993.
[108] W. Heisenberg. Mehrkörperproblem und Resonanz in der Quantenmechanik. *Z. Physik*, 38:411–426, 1926.
[109] W. Heisenberg. Zur Theorie des Ferromagnetismus. *Z. Physik*, 49:619–636, 1928.
[110] R. M. Hornreich. 90 ° magnetization curling in thin films. *J. Appl. Phys.*, 34:1071–1072, 1963.
[111] P. Hornung, M. Lewicka, and R. Pakzad, Infinitesimal isometries on developable surfaces and asymptotic theories for thin developable shells, *Journal of Elasticity*, **111(1)**, (2013).
[112] A. Hubert and R. Schäfer. *Magnetic Domains*. Springer, Berlin, 1998.
[113] A. Hubert and R. Schäfer. *Magnetic domains: the analysis of magnetic microstructures*. Springer Science & Business Media, 2008.
[114] R. Ignat. A Γ-convergence result for Néel walls in micromagnetics. *Calc. Var. PDE*, 36:285–316, 2009.
[115] R. Ignat and R. L. Jerrard. Renormalized energy between vortices in some Ginzburg-Landau models on 2-dimensional Riemannian manifolds. *ArXiv preprint arXiv:1910.02921*, 2019.
[116] R. Ignat and H. Knüpfer. Vortex energy and 360° Néel walls in thin-film micromagnetics. *Comm. Pure Appl. Math.*, 63:1677–1724, 2010.
[117] R. Ignat and M. Kurzke. Global jacobian and Γ-convergence in a two-dimensional Ginzburg-Landau model for boundary vortices. *ArXiv preprint arXiv:1910.06039*, 2019.
[118] R. Ignat and B. Merlet. Entropy method for line-energies. *Calculus of Variations and Partial Differential Equations*, 44(3-4):375–418, 2012.
[119] R. Ignat and R. Moser. A zigzag pattern in micromagnetics. *Journal de Mathématiques Pures et Appliquées. Neuvième Série*, 98(2):139–159, 2012.
[120] R. Ignat and R. Moser. Néel walls with prescribed winding number and how a nonlocal term can change the energy landscape. *Journal of Differential Equations*, 263(9):5846–5901, 2017. Doi: 10.1016/j.jde.2017.07.006.
[121] S. Jimenez-Bolanos and M. Lewicka, *Dimension reduction for thin films prestrained by shallow curvature*, Proceeding of the Royal Society A (2021).
[122] C. Kittel. Physical theory of ferromagnetic domains. *Rev. Mod. Phys.*, 21:541–583, 1949.
[123] Y. Klein, E. Efrati and E. Sharon, Shaping of elastic sheets by prescription of non-Euclidean metrics, *Science*, **315**, pp. 1116–1120, (2007).
[124] R. V. Kohn and V. Slastikov. Another thin-film limit of micromagnetics. *Archive for Rational Mechanics and Analysis*, 178(2):227–245, 2005. Doi: 10.1007/s00205-005-0372-7.
[125] H. Knüpfer and C. B. Muratov. Domain structure of bulk ferromagnetic crystals in applied fields near saturation. *J. Nonlinear Sci.*, 21:921–962, 2011.
[126] H. Knüpfer, C. B. Muratov, and F. Nolte. Magnetic domains in thin ferromagnetic films with strong perpendicular anisotropy. *Arch. Rat. Mech. Anal.*, 232:727–761, 2019.
[127] H. Knüpfer and W. Shi. Γ-limit for two-dimensional charged magnetic zigzag domain walls. arXiv:2005.02857, 2020.
[128] R. V. Kohn. Energy-driven pattern formation. In *International Congress of Mathematicians. Vol. I*, pages 359–383. Eur. Math. Soc., Zürich, 2007.
[129] R. V. Kohn and V. V. Slastikov. Another thin-film limit of micromagnetics. *Arch. Ration. Mech. Anal.*, 178:227–245, 2005.

[130] V. P. Kravchuk, D. D. Sheka, R. Streubel, D. Makarov, O. G. Schmidt, and Y. Gaididei. Out-of-surface vortices in spherical shells. *Physical Review B - Condensed Matter and Materials Physics*, 85(14):1–6, 2012. Doi: 10.1103/PhysRevB.85.144433.

[131] R. Kupferman and J.P. Solomon, A Riemannian approach to reduced plate, shell, and rod theories, *Journal of Functional Analysis* **266**, pp. 2989-3039, (2014).

[132] M. Kurzke, C. Melcher, R. Moser, and D. Spirn. Ginzburg-Landau Vortices Driven by the Landau–Lifshitz–Gilbert Equation. *Archive for Rational Mechanics and Analysis*, 199(3):843–888, 2011. Doi: 10.1007/s00205-010-0356-0.

[133] A. E. LaBonte. Two dimensional Bloch-type domain walls in ferromagnetic films. *J. Appl. Phys.*, 40:2450–2458, 1969.

[134] L. Landau and E. Lifshitz. On the theory of the dispersion of magnetic permeability in ferromagnetic bodies. *Perspectives in Theoretical Physics*, 8(153):51–65, 2012. Doi: 10.1016/b978-0-08-036364-6.50008-9.

[135] L. D. Landau and E. M. Lifshitz. *Course of Theoretical Physics*, volume 8. Pergamon Press, London, 1984.

[136] H. Le Dret and A. Raoult, The membrane shell model in nonlinear elasticity: a variational asymptotic derivation, *J. Nonlinear Sci.*, **6**, pp. 59–84, (1996).

[137] H. Le Dret and A. Raoult: The nonlinear membrane model as variational limit of nonlinear three-dimensional elasticity, *J. Math. Pures Appl.*, **75**, 1995, 551–580.

[138] J. Leliaert, M. Dvornik, J. Mulkers, J. De Clercq, M. V. Milošević, and B. Van Waeyenberge. Fast micromagnetic simulations on GPU—recent advances made with Mumax3. *J. Phys. D: Appl. Phys.*, 51:123002, 2018.

[139] M. Lewicka, Quantitative immersability of Riemann metrics and the infinite hierarchy of prestrained shell models, *Arch. Ration. Mech. Anal.*, **236**, pp. 1677–1707, (2020).

[140] M. Lewicka and D. Lucic, Dimension reduction for thin films with transversally varying prestrain: the oscillatory and the non-oscillatory case, *Communications on Pure and Applied Mathematics*, **73(9)**, pp. 1880-1932, (2020).

[141] M. Lewicka and L. Mahadevan, Geometry, Analysis and Morphogenesis: Problems and Prospects, *Bulletin of the American Mathematical Society* (2021).

[142] M. Lewicka, L. Mahadevan and R. Pakzad, The Foppl-von Karman equations for plates with incompatible strains, *Proceedings of the Royal Society A*, **467**, pp. 402-426, (2011).

[143] M. Lewicka, L. Mahadevan and R. Pakzad, Models for elastic shells with incompatible strains, *Proceedings of the Royal Society A*, **470** 20130604 (2014).

[144] M. Lewicka, L. Mahadevan and R. Pakzad, The Monge-Ampère constraint: matching of isometries, density and regularity and elastic theories of shallow shells, *Annales de l'Institut Henri Poincare (C) Non Linear Analysis*, **34(1)**, 45-67, (2017).

[145] M. Lewicka, M. Mora and R. Pakzad, A nonlinear theory for shells with slowly varying thickness, *Comptes Rendus Mathematique*, **347(3-4)**, pp. 211-216, (2009).

[146] M. Lewicka, M. Mora, and R. Pakzad, Shell theories arising as low energy Γ-limit of 3d nonlinear elasticity, *Ann. Scuola Norm. Sup. Pisa* Cl. Sci., **5(9)**, pp. 1-43, (2010).

[147] M. Lewicka, M. Mora and R. Pakzad, The matching property of infinitesimal isometries on elliptic surfaces and elasticity of thin shells, *Arch. Rational Mech. Anal.*, **200(3)**, pp. 1023-1050, (2011).

[148] M. Lewicka and P.B. Mucha, A local and global well-posedness results for the general stress-assisted diffusion systems, *Journal of Elasticity*, **123(1)**, pp. 19-41, (2016).

[149] M. Lewicka and S. Müller, The uniform Korn - Poincare inequality in thin domains, *Annales de l'Institut Henri Poincare* (C) Non Linear Analysis, **28(3)**, pp. 443-469, (2011).

[150] M. Lewicka, and S. Müller, On the optimal constants in Korn's and geometric rigidity estimates in bounded and unbounded domains, under Neumann boundary conditions, *Indiana Univ. Math. J.* **65(2)**, pp. 377-397, (2016).

[151] M. Lewicka, P. Ochoa, and R. Pakzad, Variational models for prestrained plates with Monge-Ampere constraint, *Differential and Integral Equations*, **29(9-10)**, pp. 861-898, (2015).

[152] M. Lewicka and R. Pakzad, Scaling laws for non-Euclidean plates and the $W^{2,2}$ isometric immersions of Riemannian metrics, *ESAIM: Control, Optimisation and Calculus of Variations*, **17 (4)**, pp. 1158–1173, (2011).

[153] M. Lewicka and R. Pakzad, The infinite hierarchy of elastic shell models: some recent results and a conjecture, *Fields Institute Communications*, (2010).

[154] M. Lewicka and R. Pakzad, Convex integration for the Monge-Ampere equation in two dimensions, *Analysis and PDE*, **10(3)**, pp. 695-727, (2017).
[155] M. Lewicka, A. Raoult and D. Ricciotti, Plates with incompatible prestrain of higher order, *Annales de l'Institut Henri Poincare* (C) Non Linear Analysis, **34(7)**, pp. 1883-1912, (2017).
[156] X. Li and C. Melcher. Lattice solutions in a ginzburg–landau model for a chiral magnet. *Journal of Nonlinear Science*, 30(6):3389–3420, sep 2020.
[157] F. Lin and Y. Yang. Analysis on Faddeev knots and Skyrme solitons: recent progress and open problems. *Perspectives in nonlinear partial differential equations*, 446:319–344, 2007. Doi: 10.1090/conm/446/08639.
[158] R. Lund and C. B. Muratov. One-dimensional domain walls in thin ferromagnetic films with fourfold anisotropy. *Nonlinearity*, 29:1716–1734, 2016.
[159] R. G. Lund, C. B. Muratov, and V. V. Slastikov. Edge domain walls in ultrathin exchange-biased films. *J. Nonlinear Sci.*, 30:1165–1205, 2018.
[160] R. G. Lund, C. B. Muratov, and V. V. Slastikov. One-dimensional in-plane edge domain walls in ultrathin ferromagnetic films. *Nonlinearity*, 31:728–754, 2018.
[161] F. Iurlano: Fracture and plastic models as Γ-limits of damage models under different regimes, *Adv. Calc. Var.* **6** (2013) 165–189.
[162] J. W. Hutchinson, Z. Suo: Mixed mode cracking in layered materials, *Adv. Appl. Mech.* **29** (1991) 63–191.
[163] A. A. León Baldelli, B. Bourdin, J.-J. Marigo, C. Maurini: Fracture and debonding of a thin film on a stiff substrate: analytical and numerical solutions of a one-dimensional variational model, *Cont. Mech. Thermodyn.* **25** (2013) 243–268.
[164] A. A. León Baldelli, J.-F. Babadjian, B. Bourdin, D. Henao, C. Maurini: A variational model for fracture and debonding of thin films under in-plane loadings, *J. Mech. Phys. Solids* **70** (2014) 320–348.
[165] A.A. Leòn Baldelli, B. Bourdin: On the asymptotic derivation of Winkler-type energies from 3D elasticity, *J. Elasticity* **121** (2015) 275–301.
[166] N. S. Manton. Geometry of skyrmions. *Communications in Mathematical Physics*, 111(3):469–478, 1987.
[167] R. Mattheis, K. Ramstöck, and J. McCord. Formation and annihilation of edge walls in thin-film permalloy strips. *IEEE Trans. Magn.*, 33:3993–3995, 1997.
[168] C. Melcher. The logarithmic tail of Néel walls in thin films. *Arch. Rational Mech. Anal.*, 168:83–113, 2003.
[169] C. Melcher. Chiral skyrmions in the plane. *Proceedings of the Royal Society A: Mathematical, Physical and Engineering Sciences*, 470(2172):20140394, oct 2014. Doi: 10.1098/rspa.2014.0394.
[170] C. Melcher and Z. N. Sakellaris. Curvature-stabilized skyrmions with angular momentum. *Letters in Mathematical Physics*, 109(10):2291–2304, jun 2019. Doi: 10.1007/s11005-019-01188-6.
[171] J. Milnor. *Topology from the Differentiable Viewpoint*. Princeton Landmarks in Mathematics and Physics. Princeton University Press, 1997.
[172] L. Modica. The gradient theory of phase transitions and the minimal interface criterion. *Arch. Rational Mech. Anal.*, 98:123–142, 1987.
[173] M. Morini, C. B. Muratov, M. Novaga, and V. V. Slastikov. Transverse domain walls in thin ferromagnetic strips. arXiv:2106.01338, 2021.
[174] M. Morini and V. Slastikov. Geometrically constrained walls in two dimensions. *Archive for Rational Mechanics and Analysis*, 203(2):621–692, 2012.
[175] T. Moriya. Anisotropic superexchange interaction and weak ferromagnetism. *Physical review*, 120(1):91, 1960.
[176] R. Moser. Boundary vortices for thin ferromagnetic films. *Arch. Ration. Mech. Anal.*, 174:267–300, 2004.
[177] C. B. Muratov and V. V. Osipov. Optimal grid-based methods for thin film micromagnetics simulations. *J. Comp. Phys.*, 216:637–653, 2006.
[178] C. B. Muratov and V. V. Osipov. Theory of 360° domain walls in thin ferromagnetic films. *J. Appl. Phys.*, 104:053908, 2008.
[179] C. B. Muratov and V. Slastikov. Domain structure of ultrathin ferromagnetic elements in the presence of Dzyaloshinskii-Moriya Interaction. *Proceedings of the Royal Society A: Mathematical, Physical and Engineering Sciences*, 473(2197):20160666, 2017. Doi: 10.1098/rspa.2016.0666.

[180] C. B. Muratov and X. Yan. Uniqueness of one-dimensional Néel wall profiles. *Proc. R. Soc. Lond. Ser. A*, 472:20150762, 2016.
[181] N. Nagaosa and Y. Tokura. Topological properties and dynamics of magnetic skyrmions. *Nature Nanotechnology*, 8(12):899–911, 2013. Doi: 10.1038/nnano.2013.243.
[182] J. C. Nédélec. *Acoustic and Electromagnetic Equations: Integral Representations for Harmonic Problems*, volume 144. Springer Science Business Media , 2001. Doi: DNLBO01000933132.
[183] L. Néel. Les lois de l'aimantation et de la subdivision en domaines élémentaires d'un monocristal de fer. *J. Phys. Radium*, 5:241–251, 1944.
[184] L. Néel. Les lois de l'aimantation et de la subdivision en domaines élémentaires d'un monocristal de fer. *J. Phys. Radium*, 5:265–276, 1944.
[185] L. Néel. Quelques propriétés des parois des domaines élémentaires ferromagnétiques. *Cah. Phys.*, 25:1–20, 1944.
[186] L. Néel. Energie des parois de Bloch dans les couches minces. *C. R. Hebd. Seances Acad. Sci.*, 241:533—537, 1955.
[187] NIST. The object oriented micromagnetic framework (OOMMF) project at ITL/NIST. https://math.nist.gov/oommf/.
[188] F. Otto and J. Steiner. The concertina pattern. *Calculus of Variations and Partial Differential Equations*, 39(1-2):139–181, 2010. Doi: 10.1007/s00526-009-0305-7.
[189] F. Otto and T. Viehmann. Domain branching in uniaxial ferromagnets: asymptotic behavior of the energy. *Calc. Var. Partial Differential Equations*, 38:135–181, 2010.
[190] E. Outerelo and J. Ruiz. *Mapping Degree Theory*, volume 108. American Mathematical Society, 2009.
[191] W. Pauli. Über den Einflußder Geschwindigkeitsabhängigkeit der Elektronenmasse auf den Zeemaneffekt. *Z. Physik*, 31:373–385, 1925.
[192] X. Portier and A. K. Petford-Long. The formation of 360° domain walls in magnetic tunnel junction elements. *Appl. Phys. Lett.*, 76:754–756, 2000.
[193] R. Riedel and A. Seeger. Micromagnetic treatment of Néel walls. *Phys. Stat. Sol. B*, 46:377–384, 1971.
[194] T. Roubicek, L. Scardia, C. Zanini: Quasistatic delamination problem, *Cont. Mech. Thermodyn.* **21** (2009) 223–235.
[195] M. Rührig, W. Rave, and A. Hubert. Investigation of micromagnetic edge structures of double-layer permalloy films. *J. Magn. Magn. Mater.*, 84:102–108, 1990.
[196] M. R. Scheinfein, J. Unguris, J. L. Blue, K. J. Coakley, D. T. Pierce, R. J. Celotta, and P. J. Ryan. Micromagnetics of domain walls at surfaces. *Phys. Rev. B*, 43:3395–3422, 1991.
[197] C. J. Serna, S. Veintemillas-Verdaguer, T. González-Carreño, A. G. Roca, P. Tartaj, A. F. Rebolledo, R. Costo, and M. P. Morales. Progress in the preparation of magnetic nanoparticles for applications in biomedicine. *Journal of Physics D: Applied Physics*, 42(22):224002, 2009. Doi: 10.1088/0022-3727/42/22/224002.
[198] D. D. Sheka, D. Makarov, H. Fangohr, O. M. Volkov, H. Fuchs, J. van den Brink, Y. Gaididei, U. K. Rößler, and V. P. Kravchuk. Topologically stable magnetization states on a spherical shell: Curvature-stabilized skyrmions. *Physical Review B*, 94(14):1–10, 2016. Doi: 10.1103/physrevb.94.144402.
[199] T. H.R. Skyrme. A unified field theory of mesons and baryons. *Nuclear Physics*, 31(C):556–569, 1962. Doi: 10.1016/0029-5582(62)90775-7.
[200] V. Slastikov. Micromagnetics of Thin Shells. *Mathematical Models and Methods in Applied Sciences*, 15(10):1469–1487, 2005. Doi: 10.1142/s021820250500087x.
[201] M. I. Sloika, D. D. Sheka, V. P. Kravchuk, O. V. Pylypovskyi, and Y. Gaididei. Geometry induced phase transitions in magnetic spherical shell. *Journal of Magnetism and Magnetic Materials*, 443:404–412, 2017. Doi: 10.1016/j.jmmm.2017.07.036.
[202] E. C. Stoner and E. P. Wohlfarth. A mechanism of magnetic hysteresis in heterogeneous alloys. *Philosophical Transactions of the Royal Society of London. Series A, Mathematical and Physical Sciences*, 240(826):599–642, 1948.
[203] G. Strang, R. Temam: Functions of bounded deformations, *Arch. Rational Mech. Anal.* **75** (1980) 7–21.
[204] R. Streubel, D. Makarov, Y. Gaididei, O. G. Schmidt, V. P. Kravchuk, D. D. Sheka, F. Kronast, and P. Fischer. Magnetism in curved geometries. *Journal of Physics D: Applied Physics*, 49(36):363001, sep 2016. Doi: 10.1088/0022-3727/49/36/363001.

[205] R. Streubel, E. Y. Tsymbal, and P. Fischer. Magnetism in curved geometries. *Journal of Applied Physics*, 129(21):210902, jun 2021.
[206] P. Suquet: Un espace fonctionnel pour les équations de la plasticité, *Ann. Fac. Sc. Toulouse* **1** (1979) 77–87.
[207] K. Trabelsi, Modeling of a membrane for nonlinearly elastic incompressible materials via Gamma-convergence, *Analysis and Applications*, **04**-1, 2006, 31–60.
[208] C. Truesdell, Some challenges offered to analysis by rational thermomechanics, in *Contemporary Developments in Continuum Mechanics and Partial Differential Equations*, G.M. de La Penha, L.A. Medeiros, eds., North-Holland, New York, 1978.
[209] T. Trunk, M. Redjdal, A. Kákay, M. F. Ruane, and F. B. Humphrey. Domain wall structure in permalloy films with decreasing thickness at the Bloch to Néel transition. *J. Appl. Phys.*, 89:7606–7608, 2001.
[210] R. H. Wade. Some factors in easy axis magnetization of permalloy films. *Phil. Mag.*, 10:49–66, 1964.
[211] P. Weiss. L'hypothèse du champ moléculaire et la propriété ferromagnétique. *J. Phys. Theor. Appl.*, 6:661–690, 1907.
[212] P. Weiss and G. Foëx. *Magnétisme*. Armand Colin, Paris, 1926.
[213] E. Winkler: *Die Lehre Von der Elasticität und Festigkeit*, (1867) 388.
[214] J. M. Winter. Bloch wall excitation. Application to nuclear resonance in a Bloch wall. *Phys. Rev.*, 124:452–459, 1961.
[215] Z. C. Xia, J. W. Hutchinson: Crack patterns in thin films, *J. Mech. Phys. Solids* **48** (2000) 1107–1131.
[216] P.F. Yao, Optimal exponentials of thickness in Korn's inequalities for parabolic and elliptic shells, *Annali di Matematica Pura ed Applicata*, **200(2)**, (2020).
[217] K. Zhang, Quasiconvex functions, $SO(n)$ and two elastic wells, *Annales de l'Institut Henri Poincare* (C) Non Linear Analysis, **14(6)**, pp. 759–785, (1997).